Università degli Studi del Piemonte Orientale

"Amedeo Avogadro"

Dipartimento di Scienze del Farmaco

Dottorato di Ricerca in Biotecnologie Farmaceutiche ed Alimentari

XXVII ciclo a.a. 2011-2014

Looking around neurons in Alzheimer's disease: deregulation of astrocytic calcium signalling by amyloid-β

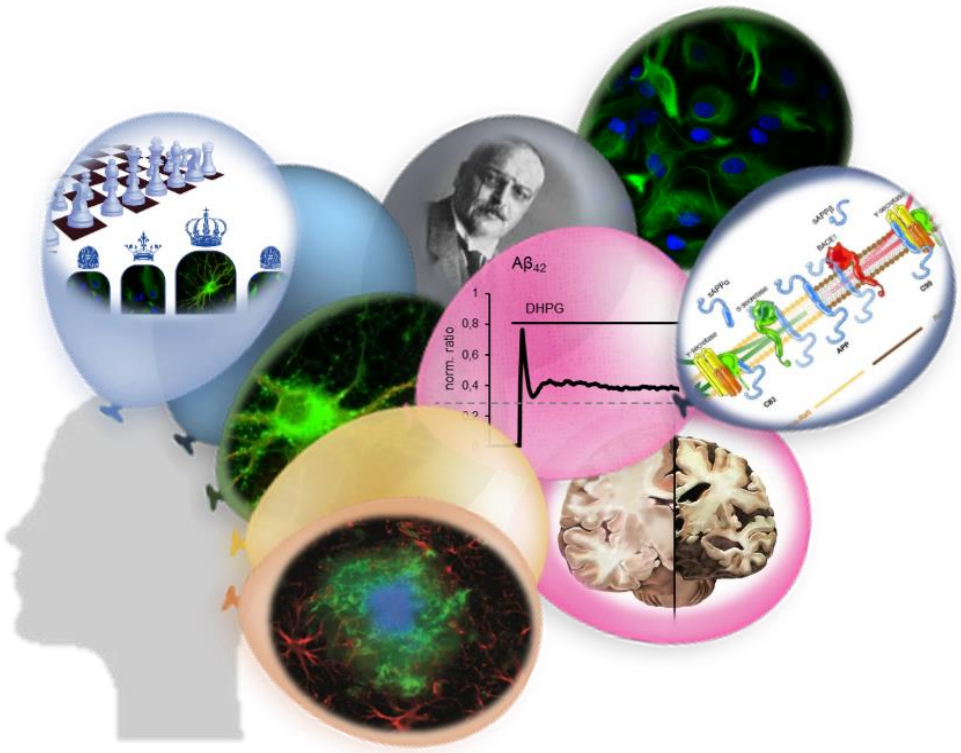

Virginia Ronco

“When you have eliminated the impossible, whatever remains, however improbable, must be the truth”

S. Holmes, Sir A.C. Doyle

To Ambra, Sarah
and Cristina

Contents

Chapter 1

Introduction

Alzheimer's disease (AD) is a devastating neurodegenerative disorder that affects increasing number of people in elderly worldwide. According to an estimate of Alzheimer's Association, the prevalence of AD in USA alone, in 2014, is 5.2 million of Americans (two-thirds of which are women), with an incidence of approximately 469.000 people. These numbers will nearly triple within the next 40 years. The AD impact is not limited to the affective field, but is also economical: total payments in USA in 2014, for all individuals with AD and other dementias, are estimated at $214 billion (www.alz.org). The most common form of AD is the late onset AD, which affects people over 60. Epidemiological studies suggest that high-calorie and fat diets, low educational level as well as history of head trauma and a sedentary life could be considered as risk factors, but how they can trigger AD is still unclear [1]. Less than 1% of AD cases have a genetic component and belong to the early onset familiar AD, which affect people younger than 60 [2, 3]. Even if AD was first described at the beginning of the 20th century by Alois Alzheimer (from who the name), is still incurable, indeed the drugs commercially available can slow down, but not heal, the pathology. In 1906, indeed, Alzheimer presented his findings of the behavioural and neuropathological changes in Frau Auguste D., a woman who died at age 51 after developing a rapidly progressive dementia: "The patient had as initial prominent presentation jealousy against the husband. Soon, a rapidly progressive weakness of memory became noticeable. She was unable to find herself oriented about her apartment… She was completely disoriented as to time and place. Occasionally, she remarked that she did not understand anything any more, that she was at a complete loss. The physician she greeted like a visitor and excused herself that she had not completed her work. Before long she shouted loudly that he wanted to cut her or she sends him away incensed with remarks which indicate that she is concerned about him regarding her female honor. At times, she is delirious, moves her bed around, calls for her husband and daughter, and appears to have auditory

hallucinations… Her ability to observe is severely disturbed. If one shows objects to her, she names these usually correctly, but immediately thereafter she has forgotten everything… She does not comprehend anymore the usage of certain objects…" [4]. The development of AD is almost imperceptible at the beginning, most often with occasional, minor lapses in recalling recent events of daily life (episodic memory). As years go by, AD patients gradually deteriorate into a marked dementia, with full disorientation, profound memory impairment, and global cognitive deficits. Many patients become immobile, confined to a chair or bed, and ultimately succumb to minor respiratory difficulties, such as aspiration or pneumonia [5].

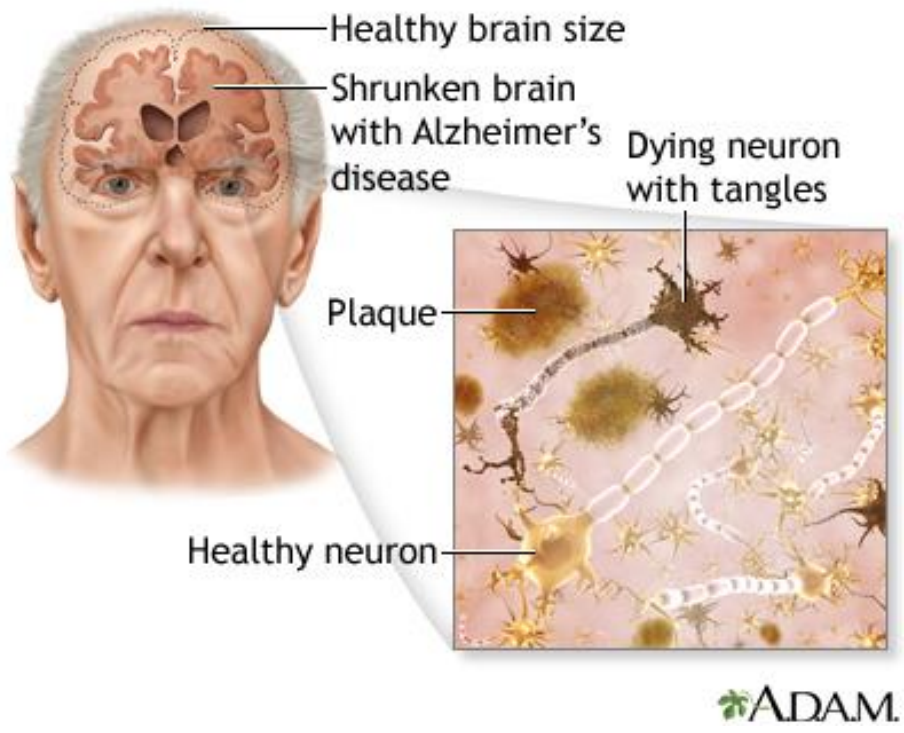

Figure 1. Scheme of the anatomical hallmarks of AD. A.D.A.M. Medical Encyclopedia

From an anatomical point of view, the brain areas involved in memory processes, including frontal and temporal lobes, of AD patients are reduced in size, due to the synaptic degeneration and neuronal loss [6]. Dissecting the brain, the hallmarks of the pathology are structures as neurofibrillary tangles (NFTs), and amyloid-β plaques (Figure 1). NFTs are intracellular fibrillar aggregates of the microtubule-associated protein tau, which is hyperphosphorylated, while plaques are extracellular deposits of fibrils, oligomers and monomers of the Amyloid β-peptide (Aβ). These structures are located mainly in brain regions involved in learning, memory and emotional behaviors such as the entorhinal cortex, hippocampus, basal forebrain and amygdala [1]. Aβ, in particular, is the protagonist of the so-called "Amyloid Hypothesis" which is the most popular and the most studied one to explain pathogenic mechanisms of the disease.

1.1 Amyloid Hypothesis

According to the amyloid hypothesis, the accumulation of Aβ and the consequent plaques formation is the result of a disequilibrium between two different cleavage pathways of the transmembrane protein Amyloid Precursor Protein (APP). One is amyloidogenic and leads to the production of Aβ fragments, expecially $A\beta_{1-40}$ and $A\beta_{1-42}$, which are the main components of the amyloid plaques, the other is the non-amyloidogenic one and is responsible for the production of the non-toxic fragment sAPPα [7]. In the amyloidogenic pathway APP is firstly cleaved by the β-secretase enzyme, an aspartyl protease (BACE 1 and 2), in the extracellular region of APP [8]. Secondly, the remaining transmembrane domain is hydrolysed in the middle by presenilin 1 (PS1), presenilin 2 (PS2) and nicastrin, which belong to the multiprotein complex γ-secretase [8, 9] and is released extracellularly. Alongside the amyloidogenic pathway, an alternative and non-amyloidigenic way of APP hydrolysis exist. In this second case, the extracellular domain is cleaved by the α-secretase instead of the β-secretase and the product of hydrolysis is the large and

soluble peptide sAPPα (Figure 2). This mechanism precludes Aβ production [10, 11].

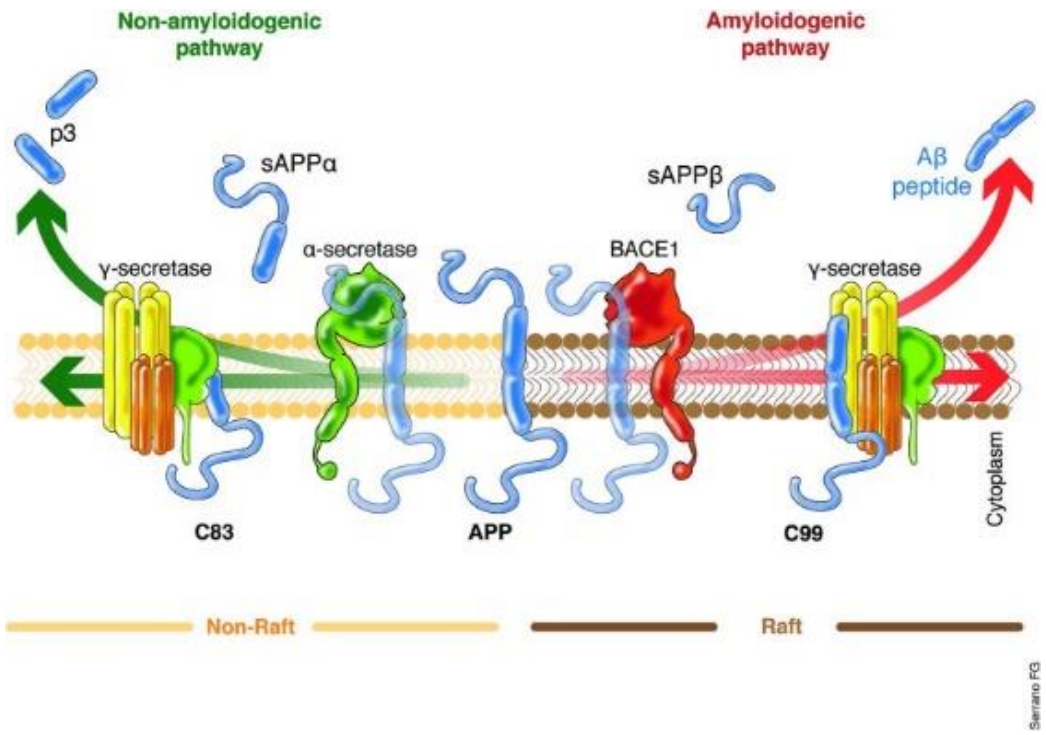

Figure 2. APP processing, critical cellular choice. The main source of Aβ production within the brain are the neurons. Two proteolytic processing pathways of APP have been described with two clear outputs. The non-amyloidogenic pathway will lead to the final release of the p3 and sAPPα, a small peptide with still poorly understood cell function. The cleaving enzymes which act to produce the sAPPα are the α- and γ-secretase. On the other hand, the activity of the β- and γ-secretase leads to the formation of the sAPPβ and the Aβ, the main neurotoxic agent described in AD. The role of the BACE is out of question and it is considered the Aβ production rate limiting enzyme. Interestingly, the recent work of Singh et al. (2013) clearly indicates that external factors might influence the expression levels of BACE, suggesting the potential up-regulation of the amyloidogenic processing of the APP. In the same context, it have been recently proposed that the APP amyloidogenic processing machinery is located in the lipid rafts rich in cholesterol. The increased lipid content within the cells, for example, as a result of increased systemic lipids levels, might also influence which APP processing machinery will be prompted to act. sAPPα/β, soluble APP fragment α/β; p3, 3-KDa peptide; BACE, β-site APP cleaving enzyme. Zolezzi et al.2014, Front Aging Neurosci. Jul 28;6:176.

Aβ monomers probably have little or no ability to disrupt synaptic functioning, but can aggregate to form oligomers (dimers seem to be the smallest synaptotoxic species), protofibrils (soluble, short fibril-shaped often "worm-like" structures), annular protofibrils (protofibrils that can form pores in membranes) and finally fibrils, which are the component of the advanced amyloid plaques. In contrast to oligomers and protofibrils, fibrils per se are unlikely candidates for memory impairment in AD, but plaque-containing insoluble fibrils can provide a source and sink for the toxic Aβ aggregate [12, 13].

The amyloid hypothesis is supported by the identification of pathological genes associated with the early onset AD. Indeed, mutations of APP itself (e.g. APPswe, the Swedish mutation, where the 670 lysine is substituted by asparagine and the 671 methionine is substituted by leucine, leading to an increase in β-secretase cleavage) as well as the enzymes involved in the amyloidogenic cascade, PS1 and PS2, have been identified and exploited in transgenic mice modelling [3, 14-16]. It should be acknowledged that these models can mimic just few histopathological features and some clinical symptoms of AD, but they don't reproduce faithfully the pathology, especially as regard the sporadic form [3]. In this thesis, the transgenic mouse model used is the triple transgenic (3xTg-AD), which presents the mutation APPswe, PS1-M146V and Tau-P301L to overexpress Aβ and hyperphosphorylated Tau. In this model, the progressive increase in Aβ peptide deposition can be detected with intracellular immunoreactivity at the third-fourth month of age, while synaptic transmission and long-term potentiation impairment is evident at the sixth month of age (www.jax.org). The amyloid hypothesis, is still a matter of debate, for example it was seen that inhibition of γ-secretase as well as β-secretase, in rat cortical neurons, decrease neuronal viability, effect which can be reverted by $A\beta_{40}$ administration [17].

Extracellular Aβ can be taken up by cells and internalised into intracellular pools. For example, Aβ can bind to the α7 nicotinic acetylcholine receptor (α7nAChR) with high affinity, leading to the receptor internalization and accumulation of Aβ intracellularly. Furthermore, Aβ can be internalized also by apolipoprotein E (APOE) receptors, which belong to the low-density lipoprotein receptors (LDLR). Neuronal Aβ uptake has also been shown to be mediated through NMDA (*N*-methyl-D-aspartate) receptors. Indeed, the blockade of this NMDA–Aβ internalization, by memantine, prevents pathogenicity [18]. The intracellular Aβ is responsible for different effects (Figure 3), which can concur to the development of the pathology. For example, Aβ can impairs the proteasome activity: Aβ can accumulate into the late endosomes, altering endosomal trafficking by the inhibition of the ubiquitin-proteasome system [19] as well as Aβ can directly inhibit proteasome [20] thus to increase Aβ itself and tau accumulation. Aβ has also been observed in mitochondria, where all subunits of the γ-secretase are located. Progressive accumulation of intracellular Aβ in mitochondria is associated with diminished enzymatic activity of respiratory chain complexes III and IV, and a reduced rate of oxygen consumption. These observations may help to explain the multitude of mitochondrial defects described in AD and mouse models of the disease [18]. Moreover, Aβ leads to calcium dishomeostasis (which will be discussed in the next chapter) and synaptic dysfunction. Indeed, the characteristic synaptic loss in AD leads to, and is linked to, a reduction in glutamatergic synapses strength and plasticity as well as an impairment in the long term potentization (LTP) to promote the long term depression (LTD), which is responsible for cognitive impairments [21-24]. LTP and LTD are dependent on NMDAR (N-methyl-D-aspartate receptors) and AMPARs (α-amino-3-hydroxy-5-methyl-4-isoxazolepropionic acid receptors). NMDAR are responsible for both LTP and LTD: high intracellular Ca^{2+} rise and synaptic NMDAR activation are required for LTP (which potentiate the glutamatergic synapses), while the internalization of synaptic NMDAR combined with the activation of perisynaptic NMDAR and a lower intracellular Ca^{2+} rise promotes the LTD. LTP induction

recruits AMPAR and promotes dendritic spine grow, while LTD is connected with spine shrinkage and synaptic loss [25]. By a mechanism not well understood, Aβ enhance LTD and impairs LTP. A possible explanation is that the Aβ blockade of glutamate uptake at the synapses could increase glutamate level in the synaptic cleft, thus to activate NMDARs first, but then desensitizing the NMDARs, leading to synaptic depression [26].

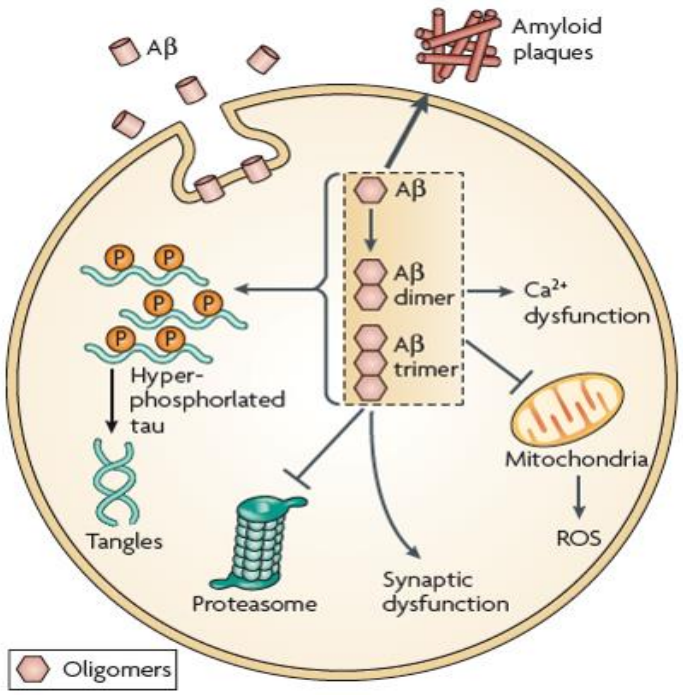

Figure 3. Amyloid-β, produced intracellularly or taken up from extracellular sources, has various pathological effects on cell and organelle function. Intracellular Aβ can exist as a monomeric form that further aggregates into oligomers, and it may be any of these species that mediate pathological events *in vivo*, particularly within a dysfunctional neuron. Evidence suggests that intracellular Aβ may contribute to pathology by facilitating tau hyperphosphorylation, disrupting proteasome and mitochondria function, and triggering calcium and synaptic dysfunction. LaFerla et al., 2007. Nat Rev Neurosci. Jul;8(7):499-509

1.2 Calcium hypothesis

Calcium (Ca^{2+}) is a ubiquitous intracellular signal, responsible for controlling numerous cellular processes [27]. The altered calcium homeostasis and signalling is one of the main features of neurons (and not only neurons) involved in AD. Such deregulation has been proposed as a key factor in the initial steps of the disease progression [28].

The fundamental role of Ca^{2+} as second messenger is ensured by its strong gradient as its cytoplasmic concentration is 50-300 nM at resting condition, but can be elevated to 1-5 µM in response to specific stimuli. This equilibrium is maintained by Calcium-ATPase and sodium/calcium ($Na+/Ca^{2+}$) exchanger on the plasma membrane (PM), where the two structures extrude Ca^{2+} from the cytosol to the extracellular space. Beside this mechanism, the sarco/endoplasmic reticulum ATPase (SERCA) pumps Ca^{2+} in the endoplasmic reticulum (ER) lumen, to create a Ca^{2+} store ready to be released at certain stimuli. Upon activation, Ca^{2+} can flow through PM channels as the voltage gated calcium channels (e.g. VGCC) or ionotropic receptors (e.g. NMDA, α7nAchR). Alternatively, Ca^{2+} can be release from the ER after stimulation of a metabotropic receptor (e.g. the metabotropic receptor for glutamate mGluRs). The G-protein linked to the receptor can activate PLC which in turn promote the generation of inositol-1,4,5-triphosphate (InsP3) which is the ligand of the receptor for InsP3 (InsP3Rs) on the ER membrane. InsP3 promote Ca^{2+} release from the ER, Ca^{2+} which can, in turn, bind the ER-resident ryanodine receptor (RyRs) to amplify ER Ca^{2+} release. The elevated micromolar cytosolic Ca^{2+} ($[Ca^{2+}]i$) reaches a concentration sufficient to trigger Ca^{2+}-dependent signalling cascade. Ca^{2+} can also flux into mitochondria matrix to activate Ca^{2+}-dependent dehydrogenases for ATP production or Ca^{2+}-dependent enzymes involved in oxygen/nitrogen species production, apoptosis/necrosis, gene expression, mitochondrial function etc. Another interesting and important mechanism involved

in Ca^{2+} homeostasis is the store operated calcium entry, but it will be discussed further.

The first calcium hypothesis of aging and AD backs to 40 years ago when Z. Khachaturian, thanks to the experiments of P. Landfield [29, 30], postulated that the chronic increase in cytosolic Ca^{2+}, and the consequent excitotoxic cell death, was a mechanism normally existing in aging. The difference between normal aging and pathological state of AD was the progression of Ca^{2+} deregulation: slow in aging, faster in AD. According to this hypothesis, the long lasting Ca^{2+} overload of the cytoplasm and of the ER induces activation of mechanisms leading to cell death [31, 32], but the exact mechanism by which this occurs is still a matter of debate. Aβ seems to play multiple and distinct roles both outside, along the plasma membrane, and inside the cells, on the endoplasmic reticulum (Figure 4). Indeed, It has been shown that Aβ has the capability to influence the plasma membrane permeability to Ca^{2+} [33], furthermore the peptide can act as a ionophore, recreating Ca^{2+} permeable pores in the plasma membrane [34-37]. The pore forming mechanism has been confirmed also by the high resolution transmission electron microscopy, revealing the presence of Aβ pores distributed in situ in cell membrane of AD post-mortem brains, but not in healthy brains [38]. Aβ can interact also with plasmalemmal Ca^{2+} channels and Ca^{2+}-permeable ionotropic receptors (e.g., NMDA or acetylcholine receptors) [39]. A direct linkage between Aβ and the nicotinic receptor α7nAchR has been reported [40-42]. Aβ can also affect the activity of NMDAR and VGCC, but the observed effects are still controversial [40, 43-45]. Inside cells, with unknown mechanisms, Aβ was reported to increase the calcium release from the endoplasmic reticulum (ER), augmenting the expression of ryanodine receptors (RyR) and their open probability in skeletal muscle [46] or, inside neurons, by the direct interaction to InsP3Rs or by affecting mGluR5 metabotropic glutamate cascade [47]. Moving to transgenic mice models, the link between genetic abnormal AD-related background and the altered Ca^{2+} homeostasis is provided by presenilins [3]. Indeed, neurons of

PS1 transgenic mice have shown an increased susceptibility to Ca^{2+}-mediated excitotoxicity, due to an abnormal Ca^{2+} release from the endoplasmic reticulum [48, 49]. This can be linked to the activity of PS1 as a leak channel [31] and the consequent excessive accumulation of Ca^{2+} in the ER, resulting in an increased InsP3R open probability and an increase in the receptor sensitivity sensitivity to InsP3 [50, 51]. These effects can be further exacerbated by increases in Ca^{2+} induced (i.e., RyR-mediated) Ca^{2+} release. Actually, the role of PS1 as a leak channel is somewhat enigmatic [52, 53], few works support the effect of PS1 on ER Ca^{2+}-leak [54, 55], but this hypothesis is still a matter of debate [56]. On the contrary, the role of RyRs and InsP3Rs in AD is strongly supported in literature. For example, the expression of RyRs was found to be elevated in PC12 expressing the PS1 mutant gene as well as in neurones from PS1 mutant knock-in mice [57]. An increase in RyR-mediated Ca^{2+} signalling was also observed in cultured neurones [58, 59], and in slices from 3xTg-AD mice (bearing mutated genes for APP, PS1, and tau) [51, 60]. Also Insp3Rs expression is augmented [61] and the inhibition of InsP3Rs can reduce Aβ calcium effects [62]. Interestingly, aberrant Ca^{2+} release has been observed in AD mice of all ages, being already present in very young animals. In this sense, deregulated Ca^{2+} can be an early marker for pathology.

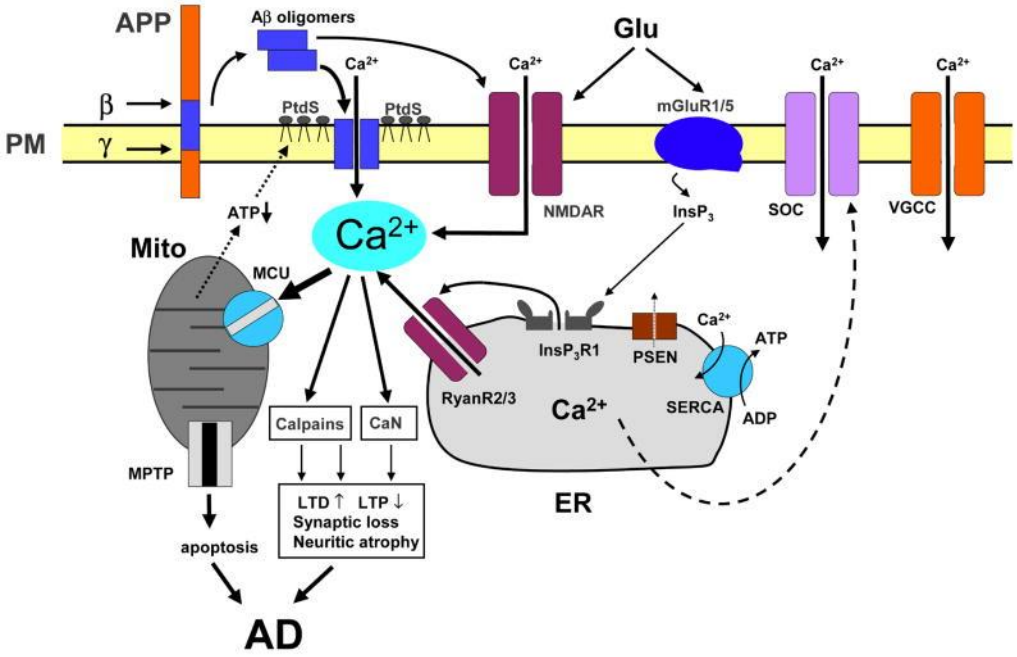

Figure 4. Calcium dysregulation in Alzheimer disease Sequential cleavages of β-amyloid precursor protein (APP) by β-secretase (β) and β-secretase (β) generate amyloid β peptide (Aβ). Aβ forms oligomers, which can insert into the plasma membrane and form Ca^{2+}-permeable pores. The association of Aβ oligomers with the plasma membrane is facilitated by binding to surface phosphatidylserine (PtdS); age and Ca^{2+}-related mitochondrial impairment leads to ATP depletion and might trigger flipping of PtdS from the inner portion of the plasma membrane to the cell surface. Reduction in ATP levels and loss of membrane integrity causes membrane depolarization, which leads to facilitation of Ca^{2+} influx through NMDAR and VGCC. Aβ oligomers can also affect activity of NMDAR, AMPAR and VGCC directly. Glutamate stimulates activation of mGluR1/5 receptors, production of InsP3 and InsP3R -mediated Ca^{2+} release from the ER. Presenilins (PS) function as an ER Ca^{2+}-leak channels and many FAD mutations impair Ca^{2+}-leak-channel function of PS, resulting in excessive accumulation of Ca^{2+} in the ER. Increased ER Ca^{2+} levels result in enhanced Ca^{2+} release through InsP3 -gated InsP3R 1 and Ca^{2+}-gated RyanR(2/3). PS might also modulate activity of InsP3R, RyanR and SERCA pump directly. The activity of store-operated Ca^{2+} channels on the plasma membrane can be affected indirectly by PS mutations through the modulation of SERCA activity. Elevated cytosolic Ca^{2+} levels result in the activation of calcineurin (CaN) and calpains and lead to facilitation of LTD, inhibition of LTP, modification of neuronal cytoskeleton, synaptic loss and neuritic atrophy. Excessive Ca^{2+} is taken up by mitochondria through mitochondrial Ca^{2+} uniporter (MCU), eventually leading to opening of mitochondrial permeability-transition pore (mtPTP) and apoptosis. Supnet and Bezprozvanny 2010 Cell Calcium Feb;47(2):183-9.

1.3 Astrocytes, a brief introduction

Before approaching to neuroglia and its complex roles in the brain, it would be appropriate a brief introduction on history and functions of these fundamental cells. The first to coin the term "neuroglia" was Rudolf Virchow in the 1858: "…If we would study the nervous system in its real relations in the body, it is extremely important to have a knowledge of that substance also which lies between the proper nervous parts, holds them together and gives the whole its form in a greater or less degree" [63]. His idea of glia as a simple connective tissue was soon overcome by Ernesto Lugaro, who collected in "Sulle funzioni della nevroglia" the efforts of the main histologists of the 19th century, the golden age of cellular histology, as Virchow himself, Santiago Ramòn y Cajal and Camillo Golgi. There he described glial cells connected to blood vessels and to synaptic cleft, the morphological changes of glial cells when exposed to a stimulus and he confirmed the protective role of glial cells against toxins [64]. Carl Ludwig Schleich, in his book *Schmerzlose Operationem*, was the first to postulate that glia and neurons were on an equal footing in maintaining brain functions, especially he believed that glia was a sort of inhibitory mechanism of the brain. According to his theory, neuronal excitation was transmitted from neuron to neuron through intercellular gaps filled with glial cells, which are the anatomical substrate responsible for controlling network excitation/inhibition by constantly changings in glial volume (swollen glial cells inhibit neuronal communication, while glial shrinkage facilitates the impulse propagation). Finally, in the 1960s Steven Kuffler, John Nicolls and Richard Orkand demonstrated electrical coupling between glial cells while Milton Brightman and Tom Reese identified the gap junctions, structures connecting the glial networks. Despite all of these findings, glia has been considered a sort of inert bystanders to the active neurons since nowadays, only the advent of modern patch-clamp and fluorescent calcium dyes techniques, has changed this image of glia as "silent" brain cells.

According to the idea of the "silent" glia, AD has been investigated mainly from a neurocentric point of view. Anyway, during the last years astrocytes have arose an increasing interest in this field. Brain can be imagined as a sort of chess game, where the king of course are neurons, but astrocytes are the other pieces as the queen or the bishop. If the king is lost, the game is lost, but in this game the main players are not the king, but the other pieces. As well as a chess game, astrocytes can play to protect their king or against the king. This second condition is what append in neurodegenerative disorders as AD.

Before describing the role of glia, it must be pointed out that glia is a general term to indicate different cell types, indeed microglia, and the macroglia (astrocytes and oligodendrocytes) belong to this [65, 66]. Microglial cells are residing cells in the central nervous system designated to the immunocompetent role. They are the brain immune system. Microglia represents almost the 10% of the total glial cells and can appear in three different states: resting, activated and phagocytic state. Resting microglia resides in every parts of the brain and is characterised by a small soma with numerous thin and highly branched processes, full of receptors and immune molecules recognition sites to detect the status of the CNS tissues. Brain injury triggers the activation of microglia, which is turned into activated state or into phagocytes, the active brain defence system. Oligodendrocytes are the glial cells, which enwrap the neuronal axons to isolate them by the myelin production and allowing the salutatory action potential propagation (the same role as Schwann cells in the peripheral nervous system). They're characterised by a small rounded cell body with four to six primary processes which branch and myelinate 10 to 30 thin (diameter <2 μm) axons. The axonal areas without myelin coating are called nodes of Ranvier and are the areas where the action potentials are generated. Astrocytes ('star-like cells') are the most abundant and diverse glial cells in the CNS, characterised by a stellate morphology with many primary processes originating from the soma. Actually, not all of the astrocytes have this kind of morphology.

Beside the "true" astrocytes (the protoplasmic astrocytes of the grey matter and the fibrous astrocytes of the white matter) belong to this class also cells without a stellate morphology e.g. radial glia. Radial glia are bipolar cells with an ovoid cell body and usually two main processes, one of them forming endfeet on the ventricular wall and the other at the pial surface. Something characteristic of all of the astrocytes is the expression of vimentin and the Glial Fibrillary Acidic Filament (GFAP), the intermediate filaments of the cytoskeleton. Indeed, vimentin and GFAP are two classical marker for astrocytes identification. Astrocytes are the cells examined in this thesis.

Looking at astrocytic physiology, astrocytes show a predominant potassium conductance, hence the negative resting potential (-80 to -90), which is near to the potassium equilibrium potential. They're non excitable cells, so after electric depolarization astrocytes can't produce a regenerative action potential. The ionic distribution across the PM is similar to other cells, except Cl^-, which is unusually high in the cytosol (30-40 mM) due to the high activity of the $Na^+/K^+/2Cl^-$ co-transporter (transport $2Cl^-$ into the cell in exchange for 1 K^+ and 1 Na^+) [65]. According to the negative resting potential, the predominant astrocytic ion channels are the potassium voltage-gated channels [66], but also voltage-gated sodium channels (Na_v) are present. The voltage-gated calcium channels (Ca_v) are involved in generating local elevations of cytosolic Ca^{2+} to control Ca^{2+}-dependent processes. They're up-regulated in reactive astrocytes, while they're usually down-regulated during glial development. Furthermore, glial cells have a multiplicity of neurotransmitter receptor both ionotropic and metabotropic. Among the ionotropic receptors, stand out the nicotinic receptors (nAchRs) and GABA receptors, as well as the muscarinic receptors (mAchRs) from the metabotropic receptors. Quite interesting are the purinergic and glutamatergic receptors. Astrocytes, indeed, belong to the "tripartite synapses" where they actively participate to the synaptic signalling also by the release of gliotransmitters: glutamate and ATP. Astrocytic purinergic

receptors are both ATP and adenosine receptors indeed, ATP can be broken down to adenosine, to be employed as a gliotransmitter in some areas. The adenosine receptors are coupled with G-proteins and can participate to the regulation of glutamate transporters expression, sensitivity of cells to glutamate, etc. ATP receptors are ionotropic (P2X) and metabotropic (P2Y). P2X7, especially, is activated by high amount of ATP (mM) and has the capability to open, in the PM, large Na^+, Ca^{2+} and K^+ permeable pores. This high ATP concentration ca be reached during neuronal damage and can activate microglia through microglial P2X7. Microglial P2X7 may play a role in AD [67] in APP processing [68] or in oxygen radical species production [69]. In astrocytes, P2X7 may mediate the release of ATP. Glutamate receptor can be divided into ionotropic (AMPA, NMDA and kainate) and metabotropic (mGluRs) receptors. AMPA (activated by α-amino-3-hydroxy-5-methyl-4-isoxazolepropionate) and kainate are non selective cation channels permeable to Na^+ and K^+ and, to a much lesser extent, Ca^{2+}. AMPA are localised on the post-synaptic membrane and are responsible for the fast post-synaptic neuronal depolarisation. The receptor for kainate can interact with AMPA to extend the AMPA depolarising effect. NMDA (receptor for N-methyl-D-aspartate) are the third type of ionotropic glutamate receptor, in contrast to the other two receptor, their channel is highly permeable to Ca^{2+}. Neuronal NMDA are blocked by Mg^{2+}, which is removed only when neuron is depolarised. These channels require the presence of the co-agonist D-serine, which can be supplied by astrocytes, to be activated. The binding of glutamate alone is not sufficient to NMDA opening. In contrast to neuronal receptors, glial NMDA are less sensitive to Mg^{2+} blockade thus to be activated also at resting potential. AMPA and NMDA are involved in the processes of long term potentiation and long term depression, which are the basis of memory processes [65, 70, 71]. Glutamate metabotropic receptor (mGluRs) are seven transmembrane proteins coupled to protein G. mGluRs can be divided into three groups: I) positive coupled with PLCγ and InsP3 pathway. They're mGluR1 and mGluR5, which can be selectively stimulated by DHPG. II) mGluR2 and mGluR3.

III) mGluR4, mGluR6, mGluR7 and mGluR8. mGluRs of group II and III are negatively coupled to adenylate cyclase, regulating the intracellular levels of cAMP. Astrocytes predominantly express mGluR3 and mGluR5 [65, 71].

1.4 Astrocytes in Alzheimer's disease and neurodegenerative disorders

As anticipated before, astrocytes play multiple functions in maintaining brain physiology. Indeed, astrocytes have a structural role, defining the shape of the grey matter and enwrapping and "fixing" neurons and synapses (a single astrocyte can envelop approximately 140,000 synapses) [72]. Astrocytes are a component of the Blood Brain Barrier (BBB) as they send their processes to the blood vessels providing a metabolic support to glia itself as well as neurons. An increased neuronal activity, followed by the activation of astrocytic Ca^{2+} signalling, leads to a fast release of vasoactive substances and vasodilatation [73]. Furthermore, astrocytes and endothelial cells can interact each other: astrocytes can release regulatory factors (e.g. TGF-β, glial derived neutrophic factor GDNF) to stimulate the formation of tight junction and polarised luminal and basal endothelial cells membrane. Endothelial cells, in turn, promote astrocytes development through leukaemia inhibitor factor (LIF) or can influence the composition in ion channels and receptors of the glial membrane [74]. Astrocytes regulate the extracellular environment, controlling extracellular concentration of ions, metabolites and neuroprotective molecules, through structures as aquaporin 4 (AQP4) or transporter for the K^+ uptake [75]. Astrocytes belong to the so called "tripartite synapse", as they directly interact with neurons by gliotransmitters release (Glu, ATP, D-serine, GABA, adenosine). This process depends on an astrocytic cytosolic Ca^{2+} rise in response to changes in neuronal synaptic activity [70]. According to this concept, astrocytes in situ are not simply spectators, listening and reacting to neuronal activity, but can also modulate the synaptic transmission, being a functional component of the synapses, as the pre- and postsynaptic compartments, in a bidirectional communication [72]. Moreover,

astrocytes can modulate the synapses by controlling the neurotransmitters level in the synaptic cleft. Indeed, they highly express transporters e.g. for glutamate, GABA and glycine, which remove the neurotransmitter to the synaptic space. Glutamate, for example, needs to be maintained at a low level to allow an efficient signalling and to avoid excitotoxic cell death. Glutamate transporters (excitatory amino acid transporter 2, EAAT2, known as glutamate-transporter 1, GLT1, in the rodents) remove the neurotransmitters from the synaptic space to the astrocytic intracellular space, where is converted by enzymes, such as glutamine synthase, into precursors as glutamine. The precursors are recycled-back to the synapses in order to be reconverted in the active transmitters again [76]. Astrocytes are connected each other by gap junction, mainly formed by Connexin 43 (CX43). This network can dissipate molecules as glutamate or can contribute to the propagation of intracellular Ca^{2+} waves, thus to, for example, rescue neurons from the glutamate mediated excitotoxicity [77]. Furthermore, astrocytes supply a small portion of D-serine, which is a fundamental co-agonist in neuronal NMDA activation [70]. Because of the primary role of astrocytes in brain homeostasis and function, is not difficult to imagine that astrocytes can play a key role in a pathological state such as in Alzheimer's disease.

The term "neurodegenerative disorder" refers to a chronic disease, which progressively leads to neurons degeneration, atrophy and death. The progression of the neurodegeneration is linked to functional and cognitive deficits, which correlates to the clinical manifestation of the pathology. As anticipated before, the disease progression cannot be arrested; indeed, the therapeutic strategies are purely symptomatic. Find a correct therapy is further complicated by the difficulties in finding the underlying cause of the pathology, indeed, even if neurons are the "victims" of the disorder, other brain cells might play a fundamental role in the disease beginning and development. The study of these cells can be a new strategy

in the neurodegeneration understanding and a breakthrough in the ambitious search of a cure.

There are many examples on the involvement of astroglia in neurodegenerative pathology. The loss of astroglia-dependent glutamate clearance and K^+ buffering is a key pathogenic step in the toxic encephalopaties after brain poisoning with heavy metals (mercury, lead, or aluminium) or in the Reye's syndrome (also called hepatic encephalopathy, is a consequence of ammonia brain poisoning). The altered glutamate and K^+ homeostasis leads to excitotoxicity and brain oedema, which are the hallmark of the pathology [78-81]. The thiamine deficiency is connected to a profound loss of astroglial glutamate transporters, triggering the excitotoxicity in the Wernicke–Korsakoff encephalopathy [82]. Recently, the involvement of astrocytes in motoneurones degeneration and death has been identified in the pathological progression of the amyotrophic lateral sclerosis (ALS). Indeed, glia atrophy, as well as astrocytes apoptosis and degeneration, are linked with neuronal damage and clinical symptoms [83, 84]. The linkage between glia and neurodegeneration in ALS seems to be glutamate excitotixicity. The down-regulation of the astroglial glutamate transporter, leads to an increase of glutamate in the synaptic cleft and the consequent exciotoxic death of motoneurones. The transgenic deletion of GLT-1/EAAT2, the glutamate transporter, in mice can recreate this key pathological feature of the disease [85]. The Familiar form of ALS presents, in astrocytes, the specific expression of the mutant human superoxide dismutase (hSOD1), which is connected with an increase in glutamate sensibility, as well as activated microglia and neurotoxicity. The astrocytic silencing of hSOD1 has been shown to slow down the disease progression [86]. An increase in glutamate vulnerability has also been observed in Huntington Disease (HD), where the expression of pathological huntingtin, characterised by a large polyQ repeat, in astrocytes, increases glutamate neurotoxicity. This effect is possibly related to a down-regulation of glutamate uptake, as in the ALS [87]. These pathologies are just few examples of the

involvement of astrocytes in neurodegenerative disorders. Indeed, astrodegeneration and astroglial death were also described for the fronto-temporal dementia, Pick's disease, fronto-temporal lobar degeneration, thalamic dementia, and HIV-associated dementia [88-90].

In Alzheimer's disease, astrocytic abnormalities have been observed in the full-blown pathology, as well as in the early phases of the disease (Figures 5 and 6). Atrophic astrocytes, characterised by a reduction in GFAP, glutamine-synthetase, and/or s100β immunoreactivity have been observed before the plaques formation in several mouse models, e.g 3xTG-AD and PDAPP-J20 mice carrying the Swedish and Indiana APP human mutations [91-94]. These atrophic changes are strongly region dependent. Indeed, they appear very early (at 1 month of age) in the entorhinal cortex, around 6 months of age in the prefrontal cortex, and at almost 12 months of age in the hippocampus of transgenic mice. Such astrodegeneration and atrophy are accompanied by reactive astrogliosis, especially in the later stages of the disease. Furthermore, reactive astrocytes surrounding the amyloid plaques have been observed in human AD brains, as well as transgenic mice brains [95]. The terms "reactive astrocytes" or "astrogliosis" refer to a finely gradated continuum of progressive changes in gene expression and cellular changes, in response to a brain insult [96]. This ancient and conserved defence enables astrocytes to delimit the damaged area and remodel the area after injury recovery. Furthermore, reactive astrocytes protect the insulted tissue by their homeostatic mechanisms: i) the uptake of potential excitotoxic glutamate ii) the protection from oxidative stress by glutathione production, iii) the anti-inflammatory effect by adenosine release, iv) Aβ degradation, v) oedema reduction vi) stabilizing extracellular fluid and ion balance [97, 98]. Severe and persisting insults (e.g. ischemia, trauma, infections, inflammation), from which recovery is impossible, trigger astrocytes proliferation, as well as a long-lasting reorganization of the damaged tissue as collagenous deposition, leading to the scar formation. In this case, the damaged area loses its

function, but astrocytes on the scar burden keep their homeostatic activities [97]. In experimental AD, Aβ triggers reactive astriogliosis predominantly in the hippocampus, while is almost absent in the entorhinal and prefrontal cortex [92-94]. This region dependence can reflect the different sensitivity of the two brain areas to AD pathology.

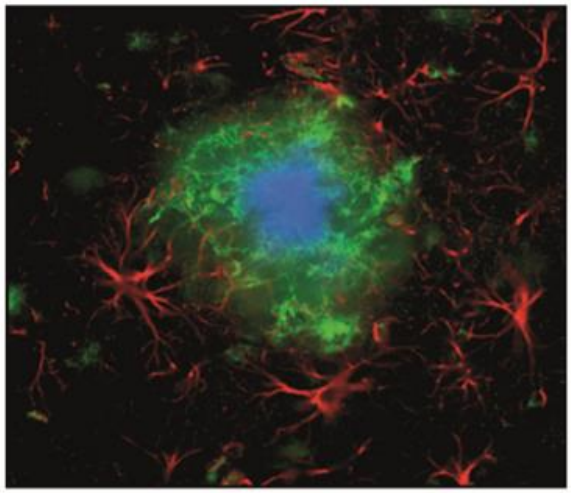

Figure 5. Astroglia assembling around a plaque in an amyloid precursor protein/presenilin 1 transgenic mouse. Astrocytes (red) are labelled using indirect immunochemistry and antibody against glial fibrillary acidic protein, while the core and periphery of the b-amlyoid (Aβ) plaque are stained using methoxy-XO4 [binding Ab fibrils; (Klunk et al. 2002)] and monoclonal antibody IC16 [binding Ab dimer, with the epitope at residues 2–8 of Ab; (Muller-Schiffmann et al. 2011)], respectively. Courtesy of Drs. Markus Kummer and Michael Heneka. V. Parpura et al. J. Neurochem (2012) 121, 4-27

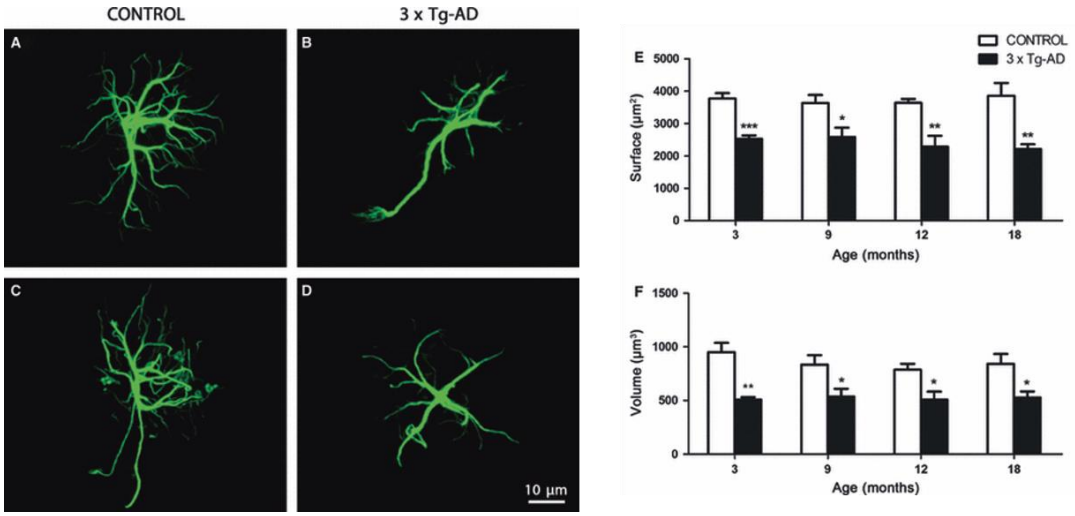

Figure 6. Atrophic astrocytes in the early stages of AD. Confocal images showing the classical morphology of GFAP-positive astrocytes in control non-Tg animals and astrocytic atrophy in the 3 × Tg-AD animals at 3 months (A and B, respectively) and 18 months (C and D, respectively) in the mPFC. Bar graphs showing the decreases in the GFAP-positive surface area and volume throughout the whole extent of the mPFC (E, F) in 3 × Tg-AD mice when compared with control animals. Bars represent mean ± SEM. Kulijewicz-Nawrot et al., J. Anat. (2012) 221, pp252-262

1.5 Astrocytic Ca^{2+} signalling and toolkit in AD

First to describe the implication of astrocytic Ca^{2+} signalling in AD, it should be acknowledged that the difficulties in generating unifying concepts are connected to the great heterogeneity in this field. Indeed, the great part of our knowledge in the implication of astrocytic Ca^{2+} in AD comes from in vitro studies on primary astrocytes, but the models used as the source of astrocytes, as well as the investigated brain areas or the quality of cultures (mixed with neurons/microglia or purely astrocytic) differ from study to study. The problem of the heterogeneity also affects the concentrations of Aβ treatments, as well as the species of Aβ (monomers, oligomers, fibrils) and the length of Aβ peptide (1–42, 1–40, or 25–35), the protocols to Aβ production and the time of Aβ treatments. The reason for this complexity could resides in the different outcomes the groups working in this field are focusing on, or

can reflect the tendency of considering astrocytes something secondary according to the neuronocentric view of AD [3].

The reported effects of Aβ administration in acute, on astrocytes, include fast $[Ca^{2+}]i$ transients [99-102], as well as Ca^{2+} oscillations [103, 104]. It should be pointed out that beside these studies there are few others that don't observe any acute effects of Aβ on astroglial $[Ca^{2+}]i$ [105-107]. Because of the experimental protocols of these two groups are similar, the opposite results should be explained by the different concentrations of Aβ used. Indeed, Ca^{2+} transients and oscillation can be trigger by micromolar Aβ concentrations, while concentrations lower than 1μM have no or less reproducible effects. A recent article postulated that low (200 pM) Aβ concentrations can modulate the α7nAChRs receptor, especially by altering the frequency and amplitude of Ca^{2+} waves, both spontaneous and evoked ones [108]. It is not easy, or it may be impossible, to define the perfect Aβ concentration to employ in experimental protocols, indeed, also in physiological conditions, as well as in AD, the Aβ concentrations may vary, for example, with the distance to the plaques [109]. The fact that only high concentrations induce reproducible effects is not, anyway, something irrelevant. Transient and waves are not the only mechanisms which can be altered by Aβ, but Aβ can also induce $[Ca^{2+}]i$ rise by other pathways [100, 103, 104] and can affect the Ca^{2+} release from intracellular stores [99, 100,102]. There are also evidences that Aβ effects could be extended to the response of astrocytes to neurotransmitters, which is altered after Aβ treatment. Interestingly the exposure of primary cortical astrocytes to 200pM of $Aβ_{25-35}$ had no effect on acute Ca^{2+} response, but significantly potentiated serotonin- and glutamate-induced $[Ca^{2+}]i$ transients [107]. This report supports the idea that Aβ is not able to induce Ca^{2+} response per se, if not at high concentration, while at low concentrations Aβ can modulate the Ca^{2+} response to other signalling molecules. Unfortunately, the study of this modulating activity of Aβ has not been followed up.

Acute effects of Aβ are not the only explored, but also sub-acute and chronical Aβ activities have been examined. Sub-acute exposure refers to period of Aβ treatment up to 12 h. The reported effects of Aβ in such conditions consist in a modest rise of basal Ca^{2+} levels (almost doubled), which was confined to a subcellular population of primary hippocampal [106] and cortical [110] astrocytes. The sub-acute treatment could also affect the mechanically induced intercellular Ca^{2+} waves, increasing the frequency and amplitude in cortical astrocytes [110], as well as the exposure of cultured cortical rat astrocytes to 5μM of Aβ42 can increase the intercellular spontaneous waves between cells in time-delayed [100]. As reported for acute Aβ treatment, literature about sub-acute treatment is contradictory. Indeed, in few studies (which, however, employed somewhat different conditions) the alterations in Ca^{2+} signalling after sub-acute Aβ treatment have not been observed [101] or, on the contrary, a decreased in basal calcium has been reported [111]. The augmented basal Ca^{2+}, also if modest, can have long-term repercussions, activating Ca^{2+} dependent signalling cascades. This was evident after chronic exposure (24–72 h) to 100nM Aβ, where hippocampal and cortical astrocytes showed an improved mGluR5 signalling, as well as the store operated calcium entry [105, 106].

Other important instruments in AD understanding are the transgenic mice models of AD, which are able to recreate just few pathological features of AD, not to recreate AD completely, but remain a good strategy to investigate alteration in astroglial Ca^{2+} signalling in a situation, which is closer to real physiological conditions. In these sense, the possible approaches are the study on primary cultures, the study on brain slices and the study *in vivo* by the cranial window. Primary astrocytes from newborn pups are employed for the investigation of the very early stages of the disease, when the histological hallmarks of AD have not developed yet, but genetic alterations have started their deleterious effects. From the point of view of this thesis, the most interesting mechanisms are the astrocytic response to glutamate through the mGluR5 receptor and the Store Operated Ca^{2+} Entry (SOCE). The SOCE is a mechanism to

refill the ER after its luminal Ca^{2+} depletion, due to the activation of InsP3Rs or RyRs and the consequent Ca^{2+} release from the ER. The protein STIM, which is a transmembrane protein on the ER membrane, detects the luminal Ca^{2+} loss and, in turn, activates the channels Orai or TRPCs (Transient Receptor Potential Channels). Orai and TRPCs opening leads the Ca^{2+} entry from the extracellular medium. Ca^{2+} is finally pumped into the ER by the SERCA pump to restore the resting ER luminal Ca^{2+} concentration. Hippocampal primary astrocytic cultures from 3xTg-AD mice have shown an increased DHPG response, as well as an augmented SOCE, compared to astrocytes from wild type animals [112, 113]. The same effects have been observed in wild type astrocytes incubated with $A\beta_{42}$ for 72 h, while the Aβ treatment on transgenic astrocytes was unaffected. Somewhat interesting is that the increased SOCE of transgenic astrocytes reaches almost the same level as that of wild type astrocytes treated with $A\beta_{42}$ for 72 h [113]. The altered Ca^{2+} signalling toolkit just described, is region specific as it has been observed in the astrocytes from the hippocampus, but not in those from the entorhinal cortex (EC) of the same animals [112]. Furthermore, entorhinal astrocytes have not shown the astrogliotic response to β-amyloid depositions in the 3xTg-AD mice. Indeed, even if transgenic astrocytes of EC are atrophic, the cell distribution and density is unaffected by the disease progression [94]. This can be explained by the absence of Aβ effects on the InsP3 pathway in EC astrocytes, where the InsP3-dependent Ca^{2+} signalling is critical for astrogliosis initiation [114]. Moreover, in a mouse model where APP was genetically deleted, the decrease of the SOCE in cortical astrocytes has been observed, while cortical astrocytes from Tg5469 mice (which overproduce human APP) showed no difference in SOCE between transgenic and wild type cells [115]. It should be pointed out that the different protocols of these experiments are difficultly comparable, anyway the increased $[Ca^{2+}]i$ through InsP3 pathway, as well as the increased SOCE in transgenic astrocytes seem to be the most accredited line. Such findings were also confirmed by an animal model of Down syndrome (Trisomy 16 mice, amyloid deposits are characteristic also in Down syndrome). Indeed, the

increase in basal $[Ca^{2+}]i$, as well as the increased Ca^{2+} release from ER, triggered by thapsigargin, which inhibit SERCA leading to ER Ca^{2+} leak [116] have been observed also in this model. The measurement of ER Ca^{2+} release triggered by thapsigargin it's a classical protocol to evaluate ER luminal Ca^{2+} storage. Data from cultured astrocytes are no longer different from evidences on brain slices. For example, astrocytes from brain slices of Tg2576 mice (overexpressing the APPK670/671L) have shown a significantly higher Ca^{2+} spikes frequency compared to wild type cells [117, 118].

Very intriguing is the possibility to measure Ca^{2+} in alive animals directly [3]. That's the example of the work of Kuchibhotla. By the technique of the two-photon microscopy, combined with the cranial window, he studied Ca^{2+} abnormalities in APP/PS1 mice. He observed an increase in the basal astrocytes Ca^{2+}, which was almost doubled, compared to the wild type. This abnormality was accompanied by the appearance of spontaneous Ca^{2+} activity, as well as synchronous hyperactivity and long-range aberrant Ca^{2+} waves in astroglial syncytia [119]. These effects were evident in the late stages of the disease, when the plaques were already present, and were not neurons dependent as tetrodotoxin was unable to block them. Similar results were obtained by Takano's group, analysing the earlier stages of the disease. On APPSwe mice of 2-4 months of age (so before the amyloid plaques accumulation) he observed a higher frequency of spontaneous Ca^{2+} oscillation, compared to the wild type. Curiously these data were confirmed only by a sub-population of 3xTG-AD astrocytes, while the increased Ca^{2+} activity was absent in Dutch/Iowa mice [120]. Nevertheless, the intravenous administration of Aβ (0.4 mg/Kg) induced an increase in astrocyte Ca^{2+} oscillations both in wild type animals and in Dutch/Iowa mice [120]. All of these studies in vivo seem to support the abnormal astrocytic Ca^{2+} signalling in AD pathology.

An interesting view of the alterations in Ca^{2+} signalling toolkit, triggered by AD, can be given by microarray analysis on human brains [3]. Indeed, changes in gene

expression associated with Ca^{2+} signalling toolkit have been highly observed in AD human brains [121]. Especially, these results support the idea of a general Ca^{2+} deregulation in AD, thus to confirm the calcium hypothesis. However, it should be pointed out that these results cannot discriminate between neurons and glia, but refer to the total brain. The comparison of astrocytes from the temporal cortex of patients with different Braak stages, revealed the decrease of 32 genes involved in the Ca^{2+} signalling pathway (as classified by Kyoto Encyclopaedia of Genes and Genomes, KEGG) in the late stages of the disease. These genes included CaMKII isoforms, RyRs, InsP3Rs and Ca^{2+}-ATPases of the plasma membrane. These findings refer to a comparison between earlier and late stages of the disease, due to the impossibility to find control brains [122]. Altered expression of proteins of the Ca^{2+} toolkit, in human AD astrocytes, has also been observed by immunohistochemistry. For example, the Ca^{2+} dependent cysteine protease, calpain-10, has recently been reported to be up-regulated in astrocytes from the temporal cortex of AD brains, but not in neurons [123]. Such effect increases with the disease progression. As calpain-10, other Ca^{2+} toolkit proteins were found up-regulated: mGluR5 [61, 105], calcineurin [124], calsenelin [125], NFκB [61], and NFAT3 [126], while a decrease in EAAT2 [126] has also been observed.

Moving back to primary astrocytes, effects of Aβ on the Ca^{2+} toolkit are not so far from those observed in human brains [3]. A chronical treatment of low concentrations (0.1–100 nM) of $A\beta_{42}$ oligomers, on rat hippocampal and cortical astrocytes, has been shown to promote the up-regulation of nicotinic acetylcholine receptors α7nAChR, α4nAChR, and β2nAChR, effect mediated at the transcriptional level [127]. Similar up-regulation of the α7nAChR subunit has been found also by PCR and immunohistochemistry in AD astrocytes from human brains [128-130]. The increased DHPG Ca^{2+} response, described before, can be explained by the increased mRNA levels, as well as proteins levels, of mGluR5 receptor and its downstream targets InsP3R1 and InsP3R2 observed in astrocytes treated with Aβ

[61, 105, 106]. mGluR5 increase has been detected also in plaque-associated astrocytes of a mutant PS1 mouse [131], as well as in post-mortem AD human brains [106]. Furthermore, also the increased SOCE in Aβ treated astrocytes can be better understood by transcriptional effects of Aβ on the expression of genes involved in this mechanism. Indeed, Aβ treatment has been reported to up-regulates Orai channels in rat hippocampal astrocytes [113]. Somewhat intriguing is the involvement of calcineurin (CaN) in Aβ transcriptional effects. Indeed, CaN overexpression has been observed in astrocytes from an AD mouse model [124], as well as in human brains [106]. CaN is a Ca^{2+}-dependent phosphatase, activated by small long-lasting increases in $[Ca^{2+}]i$ [132, 133] and the inhibition of this enzyme has been shown to block the up-regulation of InsP3R and mGluR5 induced by Aβ [106, 124]. It should be acknowledge that in vivo studies, where the CaN inhibitor FK506 was administered to APP/PS1 and Tg2576 mice models, have demonstrated that CaN inhibition was able to increases neuronal spine density, as well as dendritic arborization [134, 135]. Such inhibition could also preserves the postsynaptic density [136] and improves the mice performaces in the novel object recognition test [137]. The effects of Aβ on InsP3Rs and mGluR5 have been proposed to follow the classical pathway CaN-NFAT [126] or the non canonical one CaN-NFκB [106]. The former is supported by in vivo studies where the administration of the adenoviral vector inducing the expression of VIVIT (which disrupt the CaN/NFAT signalling) in astrocytes, was able to improve synaptic plasticity as well as cognitive function and to reduce Aβ load in APP/PS1 AD mice model [138]. The latter is supported by in vitro studies on rat hippocampal astrocytes where the inhibition of CaN, as well as the inhibition of NFκB was able to revert the up-regulation of mGluR5 and InsP3R2 induced by $Aβ_{42}$ treatment. Moreover, NFκB inhibition have no effect on Aβ triggered InsP3R1 over-expression, while it can be abolished by CaN inhibition, thus to confirm the co-existence of different pathways which might be regulated by Aβ [106].

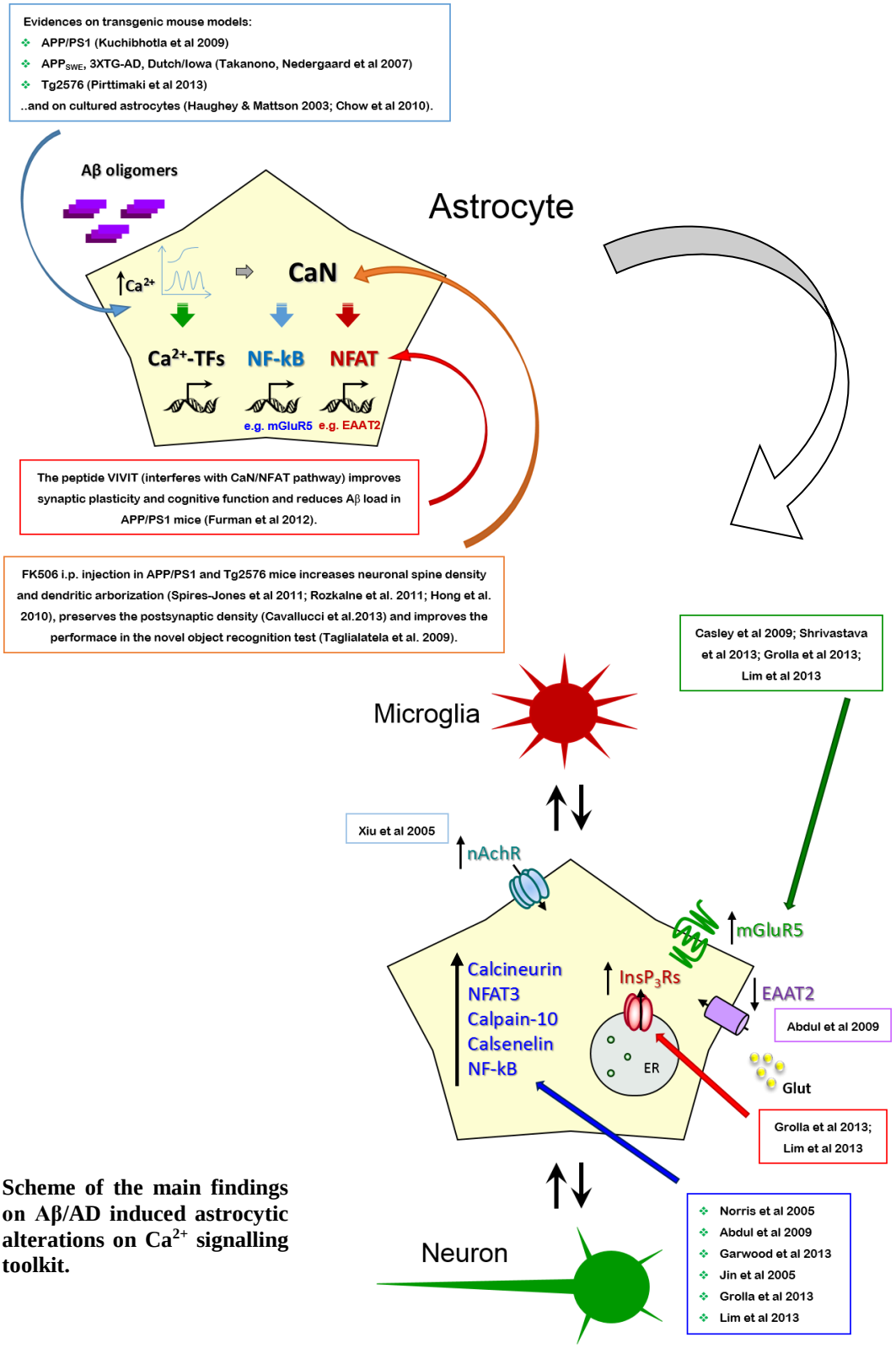

Scheme of the main findings on Aβ/AD induced astrocytic alterations on Ca^{2+} signalling toolkit.

It should be acknowledged that part of this introduction is taken from the review "Glial Calcium Signalling in Alzheimer's Disease" Lim D, Ronco V, Grolla AA, Verkhratsky A, Genazzani AA. Rev Physiol Biochem Pharmacol. 2014.

References

[1]. Mattson MP. Pathways towards and away from Alzheimer's disease. Nature. 2004 Aug 5;430(7000):631-9.

[2]. A.D.A.M. Medical Encyclopedia

[3]. Lim D, Ronco V, Grolla AA, Verkhratsky A, Genazzani AA. Glial Calcium Signalling in Alzheimer's Disease. Rev Physiol Biochem Pharmacol. 2014 Jun 17. [Epub ahead of print]

[4]. Martin JB. The integration of neurology, psychiatry, and neuroscience in the 21st century. Am J Psychiatry. 2002 May;159(5):695-704.

[5]. Selkoe DJ, Schenk D. Alzheimer's disease: molecular understanding predicts amyloid-based therapeutics. Annu Rev Pharmacol Toxicol. 2003;43:545-84. Epub 2002 Jan 10.

[6]. Dickson DW. Neuropathological diagnosis of Alzheimer's disease: a perspective from longitudinal clinicopathological studies. Neurobiol Aging. 1997 Jul-Aug;18(4 Suppl):S21-6.

[7]. Hardy J, Selkoe DJ. The amyloid hypothesis of Alzheimer's disease: progress and problems on the road to therapeutics. Science. 2002 Jul 19;297(5580):353-6.

[8]. Vassar R, Bennett BD, Babu-Khan S, Kahn S, Mendiaz EA, Denis P, Teplow DB, Ross S, Amarante P, Loeloff R, Luo Y, Fisher S, Fuller J, Edenson S, Lile J, Jarosinski MA, Biere AL, Curran E, Burgess T, Louis JC, Collins F, Treanor J, Rogers G, Citron M. Beta-secretase cleavage of Alzheimer's amyloid precursor protein by the transmembrane aspartic protease BACE. Science. 1999 Oct 22;286(5440):735-41.

[9]. Tischer E, Cordell B. Beta-amyloid precursor protein. Location of transmembrane domain and specificity of gamma-secretase cleavage. J Biol Chem. 1996 Sep 6;271(36):21914-9.

[10]. Shoji M, Golde TE, Ghiso J, Cheung TT, Estus S, Shaffer LM, Cai XD, McKay DM, Tintner R, Frangione B, et al. Production of the Alzheimer amyloid beta protein by normal proteolytic processing. Science. 1992 Oct 2;258(5079):126-9.

[11]. Kuhn PH, Wang H, Dislich B, Colombo A, Zeitschel U, Ellwart JW, Kremmer E, Rossner S, Lichtenthaler SF. ADAM10 is the physiologically relevant, constitutive alpha-secretase of the amyloid precursor protein in primary neurons. EMBO J. 2010 Sep 1;29(17):3020-32.

[12]. Klyubin I, Cullen WK, Hu NW, Rowan MJ. Alzheimer's disease Aβ assemblies mediating rapid disruption of synaptic plasticity and memory. Mol Brain. 2012 Jul 17;5:25. doi: 10.1186/1756-6606-5-25.

[13]. Glabe CG. Structural classification of toxic amyloid oligomers. J Biol Chem. 2008 Oct 31;283(44):29639-43.

[14]. Oddo S, Caccamo A, Shepherd JD, Murphy MP, Golde TE, Kayed R, Metherate R, Mattson MP, Akbari Y, LaFerla FM (2003) Triple-transgenic model of Alzheimer's disease with plaques and tangles: intracellular Ab and synaptic dysfunction. Neuron 39:409-21

[15]. Sorrentino P, Iuliano A, Polverino A, Jacini F, Sorrentino G. The dark sides of amyloid in Alzheimer's disease pathogenesis. FEBS Lett. 2014 Mar 3;588(5):641-52.

[16]. Selkoe DJ (2001) Alzheimer's disease: genes, proteins, and therapy. Physiol Rev 81:741-66

[17]. Plant LD, Boyle JP, Smith IF, Peers C, Pearson HA (2003) The production of amyloid β peptide is a critical requirement for the viability of central neurons. J Neurosci 23:5531-5

[18]. LaFerla FM (2002) Calcium dyshomeostasis and intracellular signalling in Alzheimer's disease. Nat Rev Neurosci 3:862-72

[19]. Almeida CG, Takahashi RH, Gouras GK. Beta-amyloid accumulation impairs multivesicular body sorting by inhibiting the ubiquitin-proteasome system. J Neurosci. 2006 Apr 19;26(16):4277-88.

[20]. Tseng BP, Green KN, Chan JL, Blurton-Jones M, LaFerla FM. Abeta inhibits the proteasome and enhances amyloid and tau accumulation. Neurobiol Aging. 2008 Nov;29(11):1607-18. Epub 2007 Jun 1.

[21]. Hsia AY, Masliah E, McConlogue L, Yu GQ et al. (1999) Plaque-independent disruption of neural circuits in Alzheimer's disease mouse models. Proc. Natl. Acad. Sci. 96:3228–3233.

[22]. Chapman PF, White GL, Jones MW, Cooper-Blacketer D et al. (1999) Impaired synaptic plasticity and learning in aged amyloid precursor protein transgenic mice. Nat. Neurosci. 2:271–276.

[23]. Walsh DM, Klyubin I, Fadeeva JV, Cullen WK et al. (2002) Naturally secreted oligomers of amyloid β protein potently inhibit hippocampal long-term potentiation *in vivo*. Nature. 16:535–539.

[24]. Kamenetz F, Tomita T, Hsieh H, Seabrook G, Borchelt D, Iwatsubo T, Sisodia S, Malinow R (2003) APP processing and synaptic function. Neuron 37:925-37

[25]. Kullmann DM, Lamsa KP. Long-term synaptic plasticity in hippocampal interneurons. Nat Rev Neurosci. 2007 Sep;8(9):687-99.

[26]. Li S, Hong S, Shepardson NE, Walsh DM et al. (2009) Soluble oligomers of amyloid β protein facilitate hippocampal long-term depression by disrupting neuronal glutamate uptake. Neuron. 62:788–801.

[27]. Berridge MJ, Lipp P, Bootman MD (2000) The versatility and universality of calcium signalling. Nat Rev Mol Cell Biol 1:11-21

[28]. Thibault et al., 2007 O. Thibault, J.C. Gant, P.W. Landfield Expansion of the calcium hypothesis of brain aging and Alzheimer's disease: minding the store Aging Cell, 6 (2007), pp. 307–317

[29] Khachaturian ZS. Hypothesis on the regulation of cytosol calcium concentration and the aging brain. Neurobiol Aging. 1987 Jul-Aug;8(4):345-6.

[30]. Landfield PW (1987) 'Increased calcium-current' hypothesis of brain aging. Neurobiol Aging 8:346-7

[31]. Supnet and Bezprozvanny, 2010 C. Supnet, I. Bezprozvanny The dysregulation of intracellular calcium in Alzheimer disease Cell Calcium, 47 (2010), pp. 183–189

[32]. Demuro A, Mina E, Kayed R, Milton SC, Parker I, Glabe CG. Calcium dysregulation and membrane disruption as a ubiquitous neurotoxic mechanism of soluble amyloid oligomers. J Biol Chem. 2005 Apr 29;280(17):17294-300. Epub 2005

[33]. Mark RJ, Lovell MA, Markesbery WR, Uchida K, Mattson MP (1997) A role for 4-hydroxynonenal, an aldehydic product of lipid peroxidation, in disruption of ion homeostasis and neuronal death induced by amyloid beta-peptide. J Neurochem 68:255-64

[34]. Arispe N, Rojas E, Pollard HB (1993) Alzheimer disease amyloid beta protein forms calcium channels in bilayer membranes: blockade by tromethamine and aluminum. Proc Natl Acad Sci U S A 90:567-71

[35]. Lashuel HA, Hartley D, Petre BM, Walz T, Lansbury PT, Jr. (2002) Neurodegenerative disease: amyloid pores from pathogenic mutations. Nature 418:291

[36]. Demuro A, Smith M, Parker I. Single-channel $Ca(^{2+})$ imaging implicates Aβ1-42 amyloid pores in Alzheimer's disease pathology. J Cell Biol. 2011 Oct 31;195(3):515-24.

[37] Johnson RD, Schauerte JA, Wisser KC, Gafni A, Steel DG. Direct observation of single amyloid-β(1-40) oligomers on live cells: binding and growth at physiological concentrations. PLoS One. 2011;6(8):e23970.

[38]. Inoue S. In situ Abeta pores in AD brain are cylindrical assembly of Abeta protofilaments. Amyloid. 2008 Dec;15(4):223-33.

[39]. Demuro A, Parker I, Stutzmann GE (2010) Calcium signaling and amyloid toxicity in Alzheimer disease. J Biol Chem 285:12463-8

[40]. Wang HY, Bakshi K, Shen C, Frankfurt M, Trocmé-Thibierge C, Morain P. S 24795 limits beta-amyloid-alpha7 nicotinic receptor interaction and reduces Alzheimer's disease-like pathologies. Biol Psychiatry. 2010 Mar 15;67(6):522-30

[41]. Lilja AM, Porras O, Storelli E, Nordberg A, Marutle A. Functional interactions of fibrillar and oligomeric amyloid-β with alpha7 nicotinic receptors in Alzheimer's disease. J Alzheimers Dis. 2011;23(2):335-47.

[42]. Wu MN, Li XY, Guo F, Qi JS. Involvement of nicotinic acetylcholine receptors in amyloid β-fragment-induced intracellular Ca($^{2+}$) elevation in cultured rat cortical neurons. Sheng Li Xue Bao. 2009 Dec 25;61(6):517-25.

[43]. Ye C, Walsh DM, Selkoe DJ, Hartley DM. Amyloid beta-protein induced

[44]. Ferreira IL, Bajouco LM, Mota SI, Auberson YP, Oliveira CR, Rego AC. Amyloid beta peptide 1-42 disturbs intracellular calcium homeostasis through activation of GluN2B-containing N-methyl-d-aspartate receptors in cortical cultures. Cell Calcium. 2012

[45]. Lee S, Zemianek J, Shea TB. Rapid, reversible impairment of synaptic signalling in cultured cortical neurons by exogenously-applied amyloid-β. J Alzheimers Dis. 2013;35(2):395-402.

[46]. Shtifman A, Ward CW, Laver DR, Bannister ML, Lopez JR, Kitazawa M, LaFerla FM, Ikemoto N, Querfurth HW (2010) Amyloid-beta protein impairs Ca^{2+} release and contractility in skeletal muscle. Neurobiol Aging 31:2080-90

[47]. Stutzmann GE, Mattson MP (2011) Endoplasmic reticulum Ca^{2+} handling in excitable cells in health and disease. Pharmacol Rev 63:700-27

[48]. Guo Q, Sebastian L, Sopher BL, Miller MW, Ware CB, Martin GM, Mattson MP.Increased vulnerability of hippocampal neurons from presenilin-1 mutant knock-in mice to amyloid beta-peptide toxicity: central roles of superoxide production and caspase activation. J Neurochem. 1999 Mar;72(3):1019-29.

[49]. Keller JN, Guo Q, Holtsberg FW, Bruce-Keller AJ, Mattson MP. Increased sensitivity to mitochondrial toxin-induced apoptosis in neural cells expressing mutant presenilin-1 is linked to perturbed calcium homeostasis and enhanced oxyradical production. J Neurosci. 1998 Jun 15;18(12):4439-50.

[50]. Cheung KH, Shineman D, Muller M, Cardenas C, Mei L, Yang J, Tomita T, Iwatsubo T, Lee VM, Foskett JK (2008) Mechanism of Ca^{2+} disruption in Alzheimer's disease by presenilin regulation of $InsP_3$ receptor channel gating. Neuron 58:871-83

[51]. Goussakov I, Miller MB, Stutzmann GE (2010) NMDA-mediated Ca^{2+} influx drives aberrant ryanodine receptor activation in dendrites of young Alzheimer's disease mice. J Neurosci 30:12128-37

[52]. Hammadi M, Oulidi A, Gackiere F, Katsogiannou M, Slomianny C, Roudbaraki M, Dewailly E, Delcourt P, Lepage G, Lotteau S, Ducreux S, Prevarskaya N, Van Coppenolle F (2013) Modulation of ER stress and apoptosis by endoplasmic reticulum calcium leak via translocon during unfolded protein response: involvement of GRP78. FASEB J 27:1600-9

[53]. Lang S, Erdmann F, Jung M, Wagner R, Cavalie A, Zimmermann R (2011) Sec61 complexes form ubiquitous ER Ca2+ leak channels. Channels (Austin) 5:228-35

[54]. Nelson O, Tu H, Lei T, Bentahir M, de Strooper B, Bezprozvanny I (2007) Familial Alzheimer disease-linked mutations specifically disrupt Ca^{2+} leak function of presenilin 1. J Clin Invest 117:1230-9

[55]. Tu H, Nelson O, Bezprozvanny A, Wang Z, Lee SF, Hao YH, Serneels L, De Strooper B, Yu G, Bezprozvanny I (2006) Presenilins form ER Ca^{2+} leak channels, a function disrupted by familial Alzheimer's disease-linked mutations. Cell 126:981-93

[56]. Shilling D, Mak DO, Kang DE, Foskett JK (2012) Lack of evidence for presenilins as endoplasmic reticulum Ca2+ leak channels. J Biol Chem 287:10933-44

[57]. Chan SL, Mayne M, Holden CP, Geiger JD, Mattson MP (2000) Presenilin-1 mutations increase levels of ryanodine receptors and calcium release in PC12 cells and cortical neurons. J Biol Chem 275:18195-200

[58]. Smith IF, Hitt B, Green KN, Oddo S, LaFerla FM (2005) Enhanced caffeine-induced Ca^{2+} release in the 3xTg-AD mouse model of Alzheimer's disease. J Neurochem 94:1711-8

[59]. Zhang H, Sun S, Herreman A, De Strooper B, Bezprozvanny I (2010) Role of presenilins in neuronal calcium homeostasis. J Neurosci 30:8566-80

[60]. Stutzmann GE, Smith I, Caccamo A, Oddo S, Laferla FM, Parker I (2006) Enhanced ryanodine receptor recruitment contributes to Ca^{2+} disruptions in young, adult, and aged Alzheimer's disease mice. J Neurosci 26:5180-9

[61]. Grolla AA, Fakhfouri G, Balzaretti G, Marcello E, Gardoni F, Canonico PL, DiLuca M, Genazzani AA, Lim D (2013a) Ab leads to Ca^{2+} signaling alterations and transcriptional changes in glial cells. Neurobiol Aging 34:511-22

[62]. Demuro A, Parker I. Cytotoxicity of intracellular aβ42 amyloid oligomers involves Ca2+ release from the endoplasmic reticulum by stimulated production of inositol trisphosphate. J Neurosci. 2013 Feb 27;33(9):3824-33.

[63]. Virchow R. Cellular pathology. As based upon physiological and pathological histology. Lecture XVI--Atheromatous affection of arteries. 1858. Nutr Rev. 1989 Jan;47(1):23-5.

[64]. Lugaro E (1907) Sulle Funzioni della Nevroglia. Rivista di Patologia Nervosa e Mentale.

[65]. Verkhratsky A and Butt A, Glial Neurobiology -a textbook- Wiley

[66]. Kimelberg HK, Schools GP, Cai Z, Zhou M. Freshly isolated astrocyte (FIA)preparations: a useful single cell system for studying astrocyte properties. J Neurosci Res. 2000 Sep 15;61(6):577-87.

[67]. Sanz JM, Chiozzi P, Ferrari D, Colaianna M, Idzko M, Falzoni S, Fellin R,Trabace L, Di Virgilio F. Activation of microglia by amyloid {beta} requires P2X7 receptor expression. J Immunol. 2009 Apr 1;182(7):4378-85.

[68]. Delarasse C, Auger R, Gonnord P, Fontaine B, Kanellopoulos JM. The purinergic receptor P2X7 triggers alpha-secretase-dependent processing of the amyloid precursor protein. J Biol Chem. 2011 Jan 28;286(4):2596-606.

[69]. Parvathenani LK, Tertyshnikova S, Greco CR, Roberts SB, Robertson B, Posmantur R. P2X7 mediates superoxide production in primary microglia and is up-regulated in a transgenic mouse model of Alzheimer's disease. J Biol Chem. 2003 Apr 11;278(15):13309-17.

[70]. Agulhon C, Sun MY, Murphy T, Myers T, Lauderdale K, Fiacco TA. Calcium Signaling and Gliotransmission in Normal vs. Reactive Astrocytes. Front Pharmacol. 2012 Jul 13;3:139.

[71]. Paoletti R., Nicosia S., Clementi F., Fumagalli G. Farmacologia Generale e Molecolare –textbook- UTET

[72]. Agulhon C, Petravicz J, McMullen AB, Sweger EJ, Minton SK, Taves SR, Casper KB, Fiacco TA, McCarthy KD. What is the role of astrocyte calcium in neurophysiology? Neuron. 2008 Sep 25;59(6):932-46.

[73]. Takano T, Tian GF, Peng W, Lou N, Libionka W, Han X, Nedergaard M. Astrocyte-mediated control of cerebral blood flow. Nat Neurosci. 2006 Feb;9(2):260-7.

[74]. Fan YY, Zhang JM, Wang H, Liu XY, Yang FH. Leukemia inhibitory factor inhibits the proliferation of primary rat astrocytes induced by oxygen-glucose deprivation. Acta Neurobiol Exp (Wars). 2013;73(4):485-94.

[75]. Simard M, Nedergaard M. The neurobiology of glia in the context of water and ion homeostasis. Neuroscience. 2004;129(4):877-96.

[76]. Sattler R, Rothstein JD. Regulation and dysregulation of glutamate transporters. Handb Exp Pharmacol. 2006;(175):277-303.

[77]. Seifert G, Schilling K, Steinhäuser C. Astrocyte dysfunction in neurological disorders: a molecular perspective. Nat Rev Neurosci. 2006 Mar;7(3):194-206.

[78]. Brusilow SW, Koehler RC, Traystman RJ, Cooper AJ (2010) Astrocyte glutamine synthetase: importance in hyperammonemic syndromes and potential target for therapy. Neurotherapeutics 7:452-70

[79]. Butterworth RF (2010) Altered glial-neuronal crosstalk: cornerstone in the pathogenesis of hepatic encephalopathy. Neurochem Int 57:383-8

[80]. Verkhratsky A, Rodriguez JJ, Parpura V (2013) Astroglia in neurological diseases. Future Neurol 8:149-158

[81]. Yin Z, Milatovic D, Aschner JL, Syversen T, Rocha JB, Souza DO, Sidoryk M, Albrecht J, Aschner M (2007) Methylmercury induces oxidative injury, alterations in permeability and glutamine transport in cultured astrocytes. Brain Res 1131:1-10

[82]. Hazell AS, Sheedy D, Oanea R, Aghourian M, Sun S, Jung JY, Wang D, Wang C (2009) Loss of astrocytic glutamate transporters in Wernicke encephalopathy. Glia 58:148-156

[83]. Rossi D, Volterra A (2009) Astrocytic dysfunction: Insights on the role in neurodegeneration. Brain Res Bull 80:224-232

[84]. Valori CF, Brambilla L, Martorana F, Rossi D (2014) The multifaceted role of glial cells in amyotrophic lateral sclerosis. Cell Mol Life Sci 71:287-97

[85]. Staats KA, Van Den Bosch L (2009) Astrocytes in amyotrophic lateral sclerosis: direct effects on motor neuron survival. J Biol Phys 35:337-46

[86]. Yamanaka K, Chun SJ, Boillee S, Fujimori-Tonou N, Yamashita H, Gutmann DH, Takahashi R, Misawa H, Cleveland DW (2008) Astrocytes as determinants of disease progression in inherited amyotrophic lateral sclerosis. Nat Neurosci 11:251-3

[87]. Bradford J, Shin JY, Roberts M, Wang CE, Sheng G, Li S, Li XJ (2010) Mutant huntingtin in glial cells exacerbates neurological symptoms of Huntington disease mice. J Biol Chem 285:10653-61

[88]. Broe M, Kril J, Halliday GM (2004) Astrocytic degeneration relates to the severity of disease in frontotemporal dementia. Brain 127:2214-20

[89]. Kersaitis C, Halliday GM, Kril JJ (2004) Regional and cellular pathology in frontotemporal dementia: relationship to stage of disease in cases with and without Pick bodies. Acta Neuropathol 108:515-23

[90]. Potts R, Leech RW (2005) Thalamic dementia: an example of primary astroglial dystrophy of Seitelberger. Clin Neuropathol 24:271-5

[91]. Beauquis J, Pavia P, Pomilio C, Vinuesa A, Podlutskaya N, Galvan V, Saravia F (2013) Environmental enrichment prevents astroglial pathological changes in the hippocampus of APP transgenic mice, model of Alzheimer's disease. Exp Neurol 239:28-37.

[92]. Kulijewicz-Nawrot M, Verkhratsky A, Chvatal A, Sykova E, Rodriguez JJ (2012) Astrocytic cytoskeletal atrophy in the medial prefrontal cortex of a triple transgenic mouse model of Alzheimer's disease. J Anat 221:252-62

[93]. Olabarria M, Noristani HN, Verkhratsky A, Rodriguez JJ (2010) Concomitant astroglial atrophy and astrogliosis in a triple transgenic animal model of Alzheimer's disease. Glia 58:831-838

[94]. Yeh CY, Vadhwana B, Verkhratsky A, Rodriguez JJ (2011) Early astrocytic atrophy in the entorhinal cortex of a triple transgenic animal model of Alzheimer's disease. ASN Neuro 3:271-9

[95]. Parpura V, Heneka MT, Montana V, Oliet SH, Schousboe A, Haydon PG, Stout RF Jr, Spray DC, Reichenbach A, Pannicke T, Pekny M, Pekna M, Zorec R, Verkhratsky A. Glial cells in (patho)physiology. J Neurochem. 2012 Apr;121(1):4-27. doi: 10.1111/j.1471-4159.2012.07664.x. Epub 2012 Feb 2.

[96]. Sofroniew MV. Molecular dissection of reactive astrogliosis and glial scar formation. Trends Neurosci. 2009 Dec;32(12):638-47. doi: 10.1016/j.tins.2009.08.002. Epub 2009 Sep 24.

[97]. Verkhratsky A, Sofroniew MV, Messing A, deLanerolle NC, Rempe D, Rodríguez JJ, Nedergaard M. Neurological diseases as primary gliopathies: a reassessment of neurocentrism. ASN Neuro. 2012 Apr 5;4(3).

[98]. Giaume C, Kirchhoff F, Matute C, Reichenbach A, Verkhratsky A. Glia: the fulcrum of brain diseases. Cell Death Differ. 2007 Jul;14(7):1324-35. Epub 2007

[99]. Alberdi E, Wyssenbach A, Alberdi M, Sanchez-Gomez MV, Cavaliere F, Rodriguez JJ, Verkhratsky A, Matute C (2013) Ca^{2+} -dependent endoplasmic reticulum stress correlates with astrogliosis in oligomeric amyloid b-treated astrocytes and in a model of Alzheimer's disease. Aging Cell 12:292-302

[100]. Chow SK, Yu D, Macdonald CL, Buibas M, Silva GA (2010) Amyloid b-peptide directly induces spontaneous calcium transients, delayed intercellular calcium waves and gliosis in rat cortical astrocytes. ASN Neuro 2:e00026

[101]. Jalonen TO, Charniga CJ, Wielt DB (1997) β-Amyloid peptide-induced morphological changes coincide with increased K^+ and Cl^- channel activity in rat cortical astrocytes. Brain Res 746:85-97

[102]. Stix B, Reiser G (1998) b-amyloid peptide 25-35 regulates basal and hormone-stimulated Ca^{2+} levels in cultured rat astrocytes. Neurosci Lett 243:121-4

[103]. Abramov AY, Canevari L, Duchen MR (2003) Changes in intracellular calcium and glutathione in astrocytes as the primary mechanism of amyloid neurotoxicity. J Neurosci 23:5088-95

[104]. Abramov AY, Canevari L, Duchen MR (2004) Calcium signals induced by amyloid b peptide and their consequences in neurons and astrocytes in culture. Biochim Biophys Acta 1742:81-7

[105]. Casley CS, Lakics V, Lee HG, Broad LM, Day TA, Cluett T, Smith MA, O'Neill MJ, Kingston AE (2009) Up-regulation of astrocyte metabotropic glutamate receptor 5 by amyloid-beta peptide. Brain Res.

[106]. Lim D, Iyer A, Ronco V, Grolla AA, Canonico PL, Aronica E, Genazzani AA (2013) Amyloid beta deregulates astroglial mGluR5-mediated calcium signaling via calcineurin and Nf-kB. Glia 61:1134-45

[107]. Toivari E, Manninen T, Nahata AK, Jalonen TO, Linne ML (2011) Effects of transmitters and amyloid-beta peptide on calcium signals in rat cortical astrocytes: Fura-2AM measurements and stochastic model simulations. PLoS One 6:e17914

[108]. Lee L, Kosuri P, Arancio O (2014) Picomolar amyloid-b peptides enhance spontaneous astrocyte calcium transients. J Alzheimers Dis 38:49-62

[109]. Koffie RM, Meyer-Luehmann M, Hashimoto T, Adams KW, Mielke ML, Garcia-Alloza M, Micheva KD, Smith SJ, Kim ML, Lee VM, Hyman BT, Spires-Jones TL (2009) Oligomeric amyloid beta associates with postsynaptic densities and correlates with excitatory synapse loss near senile plaques. Proc Natl Acad Sci U S A 106:4012-7

[110]. Haughey NJ, Mattson MP (2003) Alzheimer's amyloid □-peptide enhances ATP/gap junction-mediated calcium-wave propagation in astrocytes. Neuromolecular Med 3:173-80

[111]. Meske V, Hamker U, Albert F, Ohm TG (1998) The effects of b/A4-amyloid and its fragments on calcium homeostasis, glial fibrillary acidic protein and S100b staining, morphology and survival of cultured hippocampal astrocytes. Neuroscience 85:1151-60

[112]. Grolla AA, Sim JA, Lim D, Rodriguez JJ, Genazzani AA, Verkhratsky A (2013b) Amyloid-β and Alzheimer's disease type pathology differentially affects the calcium signalling toolkit in astrocytes from different brain regions. Cell Death Dis 4:e623

[113]. Ronco V, Grolla AA, Glasnov TN, Canonico PL, Verkhratsky A, Genazzani AA, Lim D (2014) Differential deregulation of astrocytic calcium signalling by amyloid-β, TNFα, IL-1β and LPS. Cell Calcium, in press

[114]. Kanemaru K, Kubota J, Sekiya H, Hirose K, Okubo Y, Iino M (2013) Calcium-dependent N-cadherin up-regulation mediates reactive astrogliosis and neuroprotection after brain injury. Proc Natl Acad Sci U S A 110:11612-7

[115]. Linde CI, Baryshnikov SG, Mazzocco-Spezzia A, Golovina VA (2011) Dysregulation of Ca^{2+} signaling in astrocytes from mice lacking amyloid precursor protein. Am J Physiol Cell Physiol 300:C1502-12

[116]. Bambrick LL, Golovina VA, Blaustein MP, Yarowsky PJ, Krueger BK (1997) Abnormal calcium homeostasis in astrocytes from the trisomy 16 mouse. Glia 19:352-8.

[117]. Pirttimaki TM, Codadu NK, Awni A, Pratik P, Nagel DA, Hill EJ, Dineley KT, Parri HR (2013) a7 Nicotinic receptor-mediated astrocytic gliotransmitter release: Ab effects in a preclinical Alzheimer's mouse model. PLoS One 8:e81828

[118]. Riera J, Hatanaka R, Uchida T, Ozaki T, Kawashima R (2011) Quantifying the uncertainty of spontaneous Ca^{2+} oscillations in astrocytes: particulars of Alzheimer's disease. Biophys J 101:554-64

[119]. Kuchibhotla KV, Lattarulo CR, Hyman BT, Bacskai BJ (2009) Synchronous hyperactivity and intercellular calcium waves in astrocytes in Alzheimer mice. Science 323:1211-5

[120]. Takano T, Han X, Deane R, Zlokovic B, Nedergaard M (2007) Two-photon imaging of astrocytic Ca^{2+} signaling and the microvasculature in experimental mice models of Alzheimer's disease. Ann N Y Acad Sci 1097:40-50

[121]. Cooper-Knock J, Kirby J, Ferraiuolo L, Heath PR, Rattray M, Shaw PJ (2012) Gene expression profiling in human neurodegenerative disease. Nat Rev Neurol 8:518-30

[122]. Simpson JE, Ince PG, Shaw PJ, Heath PR, Raman R, Garwood CJ, Gelsthorpe C, Baxter L, Forster G, Matthews FE, Brayne C, Wharton SB, Function MRCC, Ageing Neuropathology Study G (2011) Microarray analysis of the astrocyte transcriptome in the aging brain: relationship to Alzheimer's pathology and APOE genotype. Neurobiol Aging 32:1795-807

[123]. Garwood C, Faizullabhoy A, Wharton SB, Ince PG, Heath PR, Shaw PJ, Baxter L, Gelsthorpe C, Forster G, Matthews FE, Brayne C, Simpson JE, Function MRCC, Ageing Neuropathology Study G (2013) Calcium dysregulation in relation to Alzheimer-type pathology in the ageing brain. Neuropathol Appl Neurobiol 39:788-99

[124]. Norris CM, Kadish I, Blalock EM, Chen KC, Thibault V, Porter NM, Landfield PW, Kraner SD (2005) Calcineurin triggers reactive/inflammatory processes in astrocytes and is upregulated in aging and Alzheimer's models. J Neurosci 25:4649-58

[125]. Jin JK, Choi JK, Wasco W, Buxbaum JD, Kozlowski PB, Carp RI, Kim YS, Choi EK (2005) Expression of calsenilin in neurons and astrocytes in the Alzheimer's disease brain. Neuroreport 16:451-5

[126]. Abdul HM, Sama MA, Furman JL, Mathis DM, Beckett TL, Weidner AM, Patel ES, Baig I, Murphy MP, LeVine H, 3rd, Kraner SD, Norris CM (2009) Cognitive decline in Alzheimer's disease is associated with selective changes in calcineurin/NFAT signaling. J Neurosci 29:12957-69

[127]. Xiu J, Nordberg A, Zhang JT, Guan ZZ (2005) Expression of nicotinic receptors on primary cultures of rat astrocytes and up-regulation of the α7, α4 and α2 subunits in response to nanomolar concentrations of the b-amyloid peptide$_{1-42}$. Neurochem Int 47:281-90

[128]. Hellstrom-Lindahl E, Mousavi M, Zhang X, Ravid R, Nordberg A (1999) Regional distribution of nicotinic receptor subunit mRNAs in human brain: comparison between Alzheimer and normal brain. Brain Res Mol Brain Res 66:94-103

[129]. Teaktong T, Graham A, Court J, Perry R, Jaros E, Johnson M, Hall R, Perry E (2003) Alzheimer's disease is associated with a selective increase in a7 nicotinic acetylcholine receptor immunoreactivity in astrocytes. Glia 41:207-11

[130]. Yu WF, Guan ZZ, Bogdanovic N, Nordberg A (2005) High selective expression of a7 nicotinic receptors on astrocytes in the brains of patients with sporadic Alzheimer's disease and patients carrying Swedish APP 670/671 mutation: a possible association with neuritic plaques. Exp Neurol 192:215-25

[131]. Shrivastava AN, Kowalewski JM, Renner M, Bousset L, Koulakoff A, Melki R, Giaume C, Triller A (2013) b-amyloid and ATP-induced diffusional trapping of astrocyte and neuronal metabotropic glutamate type-5 receptors. Glia 61:1673-86

[132]. Dolmetsch RE, Lewis RS, Goodnow CC, Healy JI (1997) Differential activation of transcription factors induced by Ca2+ response amplitude and duration. Nature 386:855-8

[133]. Klee CB, Ren H, Wang X (1998) Regulation of the calmodulin-stimulated protein phosphatase, calcineurin. J Biol Chem 273:13367-70

[134]. Rozkalne A, Hyman BT, Spires-Jones TL. Calcineurin inhibition with FK506 ameliorates dendritic spine density deficits in plaque-bearing Alzheimer model mice. Neurobiol Dis. 2011 Mar;41(3):650-4.

[135]. Hong HS, Hwang JY, Son SM, Kim YH, Moon M, Inhee MJ. FK506 reduces amyloid plaque burden and induces MMP-9 in AβPP/PS1 double transgenic mice. J Alzheimers Dis. 2010;22(1):97-105.

[136]. Cavallucci V, Berretta N, Nobili A, Nisticò R, Mercuri NB, D'Amelio M.Calcineurin inhibition rescues early synaptic plasticity deficits in a mouse model of Alzheimer's disease. Neuromolecular Med. 2013 Sep;15(3):541-8.

[137]. Taglialatela G, Hogan D, Zhang WR, Dineley KT. Intermediate- and long-term recognition memory deficits in Tg2576 mice are reversed with acute calcineurin inhibition. Behav Brain Res. 2009 Jun 8;200(1):95-9.

[138]. Furman JL, Sama DM, Gant JC, Beckett TL, Murphy MP, Bachstetter AD, Van Eldik LJ, Norris CM (2012) Targeting astrocytes ameliorates neurologic changes in a mouse model of Alzheimer's disease. J Neurosci 32:16129-40

Chapter 2

Outline of the thesis

Among the different forms of dementia, the most common one is Alzheimer's disease (AD), which affects worldwide an increasing number of people in the old age, but not only. Modern therapies are able to slow down the symptoms of AD, but they're armless in contrasting the disease devastating progression. Furthermore, many hypotheses on AD aetiology have been proposed, but the molecular pathogenesis of AD is still a matter of debate. The most accredited one is the "Amyloid Hypothesis", which believes in the amyloid-β oligomers accumulation as the starting cause of neuronal degeneration. Furthermore, altered calcium homeostasis and signalling have been observed, which are connected to altered gene expression and excitotoxic cell death. In recent years, the neurocentric view of AD has changed and glia has emerged as a key actor in the disease development and progression. The outline of this thesis is to explore the role of glia, or better the role of astrocytes, in the early stages of AD. Indeed, the study of the interplay between neurons and glia can be a rising way in AD understanding. According to the primary role of glutamate in astrocytic communications, we focused on glutamate signalling through the metabotropic receptor mGluR5, demonstrating that the receptor itself, as well as its downstream targets, the InsP3 receptors, are up-regulated in primary astrocytes treated with nanomolar $A\beta_{42}$ oligomers concentration. This effect is mediated by calcineurin and NFκB activation and is a consequence of the calcium homeostasis perturbation. Moreover, the active state of astrocytes surrounding the amyloid plaques has been observed also in human AD brains. Because of astrogliosis is a hallmark of neuroinflammation, we next investigated if the effects of Aβ, just described, were something peculiar of Aβ or an inflammatory environment could trigger the same alterations too. For this purpose, we compared the effects of $A\beta_{42}$ oligomers on mGluR5 and InsP3Rs, as well as on calcium perturbation, with those induced by classical pro-inflammatory stimuli. We demonstrated that $A\beta_{42}$ and pro-

inflammatory stimuli behaviour is just the opposite, thus to suggest specific pathways associated with Aβ triggered perturbations.

Chapter 3

Amyloid beta deregulates astroglial mGluR5-mediated calcium signaling via calcineurin and NF-kB

Dmitry Lim[1], Anand Iyer[2], Virginia Ronco[1], Ambra A Grolla[1], Pier Luigi Canonico[1], Eleonora Aronica[2,3,4], Armando A Genazzani[1,*]

[1]Department of Pharmaceutical Sciences, Università degli Studi del Piemonte Orientale "Amedeo Avogadro", 28100, Novara, Italy.

[2]Department of (Neuro)Pathology, Academic Medical Center, University of Amsterdam, 1105 AZ Amsterdam, The Netherlands.

[3]SEIN – Stichting Epilepsie Instellingen Nederland, 2100, Heemstede, The Netherlands

[4]Swammerdam Institute for Life Sciences, Center for Neuroscience, University of Amsterdam, 1105 AZ Amsterdam, The Netherlands.

Published in Glia. 2013 Jul. Vol. 61(7):1134-45

Abstract

The amyloid hypothesis of Alzheimer's disease suggests that soluble amyloid β is an initiator of a cascade of events eventually leading to neurodegeneration. Recently, we reported that amyloid β deranged Ca^{2+} homeostasis specifically in hippocampal astrocytes by targeting key elements of Ca^{2+} signaling, such as mGluR5 and IP_3R1. In the present study we dissect a cascade of signaling events by which amyloid β deregulates glial Ca^{2+}: (i) 100 nM amyloid β leads to an increase in cytosolic calcium after 4-6 hours of treatment; (ii) mGluR5 is increased after 24 hours of treatment; (iii) this increase is blocked by inhibitors of calcineurin and NF-kB. Furthermore, we show that amyloid β treatment of glial cells leads to de-phosphorylation of Bcl10 and an increased calcineurin-Bcl10 interaction. Last, mGluR5 staining is augmented in hippocampal astrocytes of Alzheimer's disease patients in proximity of amyloid β plaques and co-localizes with nuclear accumulation of the p65 NF-kB subunit and increased staining of CaNAα. Taken together our data suggest that nanomolar

[amyloid β] deregulates Ca^{2+} homeostasis via calcineurin and its downstream target NF-kB, possibly via the cross-talk of Bcl10 in hippocampal astrocytes.

1. Introduction

Extracellular soluble amyloid β (Aβ) oligomers trigger the so called "amyloid cascade" of events in early Alzheimer's Disease (AD) pathogenesis that, with disease progression, leads to neuronal death with concomitant cognitive disturbances (Hardy and Selkoe, 2002). Yet, the exact mechanism by which Aβ initiates cellular deregulation is still a question of debate (Hardy and Selkoe, 2002).

Deregulation of cellular Ca^{2+} homeostasis has been proposed to play a role in the initial steps of disease progression (Thibault et al, 2007). According to the "calcium hypothesis" of AD, a long lasting overload of the cytoplasm and of the ER with Ca^{2+} induces activation of mechanisms leading to cell death (Supnet and Bezprozvanny, 2010). The exact mechanism by which this occurs is still a matter of debate (Tu et al., 2006; Demuro et al., 2010; Kuchibhotla et al., 2008; Kagan and Thundimadathil, 2010). A number of effectors downstream of Ca^{2+} in AD have been proposed, among which the calcium/calmodulin-dependent phosphatase calcineurin (CaN) and its direct downstream target nuclear factor of activated T cell (NFAT) (Reese and Taglialatela, 2011; Abdul et al., 2011). Glia is an established partner of neurons in the execution and regulation of brain functions, including synaptic transmission. Recent evidence indicates that it may be an important player in AD pathogenesis (Parpura et al., 2012). Reactive astrocytes, present also in normal aging, are found in AD postmortem brains, as well as in animal models, around amyloid plaques (DeWitt et al., 1998). Furthermore, Aβ provokes multiple alterations in glial homeostasis, including deregulation of Ca^{2+} signaling (Kuchibhotla et al., 2009), transcriptional changes (Peters et al., 2009) and inflammatory responses (Rubio-Perez and Morillas-Ruiz, 2012). Recently, using an *in vitro* Tat-Pro-ADAM10 model of AD (Marcello et al., 2007), we have demonstrated that in astrocytes Aβ produces

alterations of Ca^{2+} homeostasis by over-expressing mGluR5 and IP_3R1 at the transcriptional level (Grolla et al., 2013). In the present work, we dissect the molecular mechanism by which $A\beta_{42}$ leads to mGluR5 up-regulation in glia and, as a consequence, Ca^{2+}-deregulation. We now propose that $A\beta_{42}$ leads to cytosolic calcium increases, this leads to calcineurin activation, which in turn (possibly via Bcl10), activates NF-kB-dependent transcription of mGluR5. IP_3R2 appears to be controlled in a similar manner. We also provide evidence that mGluR5 staining is augmented in hippocampal astrocytes of AD patients in proximity of Aβ plaques and is co-localized with nuclear accumulation of the p65 NF-kB subunit and with increased staining of CaNAα.

2. Materials and Methods

2.1 Cell culture

Primary hippocampal astroglial cell cultures were prepared from postnatal days 1-3 (P1-P3) rat hippocampi as described previously (Fresu et al., 1999). Hippocampal glial cells were seeded in Dulbecco's Modified Eagle's Medium, supplemented with 10% fetal bovine serum, 2 mg/ml glutamine, 10 U/ml penicillin and 100 µg/ml streptomycin (Sigma, Milan, Italy). Cells were grown until confluence (2-4 days) and then were re-plated for the experiments on plates coated with 0.1 mg/ml Poly-L-lysine. The purity of cultures was assayed by immunostaining with anti-MAP2 (neuronal marker) and anti-GFAP (glial marker). No neurons were detected in glial primary cultures.

2.2 Aβ preparation

Amyloid β 1-42 ($A\beta_{42}$) was purchased either from Bachem (Bubendorf, Switzerland) or from Innovagen (Lund, Sweden). $A\beta_{42}$ oligomers were prepared as described by Giuffrida et al. (2009) with some modifications. Briefly, the peptide was dissoloved in HFIP (1,1,1,3,3,3-hexa-fluoro-2-propanol, Fluka Cat. 52512) to 1mg/ml,

monomerized by 1h incubation at 37°C, lyophilized, resuspended in dimethylsulfoxide (DMSO) at 5 mM, diluted in ice-cold MEM to 100 µM and oligomerized for 24 h at 4°C. The peptide was snap frozen and kept at -80°C. Unless otherwise stated, final concentration of $A\beta_{42}$ was 100 nM.

2.3 Antibodies and drug treatment

Primary antibodies to: mGluR5 (ab53090, for Western Blot (WB) 1:500) was from Abcam (Cambridge, UK). Anti-IP_3R1 (WB 1:500) antibody was a kind gift from Dr. Colin Taylor (University of Cambridge). Antibodies to p65 (sc-372, for immunocytochemistry (ICC) 1:50), CaNAα (sc-6123, WB 1:200), CaNAβ (sc-6124, WB 1:200), Bcl10 (sc-5611, WB 1:500) were from Santa Cruz (Santa Cruz, CA, USA). Anti-phosphoserine (p-Ser, ALX-804-167, WB 1:1000) was from Alexis (Enzo Life Sciences, Lausen, Switzerland); anti-β-actin (A1978, WB 1:4000) was from Sigma. AlexaFluor 488 secondary antibodies were from Life Sciences (Milan, Italy), peroxidase-conjugated secondary antibodies from Pierce (Rockford, IL, USA). In all experiments, FK506, Cyclosporine A, Caffeic Acid Phenethyl Ester (CAPE) and 4-Methyl-N^1-(3-phenylpropyl)benzene-1,2-diamine (JSH-23, JSH) (all from Sigma, Milan, Italy) were used at 100 nM, 1 µM, 40 µM and 20 µM, respectively, 1 hour before treatment with $A\beta_{42}$. (S)-3,5-Dihydroxyphenylglycine (DHPG), 2-Aminoethoxydiphenylborane (2-APB), nifedipine, 6,7-Dinitroquinoxaline-2,3-dione (DNQX) (all from Tocris, Bristol, UK) were used at 20 µM, 100 µM, 100 nM and 30 µM, respectively.

2.4 NF-kB luciferase assay

1x10^5 cells/well were plated in 24 well plates and 12-24 h after plating were transfected with an NF-kB-Luc reporter plasmid (Clontech) using Lipofectamine 2000 (Life Technologies, Milan). Twenty-four h after transfection, cells were treated with inhibitors and with $A\beta_{42}$ for 12-15 h. Luciferase activity was assayed using

Bright-Glo Luciferase Assay System (Promega, Milan, Italy) according to manufacturer's instruction.

2.5 Calcium imaging

Cells were loaded with Fura-2 AM as described in Grolla et al. (2013). After de-esterification (30 min at RT) the coverslip was mounted in an acquisition chamber and placed on the stage of a Leica epifluorescent microscope equipped with a S Fluor 40x/1.3 objective. Cells were excited alternatively with 340/380 nm using a monochromator Polichrome V (Till Photonics, Munich, Germany), and the fluorescence light, filtered through a bandpass 510 nm filter was collected by cooled CCD camera (Hamamatsu, Japan) and acquired by MetaFluor software. To quantify the differences in the peaks of Ca^{2+} transients the ratio values were normalized using the formula (Fi-Fo)/Fo (referred to as normalized Fura-2 ratio, norm. ratio). The cells with norm. ratio above 0.2 were considered as responders. For baseline Ca^{2+} measurements cells were treated with $A\beta_{42}$ for 3 h, then 2 μM Fura-2 was added for 30 min directly to culture medium and the cells were transferred to room temperature to avoid Fura-2 compartmentalization. At the end of each recording cells were perfused with a solution containing 10 μM ionomycin with either 10 mM Ca^{2+}, or 25 mM EGTA. Concentrations of Ca^{2+} were calculated according to Grynkiewicz et al. (1985). Data were analysed using GraphPad Prism Software (San Diego, CA, USA).

2.6 Real-time PCR

Total mRNA was extracted from 7.0x10^5 cells using QIAzol Lysis Reagent (Qiagen, Milan, Italy) according to manufacturer's instructions. First strand of cDNA was synthesised from 1 μg of total RNA using ImProm-II RT system (Promega). Real-time PCR was performed using GoTaq qPCR Master Mix (Promega) on an SFX96 Real-Time System (Biorad, Segrate, Italy). S18 ribosomal protein was used to normalize PCR product levels. Following oligonucleotide primers were used (from 5' to 3'): S18 (NM_213557) forward (Forw)-

TGCGAGTACTCAACACCAACA, reverse (Rev) CTGCTTTCCTCAACACCACA; mGluR5 (NM_017012) Forw GCCATGGTAGACATAGTGAAGAGA, Rev TAAGAGTGGGCGATGCAAAT; IP3R1 (NM_001007235) Forw GGCTACAGAGTGCCTGACCT, Rev CCATTCGTAGATCCCTCTGC; IP3R2 (NM_031046) Forw TCCAAAAGACGTTGGACACA, Rev TTCATCCCCTTCCTCTGGAT.

2.7 Immunocytochemistry

24 h before treatment, 5x10^4 glial cells were plated onto 13mm coverslips in 24 well plates. Treated cells were fixed in 4% formaldehyde in PBS for 15 minutes at room temperature (RT), permeabilized for 7 minutes in PBS with 0.1% Triton X-100 and blocked for 30 min in 2% gelatine. Then primary (1h, 37°C) and secondary (1h, RT) antibody were applied in PBS with 2% gelatin. After washing (3x5min), nuclei were stained with 4′,6-Diamidino-2-phenylindole dihydrochloride (DAPI) for 15 min at RT. Fluorescence images were acquired using a Leica epifluorescent microscope equipped with S Fluor 40x/1.3 objective using MetaMorph software.

2.8 Immunoprecipitation and Western Blot

For immunoprecipitation (IP), 3-5x10^5 glial cells were plated in 60 mm Petri dishes. On the day of experiment, cells were pretreated with inhibitors and then treated with $A\beta_{42}$ for 6 h. Cells were then scraped on ice in 300 µl IP buffer (50 mM Tris-HCl, pH=7.4, 150 nM NaCl, 1% NP-40) supplemented with protein inhibitors cocktail (PIC), 0.1 mM phenylmethanesulfonylfluoride (PMSF), and phosphatase inhibitors cocktail (all from Sigma), quantified with Micro BCA Protein Assay Kit (Pierce, Rockford IL, USA). 500 µg of total proteins were immunoprecipitated using A/G agarose beads (Santa Cruz Biotechnology, Inc., Santa Cruz, CA, USA) according to manufacturer's instructions with 2 µg primary anti-Bcl10, anti-CnAα or anti-CnAβ antibodies in 0.5 ml at 4°C O/N on a rotator shaker. After intensive washing, precipitates were dissolved in 100 µl of 1x Laemmli sample buffer and 30

µl were used for Western Blot. The raw densitometric data were expressed as ratio of Bcl10 to CaNA in Fig. 4 A and B, and as ratio of Bcl10 to p-Ser band intensities in Fig. 4 C and D. The ratios then were expressed as fold of increase as compared to control samples. For total lysates, cells were treated with $A\beta_{42}$ for 48-60 h, scraped in IP buffer and total proteins were quantified. 30-50 µg of total proteins were resolved in 5-12% gradient SDS-PAGE and blotted onto nitrocellulose membrane (GE Healthcare, Milan, Italy). Densitometric analysis was performed with Quantity One v. 4.6 software (Bio-Rad, Hercules, CA, USA).

2.9 Human material

The subjects included in this study were selected from the databases of the Departments of Neuropathology of the Academic Medical Center, University of Amsterdam (The Netherlands). Informed consent was obtained for the use of brain tissue and for access to medical records for research purposes. Tissue was obtained and used in a manner compliant with the Declaration of Helsinki. We included six hippocampal specimens of patients with Alzheimer's disease (Braak stage V and VI) and six hippocampal specimens obtained at autopsy from controls (without evidence of degenerative changes, and lacking a clinical history of cognitive impairment; Table 1). All Alzheimer's disease cases were pathologically staged according to Braak and Braak criteria [1]. All autopsies were performed within 24 h after death.

TABLE 1: Cases Included in this Study

Patients	Sex	Age	Braak's Neurofibrillary Staging	Clinical Diagnosis
1	M	89	V	Alzheimer's disease
2	F	77	V	Alzheimer's disease
3	F	90	V	Alzheimer's disease
4	F	70	VI	Alzheimer's disease
5	M	81	VI	Alzheimer's disease
6	F	88	VI	Alzheimer's disease
7	M	86	–	NC
8	M	91	–	NC
9	F	87	–	NC
10	M	79	–	NC
11	M	84	–	NC
12	F	76	–	NC

M = male; F = female; Braak's neurofibrillary staging: stage II–VI; NC = normal controls (without evidence of degenerative changes, and lacking a clinical history of cognitive impairment). Summary of clinical and neuropathological data of Alzheimer's disease and control patients.

2.10 Tissue preparation

One or two representative paraffin blocks per case (hippocampus) were sectioned, stained and assessed. Formalin fixed, paraffin-embedded tissue was sectioned at 6 µm and mounted on pre-coated glass slides (Star Frost, Waldemar Knittel GmbH, Braunschweig, Germany). Sections of all specimens were processed for haematoxylin eosin (HE), luxol fast blue (LFB) and Nissl stains as well as for immunocytochemical stainings for a number of markers described below.

2.11 Immunohistochemistry

Glial fibrillary acidic protein (GFAP; polyclonal rabbit, DAKO, Glostrup, Denmark; 1:4000), neuronal nuclear protein (NeuN; mouse clone MAB377, IgG1; Chemicon, Temecula, CA, USA; 1:1000), human leukocyte antigen(HLA)-DP, DQ, DR (HLA-DR; major histocompatibility complex class II, MHC-II; mouse clone CR3/43; DAKO, Glostrup, Denmark, 1:400), Amyloïd-β (Mouse clone 6F/3D; DAKO; 1:200), Phosphorylated Tau (pTau; mouse clone AT8; Innogenetics, Alpharetta, GA , USA; 1:5000) were used in the routine immunocytochemical analysis. For the detection of mGluR5 we used two antibodies (polyclonal rabbit ab53090, from Abcam, 1:100; polyclonal rabbit from Upstate Biotechnology, Lake Placid, NY; 1:100). For the detection of p65 we used a polyclonal rabbit (sc-372; Santa Cruz; 1:50) and for the detection of CaNAα a polyclonal goat (sc-6123, Santa Cruz; 1:50). Immunohistochemistry was carried out as previously described (Aronica et al., 2003). Single-label immunohistochemistry was developed using the Powervision kit (Immunologic, Duiven, The Netherlands) with 3,3-diaminobenzidine (Sigma, St. Louis, USA) as chromogen. For double-labeling sections were incubated with Brightvision poly-alkaline phosphatase (AP)-anti-Rabbit (Immunologic, Duiven, The Netherlands) for 30 minutes at room temperature, and washed with PBS. Sections were washed with Tris-HCl buffer (0,1 M, pH 8,2) to adjust the pH. AP activity was visualized with the alkaline phosphatase substrate kit I Vector Red (SK-5100, Vector laboratories Inc., CA, USA). To remove the first primary antibody sections were incubated at 121 °C in citrate buffer (10 mM NaCi, pH 6,0) for 10 min.

Incubation with the second primary antibody was performed overnight at 4°C. Sections with primary antibody other than rabbit were incubated with post antibody blocking from the Brightvision+ system (containing rabbit-α-mouse IgG; Immunologic, Duiven, The Netherlands). AP activity was visualized with the AP substrate kit III Vector Blue (SK-5300, Vector laboratories Inc., CA, USA). Sections incubated without the primary Abs or with the primary antibodies, followed by heating treatment were essentially blank. For the double-label immunofluorescent staining, after incubation with the primary antibodies overnight at 4 °C, incubated for 2h at room temperature with Alexa Fluor® 568-conjugated anti-rabbit and Alexa Fluor® 488 anti-mouse IgG or anti-goat IgG (1:100, Molecular Probes, The Netherlands). Sections were mounted with Vectashield containing DAPI (targeting DNA in the cell nucleus; blue emission) and analyzed by means of a laser scanning confocal microscope (Leica TCS Sp2, Wetzlar, Germany). Sections were then analyzed by means of a laser scanning confocal microscope (Leica TCS Sp2, Wetzlar, Germany).

3. Results

3.1 $A\beta_{42}$-induced up-regulation of astroglial calcium signaling is calcineurin and NF-kB-dependent.

In the first instance, we performed Fura-2 measurements of Ca^{2+} transients induced by the mGluR agonist DHPG (20 μM) in astrocytes pretreated with the CaN inhibitor FK506 and stimulated with $A\beta_{42}$ for 48-60 h. As shown in Fig. 1, $A\beta_{42}$ significantly augmented the amplitude of the DHPG-induced Ca^{2+} transient (Fig. 1 A-b) as compared to control cells (Fig. 1 A-a). Pre-treatment with FK506 reduced significantly the peak of the Ca^{2+} transient and reduced significantly also the fraction of cells responding to DHPG (Fig. 1 B). Recent publications have described CaN-dependent activation of NF-kB in the immune system (Frischbutter et al., 2011; Palkowitsch et al., 2011). Furthermore, analysis of the promoter regions of the

mGluR5 gene revealed no presence of NFAT binding site, a direct classical downstream CaN target, but of an NF-kB binding site, present in the second of three active promoter regions (Corti et al., 2003). We thus performed identical experiments using two inhibitors of NF-kB nuclear translocation, namely CAPE and JSH. Pretreatment with CAPE and JSH did not reduce significantly the Ca^{2+} peak amplitude, but dramatically reduced the fraction of responding astrocytes (Fig. 1 A-d; Fig. 1 B). Thus, it is plausible that alterations of mGluR5 signaling, induced by $A\beta_{42}$, are controlled by CaN but also by NF-kB.

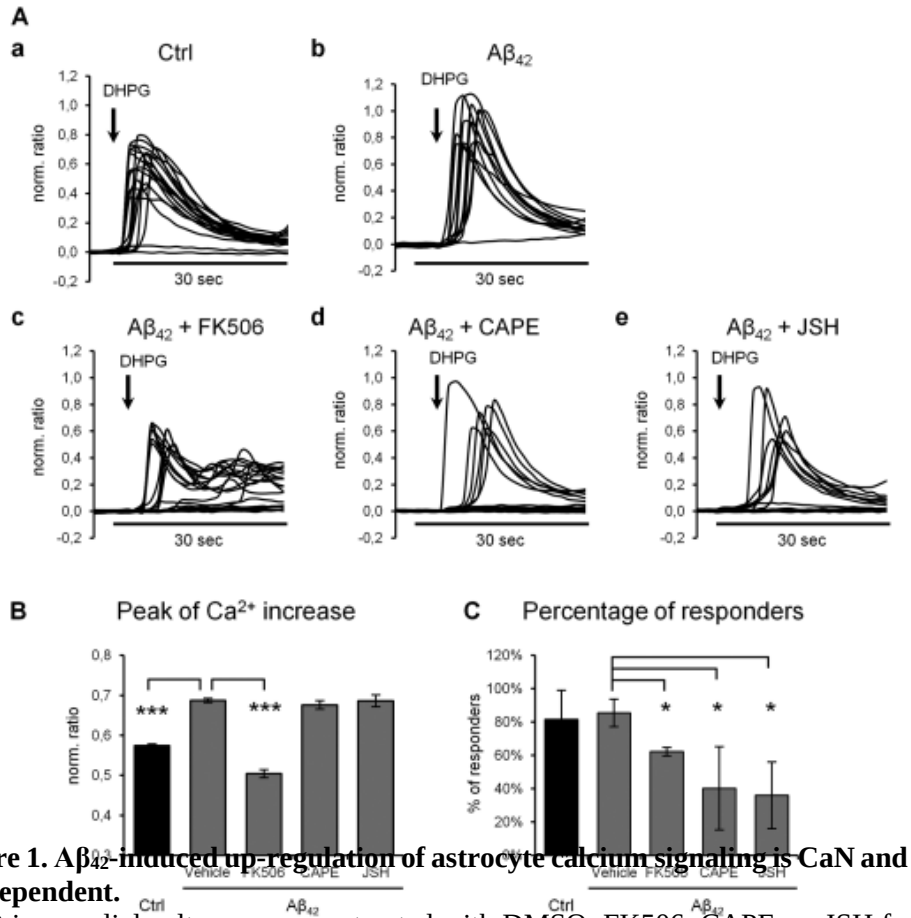

Figure 1. $A\beta_{42}$-induced up-regulation of astrocyte calcium signaling is CaN and NF-kB-dependent.
(**A**) Primary glial cultures were pretreated with DMSO, FK506, CAPE, or JSH for 1 h and then either non-stimulated (a) or stimulated with 100 nM $A\beta_{42}$ (b-e) for 48 h. Representative experiments for each condition are shown. (**B**) Summarizing histograms of Ca^{2+}-peaks of responding cells (Norm.Fura.Ratio > 0.2) expressed as mean ± SEM; (**C**) Summarizing Histogram illustrating the percentage of responding cells for each condition (mean ± SD).

3.2 $A\beta_{42}$-induced CaN-mediated up-regulation of mGluR5 and IP_3R2 is NF-kB-dependent, but up-regulation of IP_3R1 is not.

Treatment of astrocytes with $A\beta_{42}$ induced a significant increase in mGluR5 expression (Fig. 2 A). Pretreatment with inhibitors of both CaN and NF-kB abrogated $A\beta_{42}$-induced up-regulation of mGluR5 at both the mRNA (Fig. 2 A-a) and protein levels (Fig. 2 A-b). Previously, we demonstrated that both neuronal and glial splice variants of IP_3R1 were up-regulated in glial cells in a CaN-dependent manner (Grolla et al, 2013). Thus, we investigated if $A\beta_{42}$-induced over-expression of IP_3R1 was also dependent on NF-kB activation. Fig. 2 B-a shows that both FK506 and CsA restored the effect of $A\beta_{42}$ on IP_3R1 mRNA levels, but both inhibitors of nuclear NF-kB translocation, CAPE and JSH, failed to do so. The data therefore support the notion that this receptor is regulated by the direct CaN target NFAT (Graef et al., 1999; Groth and Mermelstein, 2003). In astrocytes, however, IP_3R2 is the dominant isoform of the IP_3 receptors (Sharp et al., 1999). Thus, we decided to analyse IP_3R2 expression by real-time PCR. IP_3R2 was up-regulated by $A\beta_{42}$ treatment and inhibitors of both CaN and NF-kB were able to abolish this up-regulation (Fig. 2 B-b).

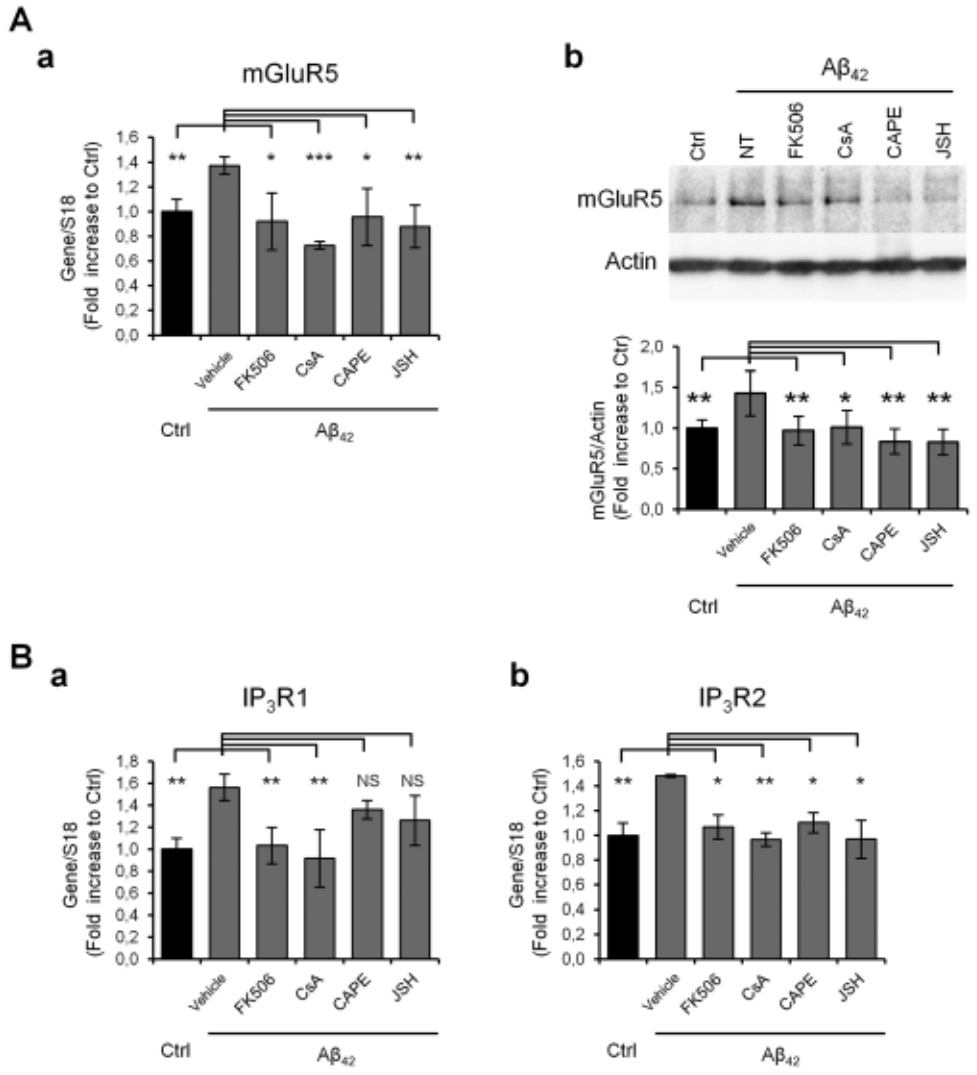

Figure 2. Aβ$_{42}$-induced and CaN-mediated up-regulation of mGluR5 and IP$_3$R2 is NF-kB-dependent, but up-regulation of IP$_3$R1 is not.

(**A**) Real-time PCR (a) and WB analysis (b) of mGluR5 in primary glial cultures stimulated with Aβ$_{42}$ for 24 h or 48 h, respectively. (**B**) Real-time PCR of IP$_3$R1 and IP$_3$R2 in primary glial cultures stimulated with Aβ$_{42}$ for 24 hours. Data were normalized to S18 ribosomal protein subunit mRNA or actin and expressed as mean ± SD reported to control. Data are from at least 5 independent cultures performed in triplicate (RT-PCR) or from three independent cultures (WB). *, $p < 0.05$; **, $p < 0.01$; ***, $p < 0.001$.

3.3 $A\beta_{42}$-induced calcineurin activation in astrocytes is calcium dependent.

Next, we investigated possible mechanisms by which $A\beta_{42}$ may activate CaN and then NF-kB. Several possibilities have been proposed, including the incorporation of the $A\beta_{42}$ peptide in the plasma membrane and the formation of a pore permeable to cations (Kawahara and Kuroda, 2000) or the activation by $A\beta_{42}$ of calpain, which in turn can cleave and activate CaN (Abdul et al., 2011). Furthermore, Aβ was shown to produce Ca^{2+} oscillations in astrocytes in mixed neuronal/glial cultures (Abramov et al., 2004). We therefore investigated whether Aβ could lead to cytosolic calcium increases in glial cells. In our hands, acute $A\beta_{42}$ treatment (up to 1 μM) in primary glial cultures did not produce any notable change in cytosolic Ca^{2+} concentrations in the first hour of treatment (data not shown). Yet, after 4-6 h of treatment, cells treated with 100 nM Aβ displayed a statistically significant increase in free cytosolic Ca^{2+} (Fig. 3 A-a). As shown in Fig. 3 A-b, this significant increase was not homogeneous, but was given by a sub-group of astrocytes which increased basal Ca^{2+} to 100-150 nM. Pre-incubation with the calcium chelator BAPTA-AM abolished the elevation of cytosolic [Ca^{2+}] (data not shown). Next we investigated the effect of BAPTA on $A\beta_{42}$-induced up-regulation of mGluR5 mRNA. One hour pre-incubation with BAPTA-AM completely abolished mGluR5 mRNA up-regulation induced by $A\beta_{42}$ (Fig. 3 B-a). The same result was obtained for IP_3R1 and IP_3R2 genes (Fig. 3 B-b,c), indicating that elevation of cytosolic [Ca^{2+}] is required for the activation of CaN. We next used a range of Ca^{2+} channel blockers to investigate whether we could pin-point the source of the Ca^{2+}-increase. Neither nifedipine (100 nM) nor DNQX (30 μM) had a significant effect (data not shown), while 2-APB (100 μM) blocked such up-regulation for all three genes, mGluR5, IP_3R1 and IP_2R2 (Fig. 3 B), indicating that TRP channels may be implicated in $A\beta_{42}$-induced elevation of cytosolic [Ca^{2+}]. Yet, 2-APB has been shown to be a rather non-specific inhibitor, and it is therefore difficult to draw conclusions.

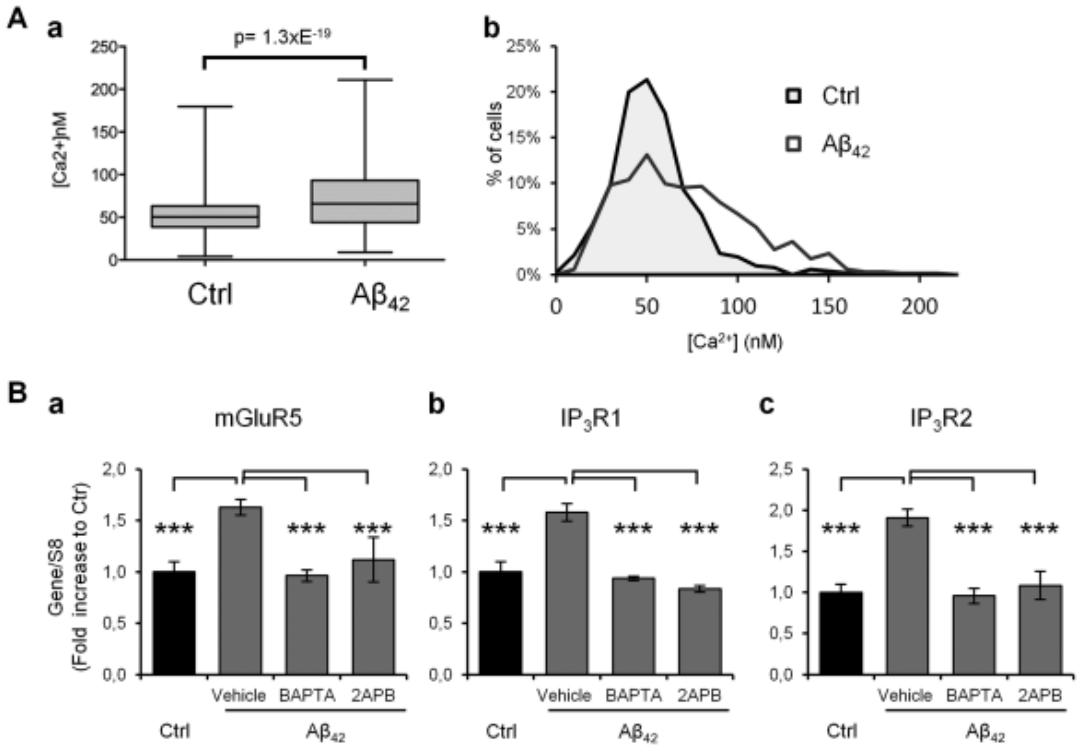

Figure 3. Cytosolic Ca^{2+} elevation is required for the $A\beta_{42}$-induced calcineurin activation.

(**A**) Whisker box graph (a) representing mean ± SD of 515 control cells and 694 cells stimulated with $A\beta_{42}$ for 4-6 h from 2 independent cell preparations (12 coverslips each) and frequency distribution plot (b) of baseline Ca^{2+} concentration in control and $A\beta_{42}$-treated cells. (**B**) Real-time PCR of the indicated genes in cells pre-treated for 2 h with 5 μM BAPTA-AM or 100 μM 2-APB prior to $A\beta_{42}$ addition for 24 h. Data were normalized to S18 ribosomal protein subunit mRNA or actin and expressed as mean ± SD reported to control. All differences are significant at $p < 0.001$ for three independent experiments.

3.4 Calcineurin interacts with and de-phosphorylates Bcl10 in $A\beta_{42}$-treated glial cells.

In the immune system, it has recently been reported that CaN interacts with and de-phosphorylates B cell lymphoma 10 (BCL10) and this leads to activation of NF-kB (Frischbutter et al., 2011; Palkowitsch et al., 2011). Therefore, we investigated if the two major CaN isoforms, CaNAα and CaNAβ, interact with Bcl10 and if this interaction results in de-phosphorylation of Bcl10. Fig. 4 A and B show that both CaNAα and CaNAβ interact with Bcl10 when CaNAα or CaNAβ were immunoprecipitated using isoform-specific antibodies. Moreover, densitometric analysis revealed that CaNA/Bcl10 interaction is augmented in $A\beta_{42}$-treated glial cultures. Interestingly, both CaN inhibitors, FK506 and CsA, significantly attenuated the interaction of Bcl10 with CaNAα, the most expressed isoform of CaNA, in $A\beta_{42}$-treated cells, while neither FK506 nor CsA had any significant effect on Bcl10 interaction with CaNAβ. Similar results were obtained when glial lysates were immunoprecipitated with anti-Bcl10 antibody and precipitates were probed with anti-CaNAα or anti-CaNAβ antibodies (Fig. 4 C). To assess de-phosphorylation of Bcl10 by CaN, we first immunoprecipitated the lysates with anti-Bcl10 antibody and then probed precipitates with antibody recognizing phosphorylated serine residues (p-Ser). To normalize intensities of the bands the ratio Bcl10/p-Ser was used for statistical tests. As shown in Fig. 4 D, $A\beta_{42}$ significantly increased Bcl10/p-Ser ratio indicating augmented of Bcl10 de-phosphorylation. This effect was completely reversed by FK506 and attenuated by CsA. These data indicate that in glial cells CaN may activate NF-kB through de-phosphorylation of Bcl10.

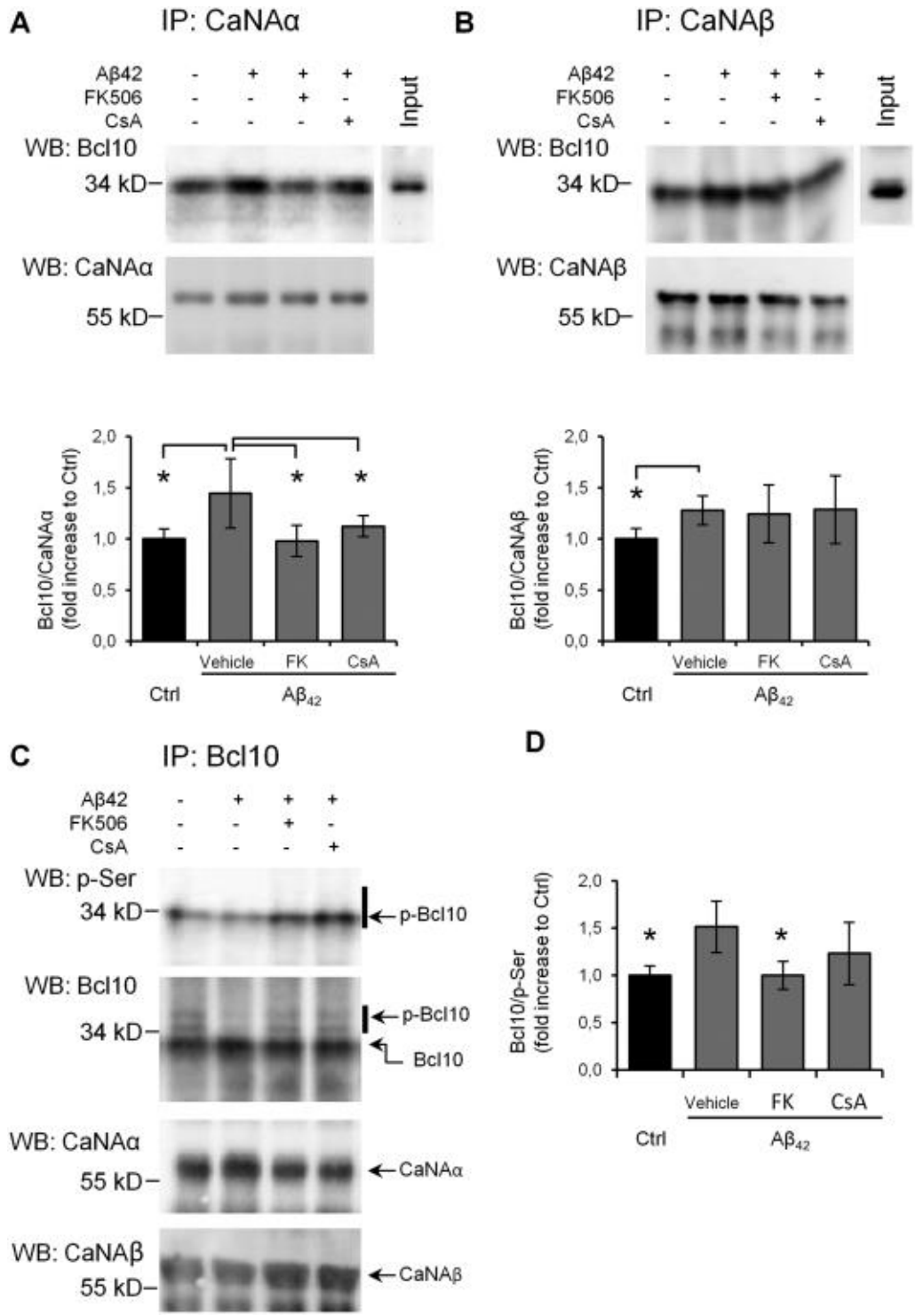
A
IP: CaNAα
Aβ42 - + + +
FK506 - - + -
CsA - - - +
Input
WB: Bcl10
34 kD–
WB: CaNAα
55 kD–
B
IP: CaNAβ
Aβ42 - + + +
FK506 - - + -
CsA - - - +
Input
WB: Bcl10
34 kD–
WB: CaNAβ
55 kD–
Bcl10/CaNAα (fold increase to Ctrl)
2,0
1,5
1,0
0,5
0,0
*
*
*
Vehicle
FK
CsA
Ctrl
Aβ42
Bcl10/CaNAβ (fold increase to Ctrl)
2,0
1,5
1,0
0,5
0,0
*
Vehicle
FK
CsA
Ctrl
Aβ42
C
IP: Bcl10
Aβ42 - + + +
FK506 - - + -
CsA - - - +
WB: p-Ser
34 kD–
p-Bcl10
WB: Bcl10
34 kD–
p-Bcl10
Bcl10
WB: CaNAα
55 kD–
CaNAα
WB: CaNAβ
55 kD–
CaNAβ
D
Bcl10/p-Ser (fold increase to Ctrl)
2,0
1,5
1,0
0,5
0,0
*
*
Vehicle
FK
CsA
Ctrl
Aβ42

Figure 4. Calcineurin interacts with and de-phosphorylates Bcl10 in $A\beta_{42}$-treated glial cells.
(**A**; **B**) Representative results and densitometric analysis of the effect of $A\beta_{42}$, FK506 or CsA on the interaction of Bcl10 with CaNAα and with CaNAβ. Lysates of primary glial cultures treated with $A\beta_{42}$ for 5 h were immunoprecipitated with anti-CaNAα and anti – CaNAβ primary antibody. Precipitates were probed with anti Bcl10 antibodies (upper bands) and with anti-CaNA (lower bands). Data in histograms are expressed as ratio of Bcl10/CaN, expressed as mean ± SD and reported to control. The differences are significant at $p < 0.05$ for 3 independent IP for each condition. (**C**) Representative results and densitometric analysis of the effect of $A\beta_{42}$, FK506 or CsA on the de-phosphorylation of Bcl10 and interaction with CaNAα and with CaNAβ. After 5 h of incubation with $A\beta_{42}$, cells were lysed and immunoprecipitated with primary anti-Bcl10 antibody. The precipitates were probed with anti-phospho serine (p-Ser), anti-Bcl10, anti-CaNAα and anti CaNAβ primary antibodies. (**D**) The Bcl10/p-Ser ratios are expressed as mean ± SD and reported to control. Differences are significant at $p < 0.05$ for 6 IPs form 3 independent glial cultures.

3.5 Calcineurin mediates $A\beta_{42}$-induced NF-kB activation and p65 nuclear translocation in astrocytes.

Next, we investigated if $A\beta_{42}$-induced activation of CaN may result in nuclear translocation of NF-kB. Fig. 5 A shows that the NF-kB-Luc reporter gene was significantly activated by $A\beta_{42}$ treatment. The effect was abolished when cells were pretreated with FK506, CsA, CAPE or JSH. Then, we performed immunocytochemistry to visualize accumulation of p65 NF-kB subunit in the nuclear compartment. As shown in Fig. 5 B and 5 C, stimulation with $A\beta_{42}$ for 5-9 hours resulted in a clear nuclear localization of p65 in 42.7 ± 8.4% of astrocytes which is significantly more than in control cells (11.3 ± 3.01%, $p < 0.001$). Blockers of both CaN and NF-kB strongly inhibited translocation of p65 to the nucleus, confirming the results obtained using the NF-kB-luc reporter.

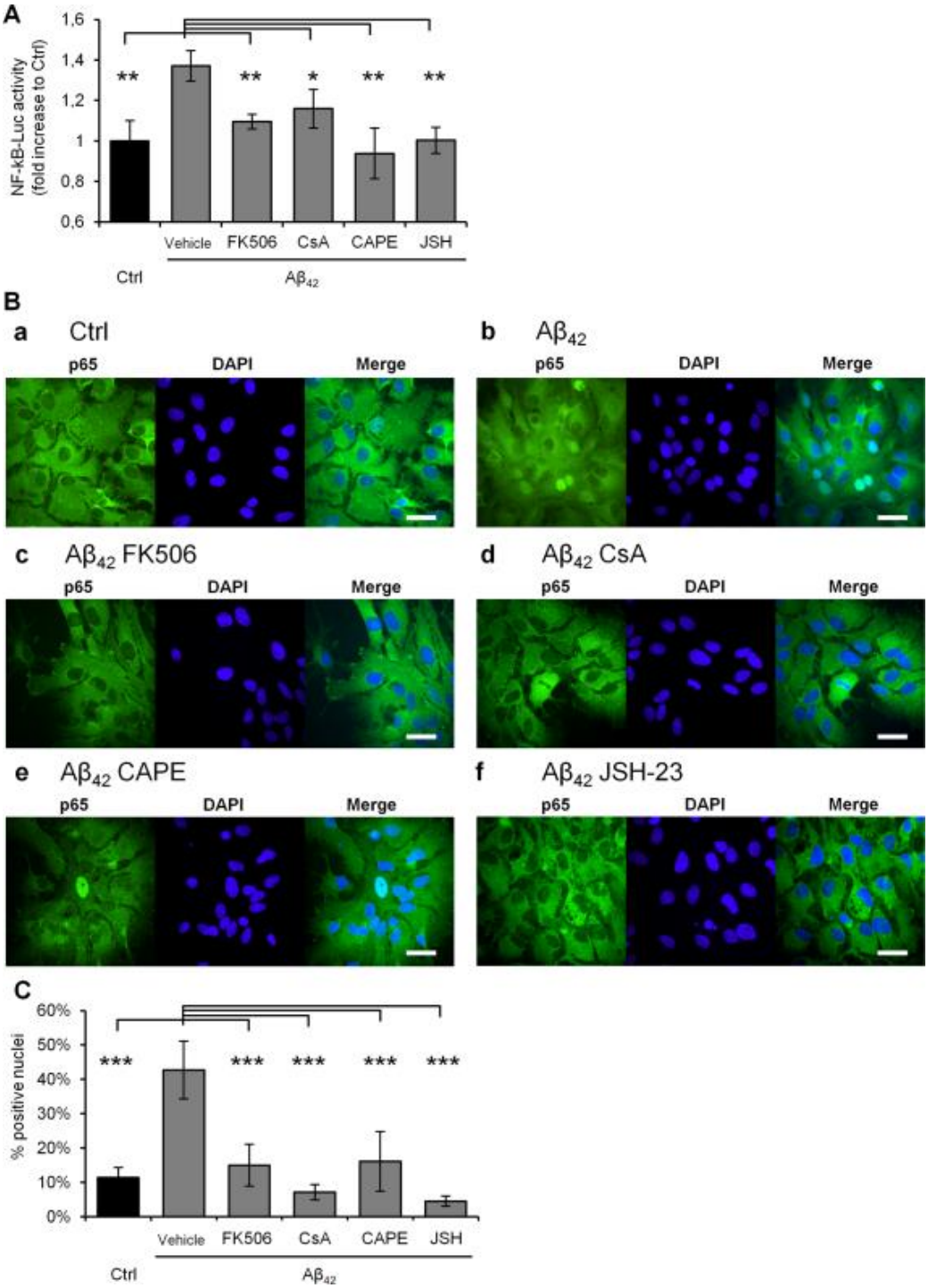
A
NF-kB-Luc activity (fold increase to Ctrl)
1,6
1,4
1,2
1
0,8
0,6
**
**
*
**
**
Vehicle
FK506
CsA
CAPE
JSH
Ctrl
Aβ42
B
a Ctrl
b Aβ42
c Aβ42 FK506
d Aβ42 CsA
e Aβ42 CAPE
f Aβ42 JSH-23
p65
DAPI
Merge
C
% positive nuclei
60%
50%
40%
30%
20%
10%
0%
***
***
***
***
***
Vehicle
FK506
CsA
CAPE
JSH
Ctrl
Aβ42

Figure 5. Calcineurin mediates $A\beta_{42}$-induced NF-kB activation and p65 nuclear translocation in astrocytes.
(**A**) NF-kB-Luc reporter assays in cells treated with FK506, CsA, CAPE or JSH 1 h prior to stimulation with $A\beta_{42}$ for 18 h. Data are expressed as mean ± SD of fold increase of luciferase activity of samples over control in five independent experiments performed in triplicate. (**B**) Immunocytochemical analysis of nuclear translocation of p65 subunit of NF-kB of primary astrocytes preincubated with the indicated compounds and stimulated with $A\beta_{42}$. Cells were fixed after 6 h of $A\beta_{42}$ treatment, permeabilized and stained with primary anti-p65 antibody followed by 488-Alexa conjugated secondary antibody (green). Nuclei were counterstained with DAPI (blue). (**C**) quantification of nuclar staining og NF-kB from 6 coverslips (10 fields each) from 3 independent experiments. Data show mean ± SD, all differences were significant at $p < 0.001$. Scale bar in **B**: 25 μm.

3.6 mGluR5 is up-regulated in astrocytes located close to Aβ plaques in AD patient's hippocampus.

In adult control hippocampus, mGluR5 is expressed throughout the CA pyramidal cells. No detectable immunoreactivity (IR) was observed in glial cells (Fig. 6 A-B). In AD hippocampus, strong mGluR5 IR was detected throughout the different hippocampal regions, particularly around Aβ deposits associated with pTAU positive dystrophic neurites (Fig. 6 C-F). Double labeling experiments confirmed the increased expression of mGluR5 in astrocytes (GFAP positive cells) of AD patients in proximity of Aβ plaques (Fig. 6 D-H). Only occasionally co-localisation with a microglial marker (HLA-DR) was observed (not shown). Double labeling with p65 and CaNAα showed co-localization with mGluR5 in astrocytes of AD hippocampus (Fig. 6 I-J).

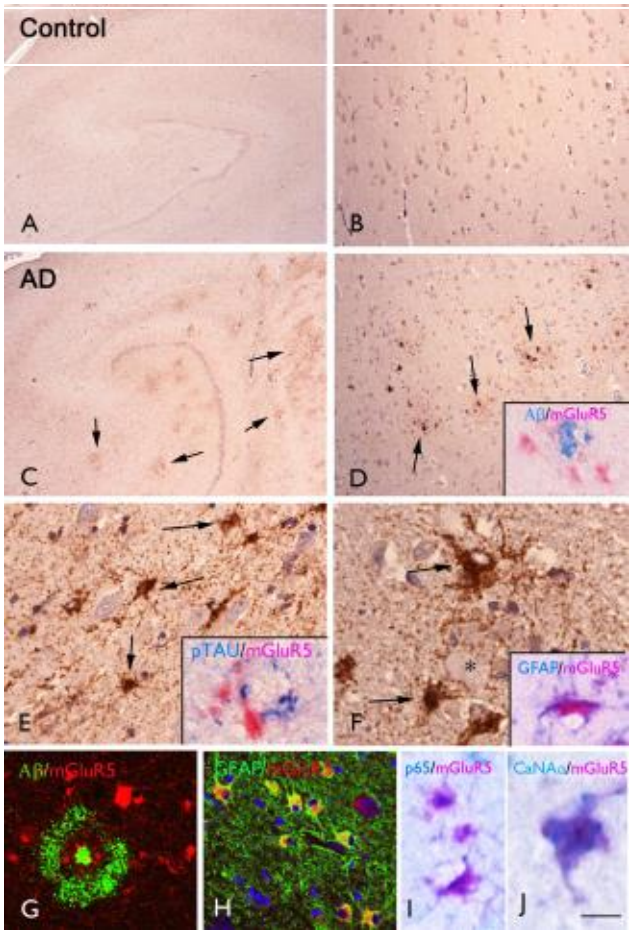

Figure 6. mGluR5 is up-regulated in astrocytes located close to Aβ plaques in AD patients.

Panels **A**-**B**: control hippocampus with expression of mGluR5 throughout the CA pyramidal cells (CA1 is shown in panel **B**). Panels **C**-**J**: Alzheimer' s disease (AD; stage VI) showing increased expression throughout the hippocampus, around amyloid plaques (arrows; CA1 is shown in panel **D**); insert in **D** shows mGluR5 positive cells around amyloid β (Aβ) immunoreactivity. Panel **E**: strong mGluR5 immunoreactivity (IR) in astrocytes is observed in the CA1 around pyramidal neurons (arrows); insert in **E** shows mGluR5 positive cells around dystrophic neurites (expressing hyperphosphorylated tau; pTAU), associated with an amyloid plaque. Panel **F** shows high magnification of mGluR5 positive astrocytes (arrows) around an amyloid plaque (asterisk); insert in **F** shows expression of mGluR5 in an astrocyte (GFAP positive cell). Panel **G**: confocal image showing expression of mGluR5 (red) around Aβ deposits (green). Panel **H**: confocal image showing co-localization (yellow) of mGluR5 (red) with GFAP (green). Panels **I** and **J**: co-localization (purple) of mGluR5 with p65 (**I**) and calcineurin α (CaNAα; **J**). Scale bar in **A**, **C**: 400 µm; **B**, **D**: 160 µm; **E**, **G**, **H**: 40 µm; **F**, **I**: 25 µm; **J**: 20 µm.

4. Discussion

In the present study we have investigated the effects of $A\beta_{42}$ oligomers on the astroglial signaling cascade, which includes CaN, mGluR5, and IP_3 receptors. Our principal findings are: (1) In hippocampal astrocytes, activation of CaN by $A\beta_{42}$ requires elevation of cytosolic [Ca^{2+}] via Ca^{2+} entry from the extracellular milieu; (2) CaN activation leads to nuclear translocation of the transcription factor NF-kB, possibly via de-phosphorylation of Bcl10, that up-regulates expression of both mGluR5 and IP_3R2; (3) A similar pathway involving CaN, but not NF-kB, controls IP_3R1 expression; (4) these transcriptional changes have repercussions on mGluR5 activation and calcium homeostasis in glial cells. We also provide evidence that this pathway may be relevant to AD: in the hippocampus of AD patients, mGluR5 is found to be over-expressed in concomitance with over-expression of CaNAα and with p65 NF-kB subunit in GFAP-positive astrocytes located in proximity to Aβ aggregates. These data are in line with previous report by Norris et al. (2005) describing CaN-immunoreactive astrocytes surrounding amyloid plaques in APP/PS1 Tg mice. We therefore propose the signaling cascade illustrated in Figure 7.It should be acknowledged that while our claim is that the data presented is relevant to AD, there is still controversy on whether Aβ is the key driver of the disease, or whether it represents a corollary phenomenon, for example of a more generalized protein mis-processing (Aguzzi and Haass, 2003). Furthermore, it remains to be ascertained whether Aβ induces a specific astrocyte activation or whether other astrocyte insults are able to induce similar effects. Therefore, a re-arrangement of the calcium signaling machinery via CaN could be a specific phenomenon linked to AD or might have a more general function in reactive astrocytes or astrogliosis.Furthermore, while the obvious context of our experiments would be placed around an increase in Aβ from neurons, we and others have previously shown that Aβ can be produced by astroglia (Rossner et al., 2005; Bettegazzi et al., 2011; Grolla et al., 2013). In this context, our experiments could also support a primary

pivotal role of astroglia in the pathogenesis of the disease, as suggested by others (Yeh et al., 2011; Kulijewicz et al., 2012). Indeed, early astrocyte atrophy has been reported in a mouse model of Alzheimer's disease (Rodriguez and Verkhratsky, 2011; Verkhratsky et al., 2012).Independently of these considerations, there is an increasing evidence that CaN is involved in AD pathogenesis (Reese and Taglialatela, 2011). Activation of CaN specifically in astrocytes has been proposed to have a role in AD and in other pathological conditions (Norris et al., 2005; Sama et al., 2008; Abdul et al., 2009; Fernandez et al., 2012; Grolla et al., 2013; Jin et al., 2012; Furman et al., 2012) although the mechanisms of its activation remain largely unknown. CaN could be directly activated by calcium entering via channel-like structures formed by Aβ (Kagan and Thundimadathil, 2010), via Ca^{2+}-permeable channels on the plasma membrane modulated by Aβ (Pellistri et al., 2008), or indirectly via the cleavage of the CaNA auto-inhibitory domain by calpain (Abdul et al., 2011). In our experiments, we used nanomolar [$A\beta_{42}$], compatible with the [Aβ] found in the cerebro-spinal fluid of AD patients (Mehta et al., 2001). We report that the acute treatment of cultured astrocytes with 100 nM $A\beta_{42}$ did not change baseline [Ca^{2+}] for up to 1 hour of recording. However, when cells were taken for Ca^{2+} imaging 4-6 h after $A\beta_{42}$ addition, a fraction of cells had elevated [Ca^{2+}]cyt in a range of 100-150 nM, which is in line with [Ca^{2+}]cyt necessary to activate CaN in cerebellar granule neurons (Guerini et al., 1999). Abdul et al. (2009) reported nuclear translocation of NFAT-EGFP reporter already 15 minutes after addition of similar [Aβ], indicating that in their experiment Aβ-induced CaN activation occurred significantly earlier than in our experiments. At least two factors may account for this discrepancy: i) different procedures of preparation of Aβ which could affect effective concentration oligomeric Aβ; and ii) different protocols of preparations primary astroglial cultures. Furthermore, all CaN-dependent changes in mRNA expression were abolished by clamping cytosolic Ca^{2+}, and indicate that involvement of cation channels is possible in the $A\beta_{42}$-induced Ca^{2+} entry. Last, we find that 2-APB, a non-specific cation blocker abolishes the effect.CaN inhibitors have been

widely used as immunosuppressants and most of their actions can be reconciled with inhibition of NFAT-dependent transcription (Lee and Burckart, 1998). Astroglial CaN-NFAT signaling has been characterized by several groups (Canellada et al., 2008; Sama et al., 2008; Pérez-Ortiz et al., 2008; Furman et al., 2010). Recently, it was proposed that CaN is an essential for activation of NF-kB in immune cells (Palkowitsch et al., 2011; Frischbutter et al., 2011) where Bcl10, a member of the so called CBM complex, interacts with and is de-phosphorylated by CaN to recruit other two CBM members, mucosa-associated lymphoid tissue lymphoma translocation protein 1 (MALT1) and caspase recruitment domain membrane-associated guanylate kinase protein 1 (CARMA1) in a ternary complex, whose downstream effects are degradation of IkB and nuclear translocation of NF-kB. This may therefore constitute a parallel pathway that mediates calcineurin's actions in the immune system. Thus, we decided to investigate if CaN interacts with Bcl10 also in glial cells. We found that, in fact, this was the case. Both CaNAα and CaNAβ co-immunoprecipitated with Bcl10 in glial cultures. Moreover, in our experiments, stimulation with $A\beta_{42}$ significantly augmented this interaction in which Bcl10 was also de-phosphorylated. As the effect of CaN and NF-kB inhibitors overlap in our experiments for mGluR5 and IP_3R2, we propose this pathway as being responsible. Yet, it has been proposed also that, in astrocytes, CaN activates NF-kB via interaction with Forkhead box O (FoxO) transcription factor 3 (Foxo3) in TNFα-stimulated cells (Fernandez et al., 2012). Interestingly, Foxo3 may also be activated downstream of Bcl10 and Ikk signaling cascade (Luron et al., 2012).The Ca^{2+}-CaN-NF-kB pathway activation, in our system, leads to a profound remodeling of Ca^{2+}-handling capacity of astrocytes. As such, it might be suggested that, in AD brains, this would lead to profound changes in astroglial Ca^{2+}-dependent processes, including gliotransmission and reactive inflammation. As such, these could participate actively in the pathogenesis of the disease.In support of the occurrence of these phenomena in AD, we also show that in hippocampi from human AD brains,

mGluR5 was over-expressed with CaNAα in GFAP-positive astrocytes in proximity to amyloid plaques and co-localized with p65.

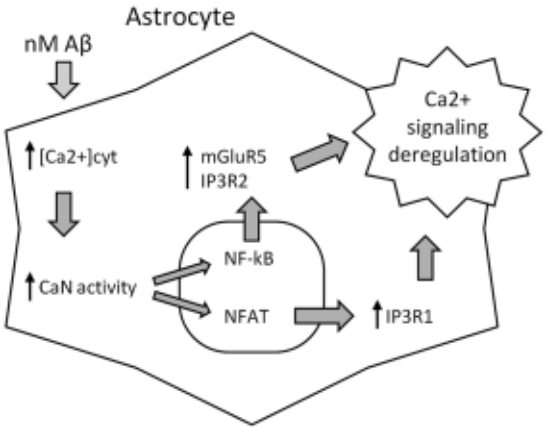

Figure 7. Scheme of the proposed mechanism of the Aβ-induced deregulation of Ca^{2+} signaling in astrocytes.

Acknowledgements

We thank Dr. Colin Taylor for anti-IP_3R1 antibody and Dr. Christian Zurlo for the help in maintenance of animals. We are grateful to J.J. Anink for his technical help. This work was supported by Fondazione Cariplo (grant n° 2008-2319 to AAG, DL); and by the EU FP7 project DEVELAGE (Grant Agreement N 278486 to EA, AI). Authors declare no conflict of interests.

References

Abdul HM, Baig I, Levine H 3rd, Guttmann RP, Norris CM. 2011. Proteolysis of calcineurin is increased in human hippocampus during mild cognitive impairment and is stimulated by oligomeric Abeta in primary cell culture. Aging Cell 10:103-113.

Abdul HM, Sama MA, Furman JL, Mathis DM, Beckett TL, Weidner AM, Patel ES, Baig I, Murphy MP, LeVine H 3rd, Kraner SD, Norris CM. 2009. Cognitive decline in Alzheimer's disease is associated with selective changes in calcineurin/NFAT signaling. J Neurosci 29:12957-12969.

Abramov AY, Canevari L, Duchen MR. 2004. Calcium signals induced by amyloid beta peptide and their consequences in neurons and astrocytes in culture. Biochim Biophys Acta 1742 81-87. Aguzzi A, Haass C. 2003. Games played by rogue proteins in prion disorders and Alzheimer's disease. Science 302:814-818.

Aronica E, Gorter JA, Jansen GH, van Veelen CW, van Rijen PC, Ramkema M, Troost D. 2003. Expression and cell distribution of group I and group II metabotropic glutamate receptor subtypes in taylor-type focal cortical dysplasia. Epilepsia 44:785-795.

Bettegazzi B, Mihailovich M, Di Cesare A, Consonni A, Macco R, Pelizzoni I, Codazzi F, Grohovaz F, Zacchetti D. 2011. beta-Secretase activity in rat astrocytes: translational block of BACE1 and modulation of BACE2 expression. Eur J Neurosci 33:236-243.

Braak H, Alafuzoff I, Arzberger T, Kretzschmar H, Del Tredici K. 2006. Staging of Alzheimer disease-associated neurofibrillary pathology using paraffin sections and immunocytochemistry. Acta Neuropathol 112:389-404.

Canellada A, Ramirez BG, Minami T, Redondo JM, Cano E. 2008. Calcium/calcineurin signaling in primary cortical astrocyte cultures: Rcan1-4 and cyclooxygenase-2 as NFAT target genes. Glia 56:709-722.

Corti C, Clarkson RW, Crepaldi L, Sala CF, Xuereb JH, Ferraguti F. 2003. Gene structure of the human metabotropic glutamate receptor 5 and functional analysis of its multiple promoters in neuroblastoma and astroglioma cells. J Biol Chem 278:33105-33119.

Demuro A, Parker I, Stutzmann G E. 2010. Calcium signaling and amyloid toxicity in Alzheimer disease. J Biol Chem 285:12463-12468.

DeWitt DA, Perry G, Cohen M, Doller C, Silver J. 1998. Astrocytes regulate microglial phagocytosis of senile plaque cores of Alzheimer's disease. Exp Neurol 149:329-40.

Fernandez AM, Jimenez S, Mecha M, Dávila D, Guaza C, Vitorica J, Torres-Aleman I. 2012. Regulation of the phosphatase calcineurin by insulin-like growth factor I unveils a key role of astrocytes in Alzheimer's pathology. Mol Psychiatry 17:705-718.

Fresu L, Dehpour A, Genazzani A A, Carafoli E, Guerini D. 1999. Plasma membrane calcium ATPase isoforms in astrocytes. Glia 28:150-155.

Frischbutter S, Gabriel C, Bendfeldt H, Radbruch A, Baumgrass R. 2011. Dephosphorylation of Bcl-10 by calcineurin is essential for canonical NF-κB activation in Th cells. Eur J Immunol 41:2349-2357.

Furman JL, Artiushin IA, Norris CM. 2010. Disparate effects of serum on basal and evoked NFAT activity in primary astrocyte cultures. Neurosci Lett 469:365-369.

Furman JL, Sama DM, Gant JC, Beckett TL, Murphy MP, Bachstetter AD, Van Eldik LJ, Norris CM. 2012. Targeting astrocytes ameliorates neurologic changes in a mouse model of Alzheimer's disease. J Neurosci 32:16129-16140.

Giuffrida ML, Caraci F, Pignataro B, Cataldo S, De Bona P, Bruno V, Molinaro G, Pappalardo G, Messina A, Palmigiano A, Garozzo D, Nicoletti F, Rizzarelli E, Copani A. 2009. Beta-amyloid monomers are neuroprotective. J Neurosci 29:10582-10587.

Graef IA, Mermelstein PG, Stankunas K, Neilson JR, Deisseroth K, Tsien RW, Crabtree GR. 1999.

L-type calcium channels and GSK-3 regulate the activity of NF-ATc4 in hippocampal neurons. Nature 401:703-708.

Grolla AA, Fakhfouri G, Balzaretti G, Marcello E, Gardoni F, Canonico PL, Diluca M, Genazzani AA, Lim D. 2013. Aβ leads to Ca(2+) signaling alterations and transcriptional changes in glial cells. Neurobiol Aging 34:511-522.

Groth RD, Mermelstein PG. 2003. Brain-derived neurotrophic factor activation of NFAT (nuclear factor of activated T-cells)-dependent transcription: a role for the transcription factor NFATc4 in neurotrophin-mediated gene expression. J Neurosci 23:8125-8134.

Grynkiewicz G, Poenie M, Tsien RY. 1885. A new generation of Ca2+ indicators with greatly improved fluorescence properties. J Biol Chem 260:3440-3450.

Guerini D, García-Martin E, Gerber A, Volbracht C, Leist M, Merino CG, Carafoli E. 1999. The expression of plasma membrane Ca2+ pump isoforms in cerebellar granule neurons is modulated by Ca2+. J Biol Chem 274:1667-1676.

Hardy J, Selkoe DJ. 2002. The amyloid hypothesis of Alzheimer's disease: progress and problems on the road to therapeutics. Science 297:353-356.

Jin SM, Cho HJ, Kim YW, Hwang JY, Mook-Jung I. 2012. Aβ-induced Ca(2+) influx regulates astrocytic BACE1 expression via calcineurin/NFAT4 signals. Biochem Biophys Res Commun 425:649-655.

Kagan BL, Thundimadathil J. 2010. Amyloid peptide pores and the beta sheet conformation. Adv Exp Med Biol 677:150-167.

Kawahara M, Kuroda Y. 2000. Molecular mechanism of neurodegeneration induced by Alzheimer's beta-amyloid protein: channel formation and disruption of calcium homeostasis. Brain Res Bull 53:389-397.

Kuchibhotla K V, Goldman ST, Lattarulo CR, Wu HY, Hyman BT, Bacskai BJ. 2008. Abeta plaques lead to aberrant regulation of calcium homeostasis in vivo resulting in structural and functional disruption of neuronal networks. Neuron 59:214-225.

Kuchibhotla KV, Lattarulo CR, Hyman BT, Bacskai BJ. 2009. Synchronous hyperactivity and intercellular calcium waves in astrocytes in Alzheimer mice. Science 323:1211-1215.

Kulijewicz-Nawrot M, Verkhratsky A, Chvátal A, Syková E, Rodríguez JJ. 2012. Astrocytic cytoskeletal atrophy in the medial prefrontal cortex of a triple transgenic mouse model of Alzheimer's disease. J Anat 221:252-262.

Lee JI, Burckart GJ. 1998. Nuclear factor kappa B: important transcription factor and therapeutic target. J Clin Pharmacol 38:981-993.

Luron L, Saliba D, Blazek K, Lanfrancotti A, Udalova IA. 2012. FOXO3 as a new IKK-ε-controlled check-point of regulation of IFN-β expression. Eur J Immunol 42:1030-1037.

Marcello E, Gardoni F, Mauceri D, Romorini S, Jeromin A, Epis R, Borroni B, Cattabeni F, Sala C, Padovani A, Di Luca M. 2007. Synapse-associated protein-97 mediates alpha-secretase ADAM10 trafficking and promotes its activity. J Neurosci 27:1682-1691.

Mehta PD, Pirttila T, Patrick BA, Barshatzky M, Mehta SP. 2001. Amyloid beta protein 1-40 and 1-42 levels in matched cerebrospinal fluid and plasma from patients with Alzheimer disease. Neurosci Lett 304:102-106.

Norris CM, Kadish I, Blalock EM, Chen KC, Thibault V, Porter NM, Landfield PW, Kraner SD. 2005. Calcineurin triggers reactive/inflammatory processes in astrocytes and is upregulated in aging and Alzheimer's models. J Neurosci 25(18):4649-4658.

Palkowitsch L, Marienfeld U, Brunner C, Eitelhuber A, Krappmann D, Marienfeld RB. 2011. The Ca2+-dependent phosphatase calcineurin controls the formation of the Carma1-Bcl10-Malt1 complex during T cell receptor-induced NF-kappaB activation. J Biol Chem 286:7522-7534.

Parpura V, Heneka MT, Montana V, Oliet SH, Schousboe A, Haydon PG, Stout RF Jr, Spray DC, Reichenbach A, Pannicke T, Pekny M, Pekna M, Zorec R. 2012. Glial cells in (patho)physiology. J Neurochem 121:4-27.

Pellistri F, Bucciantini M, Relini A, Nosi D, Gliozzi A, Robello M, Stefani M. 2008. Nonspecific interaction of prefibrillar amyloid aggregates with glutamatergic receptors results in Ca2+ increase in primary neuronal cells. J Biol Chem 283:29950-29960.

Pérez-Ortiz JM, Serrano-Pérez MC, Pastor MD, Martín ED, Calvo S, Rincón M, Tranque P. 2008. Mechanical lesion activates newly identified NFATc1 in primary astrocytes: implication of ATP and purinergic receptors. Eur J Neurosci 27:2453-2465.

Peters O, Schipke CG, Philipps A, Haas B, Pannasch U, Wang LP, Benedetti B,Kingston AE, Kettenmann H. 2009. Astrocyte function is modified by Alzheimer's disease-like pathology in aged mice. J Alzheimers Dis 18:177-189.

Reese LC, Taglialatela G. 2011. A role for calcineurin in Alzheimer's disease. Curr Neuropharmacol 9:685-692.

Rodríguez JJ, Verkhratsky A. Neuroglial roots of neurodegenerative diseases? Mol Neurobiol. 2011 Apr;43(2):87-96.

Rossner S, Lange-Dohna C, Zeitschel U, Perez-Polo JR. 2005. Alzheimer's disease beta-secretase BACE1 is not a neuron-specific enzyme. J Neurochem 92:226-234.

Rubio-Perez JM, Morillas-Ruiz JM. 2012. A review: inflammatory process in Alzheimer's disease, role of cytokines. ScientificWorldJournal. 2012:756357.

Sama MA, Mathis DM, Furman JL, Abdul HM, Artiushin IA, Kraner SD, Norris CM. 2008. Interleukin-1beta-dependent signaling between astrocytes and neurons depends critically on astrocytic calcineurin/NFAT activity. J Biol Chem 283:21953-21964.

Sharp AH, Nucifora FC Jr., Blondel O, Sheppard CA, Zhang C, Snyder SH, Russell JT, Ryugo DK, Ross CA. 1999. Differential cellular expression of isoforms of inositol 1,4,5-triphosphate receptors in neurons and glia in brain. J Comp Neurol 406:207-220.

Supnet C, Bezprozvanny I. 2010. The dysregulation of intracellular calcium in Alzheimer disease. Cell Calcium 47:183-189.

Thibault O, Gant JC, Landfield PW. 2007. Expansion of the calcium hypothesis of brain aging and Alzheimer's disease: minding the store. Aging Cell 6:307-317.

Tu H, Nelson O, Bezprozvanny A, Wang Z, Lee SF, Hao YH, Serneels L, De Strooper B, Yu G, Bezprozvanny I. 2006. Presenilins form ER Ca2+ leak channels, a function disrupted by familial Alzheimer's disease-linked mutations. Cell 126:981-993.

Verkhratsky A, Sofroniew MV, Messing A, deLanerolle NC, Rempe D, Rodríguez JJ, Nedergaard M. 2012. Neurological diseases as primary gliopathies: a reassessment of neurocentrism. ASN Neuro 4:art:e00082.doi:10.1042/AN20120010.

Yeh CY, Vadhwana B, Verkhratsky A, Rodríguez JJ. 2011. Early astrocytic atrophy in the entorhinal cortex of a triple transgenic animal model of Alzheimer's disease. ASN Neuro 3:271-279.

SUPPLEMENTARY MATERIALS

Index

Supplementary Experimental Procedure.

Antibodies and reagents.

Primary antibodies to: mGluR5 (ab53090, for Western Blot (WB) 1:500) was from Abcam (Cambridge, UK). Anti-IP3R1 (WB 1:500) antibody was a kind gift from Dr. Colin Taylor (University of Cambridge). Antibodies to p65 (sc- 372, for immunocytochemistry (ICC) 1:50), CaNAα (sc-6123, WB 1:200), CaNAβ (sc-6124, WB 1:200), Bcl10 (sc-5611, WB 1:500) were from Santa Cruz (Santa Cruz, CA, USA). Anti-phosphoserine (p-Ser, ALX-804-167, WB 1:1000) was from Alexis (Enzo Life Sciences, Lausen, Switzerland); anti-β- actin (A1978, WB 1:4000) was from Sigma. AlexaFluor 488 secondary antibodies were from Life Sciences (Milan, Italy), peroxidase-conjugated secondary antibodies from Pierce (Rockford, IL, USA). (S)-3,5- Dihydroxyphenylglycine (DHPG) from Tocris Bioscience (Bristol, UK). ***Immunocytochemistry*** Glial fibrillary acidic protein (GFAP; polyclonal rabbit, DAKO, Glostrup, Denmark; 1:4000), neuronal nuclear protein (NeuN; mouse clone MAB377, IgG1; Chemicon, Temecula, CA, USA; 1:1000), human leukocyte antigen(HLA)-DP, DQ, DR (HLA-DR; major histocompatibility complex class II, MHC-II; mouse clone CR3/43; DAKO, Glostrup, Denmark, 1:400), Amyloïd-β (Mouse clone 6F/3D; DAKO; 1:200), Phosphorylated Tau (pTau; mouse clone AT8; Innogenetics, Alpharetta, GA , USA; 1:5000) were used in the routine

immunocytochemical analysis. For the detection of mGluR5 we used two antibodies (polyclonal rabbit ab53090, from Abcam, 1:100; polyclonal rabbit from Upstate Biotechnology, Lake Placid, NY; 1:100). For the detection of p65 we used a polyclonal rabbit (sc-372; Santa Cruz; 1:50) and for the detection of CaNAα a polyclonal goat (sc-6123, Santa Cruz; 1:50).

Supplementary Table 1. Oligonucleotide primers used for quantitative realtime (real-time) and semiquantitative (SQ) PCR.

Gene Assession number	**Forward Reverce**	**Sequence 5' to 3'**
mGluR5 NM_017012	Forward Reverce	GCCATGGTAGACATAGTGAAGAGA TAAGAGTGGGCGATGCAAAT
IP3R1 NM_001007235	Forward Reverce	GGCTACAGAGTGCCTGACCT CCATTCGTAGATCCCTCTGC
IP3R2 NM_031046	Forward Reverce	TCCAAAAGACGTTGGACACA TTCATCCCCTTCCTCTGGAT
S18 NM_213557	Forward Reverce	TGCGAGTACTCAACACCAACA CTGCTTTCCTCAACACCACA

Supplementary Table2. Cases included in this study. Summary of clinical and neuropathological data of Alzheimer's disease and control patients

Patients	Sex	Age	Braak's Neurofibrillary Staging	Clinical diagnosis
1	M	89	V	Alzheimer's Disease
2	F	77	V	Alzheimer's Disease
3	F	90	V	Alzheimer's Disease
4	F	70	VI	Alzheimer's Disease
5	M	81	VI	Alzheimer's Disease
6	F	88	VI	Alzheimer's Disease
7	M	86	-	NC
8	M	91	-	NC
9	F	87	-	NC
10	M	79	-	NC
11	M	84	-	NC
12	F	76	-	NC

M = male; F = female; Braak's Neurofibrillary Staging: stage II-VI; NC: normal controls (without evidence of degenerative changes, and lacking a clinical history of cognitive impairment).

Chapter 4

Differential deregulation of astrocytic calcium signalling by amyloid-β, TNFα, IL-1β and LPS

Virginia Ronco[1], Ambra A Grolla[1], Toma N Glasnov[2], Pier Luigi Canonico[1], Alexei Verkhratsky[3,4], Armando A Genazzani[1*], Dmitry Lim[1].

[1]Department of Pharmaceutical Sciences, Università degli Studi del Piemonte Orientale "Amedeo Avogadro", 28100, Novara, Italy.
[2]Christian Doppler Laboratory for Flow Chemistry (CDLFC), Institute of Chemistry, Karl-Franzens-University Graz, Heinrichstrasse 28, A-8010 Graz, Austria.
[3]Faculty of Life Sciences, University of Manchester, Manchester M13 9PL, UK
[4]IKERBASQUE, Basque Foundation for Science, 48011, Bilbao,, 48011, Bilbao, Spain and Department of Neurosciences, University of the Basque Country UPV/EHU & CIBERNED, 48940 Leioa, Spain

Published in Cell Calcium. 2014 Apr. Vol. 55(4):219-29

Abstract

In Alzheimer's disease (AD), astrocytes undergo complex morphological and functional changes that include early atrophy, reactive activation and Ca^{2+} deregulation. Recently, we proposed a mechanism by which nanomolar $A\beta_{42}$ deregulate mGluR5 and $InsP_3$ receptors, key elements of astrocytic Ca^{2+} signalling toolkit. To evaluate the specificity of these changes, we have now investigated whether the effects on Ca^{2+} of $A\beta_{42}$ can be reproduced by pro-inflammatory agents (TNFα, IL-1β, LPS). Here we report that $A\beta_{42}$ (100 nM, 72 h) significantly increased mRNA levels of mGluR5, $InsP_3R1$ and $InsP_3R2$ while pro-inflammatory agents reduced their levels. Furthermore, DHPG-induced Ca^{2+} signals and store operated

Ca^{2+} entry (SOCE) were augmented in $A\beta_{42}$-treated cells due to up-regulation of a set of Ca^{2+} signalling-related genes including TRPC1 and TRPC4. Opposite changes were observed when astrocytes were treated with TNFα, IL-1β and LPS. Last, the effects observed on SOCE by treating wild-type astrocytes with $A\beta_{42}$ were observable in untreated astrocytes from 3xTg-AD animals, suggesting a link to the AD pathology. Our results demonstrate that effects of $A\beta_{42}$ on astrocytic Ca^{2+} signalling differ from and may contrast to the effects of pro-inflammatory agents.

1. Introduction

Astrocytes undergo changes in virtually all neurological diseases, and these changes may either protect against or contribute to pathological developments [1]. An important part of the astroglial defensive programme is represented by reactive astrogliosis triggered by poly-aetiological brain insults [2]. The term “activated" or "reactive" astrocytes groups an array of complex processes affecting astrocytic physiology in a context-dependent manner.

In Alzheimer’s disease (AD), activated astrocytes occur in the late stages of the disease and indeed, in post-mortem brains of Alzheimer’s disease patients, as well as in the brains of model animals, hypertrophic reactive astrocytes surround and penetrate amyloid plaques. Recent findings also suggest that astrocytes may contribute to the early stages of the disease [3] while soluble □-amyloid (A□) may trigger astroglial remodelling that in turn might have repercussions on neurons. In an animal model of AD, for example, basal calcium signalling was found elevated in earlier stages of the disease [4]. Likewise, hippocampal astrocytes have been shown to be atrophic in the entorhinal and mid-prefrontal cortex of the 3xTg-AD mice as early as 1 to 3 months [5,6], and alterations in Ca^{2+} homeostasis are already found in cultured astrocytes from early post-natal 3xTg-AD animals [7].

Recently, we and others have shown that pathologically relevant (100 nM) concentrations of $A\beta_{42}$ oligomers evoke subtle changes in the calcium signalling machinery of cultured hippocampal astrocytes, and that these changes can be, at least in part, re-conducted to gene expression changes mediated by calcineurin [8–11]. Remodelling of the astroglial Ca^{2+} signalling toolkit arises from specific actions of $A\beta_{42}$, as calcium channel blockers (i.e. 2-APB) can block the effects observed, and are specific to selected brain areas, for example these effects are observed in hippocampal but not in entorhinal astrocytes [7].

Astrocytic activation can be also triggered by cytokines released from activated microglia with the pivotal role assigned to interleukin-1 (IL-1β) [12]. For example, interleukin 1β (IL-1β), tumour necrosis factor α (TNFα) and bacterial toxin lipopolysaccharide (LPS) are able to induce transcriptional changes [13] and inflammatory responses [14] in astrocytes.

In the present study we aimed at further understanding whether $A\beta_{42}$ is similar in its actions to other pro-inflammatory agents (TNFα, IL-1β and LPS) or whether it induces a unique signature on expression of activation-related genes and on astrocytic Ca^{2+} signalling. In the course of this study we found that in primary cultured hippocampal astrocytes $A\beta_{42}$ and pro-inflammatory agents exert opposite effects on the metabotropic Ca^{2+} signalling pathway and on store-operated Ca^{2+} entry (SOCE), suggesting that $A\beta_{42}$ is unique in its actions on astrocytes.

2. Materials and Methods

2.1. Cell cultures

For rat astrocyte cultures, Sprague Dawley postnatal days 1-3 (P1-P3) pups were used. For 3xTg-AD mice [15], astroglial cultures were derived from P5-P7 3xTg-AD or wild type pups. Purified astrocytic cultures were prepared as described previously [16]. Hippocampi were dissected from rodent brains, minced and dissociated by incubation with trypsin (0.5 mg/ml, 20 min) followed by gentle

triturating in Hanks′ Balanced Salt Solution (HBSS, Sigma) supplemented with 10% foetal bovine serum (FBS, Immunological Sciences, Rome, Italy), 20 U/ml DNase and 3 mM $MgCl_2$ (both from Sigma). The dissociated cells were then centrifuged at 250 xg, resuspended in Dulbecco's Modified Eagle's Medium, supplemented with 10% FBS, 2mg/ml glutamine, 10U/ml penicillin and 100ug/ml streptomycin (Sigma) and plated in 75 cm^2 flasks (Falcon, BD) treated with 0.1 mg/ml Poly-L-lysine (PLL, Sigma). After confluence (2-4 days) cells were shaked on an orbital shaker to remove microglial contamination (320 rpm, 1-2 h) and re-plated for the experiments on PLL coated plates. Cell culture purity was confirmed by immunostaining with anti-MAP2 (neuronal marker), anti-Iba1 (microglial marker) and anti-GFAP (astroglial marker). Microglial cells were either absent or very sparse, depending on the cell culture, while neurons were absent.

2.2. Aβ preparation

Amyloid β 1-42 ($A\beta_{42}$) oligomers were prepared as described previously [11]. In brief, $A\beta_{42}$ (Innovagen, Lund, Sweden), was dissolved in HFIP (1,1,1,3,3,3-hexa-fluoro-2-propanol, Fluka Cat. 52512) to 1mg/ml, monomerized by 1h incubation at 37°C, lyophilized, resuspended in dry dimethylsulfoxide (DMSO) at 5 mM, diluted in ice-cold MEM to 100 μM and oligomerized for 24h at 4°C. The peptide aliquots were snap frozen and stored at -80°C. In all experiments $A\beta_{42}$ was used at a final concentration of 100 nM. Final DMSO concentration was 0.005%, that was also added to control cells.

2.3. Reagents and drug treatment

IL-1β and TNFα were purchased from ProSpec (Ness-Ziona, Israel) and were used at the final concentration of 10 ng/ml and 20 ng/ml respectively. LPS from Enzo Lifescience (New York, US) was used at the final concentration of 100ng/ml. In all experiments FK506 and 4-Methyl-N1-(3-phenylpropyl)benzene-1,2-diamine (JSH-23, JSH), from Sigma, were used at 100 nM and 20 μM respectively, 2 hours before

Aβ42, IL-1β, TNFα or LPS treatment. (S)-3,5-Dihydroxyphenylglycine (DHPG) and tert-Butylhydroquinone (tBHQ) were from Tocris (Bristol, UK) and both were used at the final concentrations of 50 μM. Thapsigargin was from Sigma.

2.4. Synthesis of Pyr6 and Pyr10 compounds

Pyr6 and Pyr10 compounds were prepared as described previously [17,18]. Their biological characterization has been published elsewhere [19]. Stock solutions of both compounds were in DMSO, and final DMSO concentration was 0.1%, that was also added to control cultures.

2.5. Calcium imaging

For Ca^{2+} imaging, astrocytes grown onto 24 mm round coverslips were loaded with Fura-2/AM (Life Technologies, Milan, Italy) in the presence of 0.01% Pluronic F-127 (Life Technologies) and 10 μM sulfinpyrazone (Sigma) in KRB solution (Krebs-Ringer modified buffer: 125 mM NaCl, 5 mM KCl, 1 mM Na_3PO_4, 1 mM $MgSO_4$, 5.5 mM glucose, 20 mM HEPES, pH 7.4) supplemented with 2 mM $CaCl_2$. After washing and de-esterification the coverslips were mounted in an acquisition chamber on the stage of a Leica epifluorescent microscope equipped with a S Fluor 40x/1.3 objective. Cells were alternatively excited at 340/380 nm by the monochromator Policrome V (Till Photonics, Munich, Germany) and the fluorescent signal was collected by a CCD camera (Hamamatsu, Japan) through bandpass 510 nm filter; the experiments were controlled and images analysed with MetaFluor (Molecular Devices, Sunnyvale, CA, US) software. To quantify the difference in the amplitude of Ca^{2+} transients, the ratio values were normalized according to the formula $(\Delta F)/F_0$ (referred to as norm. ratio). The cells with norm. ratio above 0.1 were considered as responders and used for further analysis.

2.6. Real-time PCR

Total mRNA was extracted from 7.0x10^5 cells using QIAzol Lysis Reagent (Quiagen, Milan, Italy) and retro-transcribed to cDNA using ImProm-II RT system (Promega, Milan, Italy). Real-time PCR was performed using GoTaq qPCR master mix according to manufacturer's instructions (Promega, Milan, Italy) on a SFX96 Real-time system (Biorad, Segrate, Italy). For normalization of the raw qPCR data, three housekeeping genes were tested: i) glyceraldehyde-3-phosphate dehydrogenase (GAPDH), ii) S18 ribosomal subunit and iii) polymerase (RNA) II (DNA directed) polypeptide A (RP2a). S18 exhibited the highest stability across the treatments and was used for normalization of raw data in all qPCR experiments. For single treatments (JSH-23 or $A\beta_{42}$, TNFα, IL-1β or LPS alone) the relative gene expression was normalized to control samples. For double treatments (pre-treatment with JSH-23 and stimulation with $A\beta_{42}$, TNFα, IL-1β or LPS, Fig. 3A-D) the data were normalized to its respective control. Oligonucleotide primers used for real-time PCR are listed in Supplementary Table 1.

2.7. Western Blot

3-5x10^5 glial cells were plated in 60 mm Petri dishes and treated with $A\beta_{42}$, TNFα, IL-1β and LPS. At the indicated time-points the cells were lysed in 60 µL Laemmli sample buffer (Bio-Rad) and 15 µL of each sample was run on 10% SDS-PAGE, blotted onto nitrocellulose membrane and probed with rabbit polyclonal anti-IkBα antibody (1:1000, cat. cs-371, Santa Cruz Dallas, TX, US). After incubation with anti-rabbit HRP conjugated secondary antibodies, luminescent signals, produced by ECL substrate (Pierce, Thermo Scientific, Rockford, IL, USA) were imaged with ChemiDoc system using Quantity One v. 4.6 software (Bio-Rad, Segrate, Italy). For normalization, the membrane was probed with anti-β-actin (A1978, 1:4000, Sigma, Milano, Italy) antibody.

2.8. Immunocytochemistry

For immunocytochemical analysis 5 x 10^4 astrocytes were plated onto PLL-treated (0.5 mg/ml) 13 mm coverslips in 24-well plates. 72 hours after treatment cells were fixed for 20 min in 4% formaldehyde in PBS and permeabilized form 8 min with 0.1% Triton X-100 (all at 4°C). Then primary anti-glial fibrillary acidic protein (GFAP, 1h, 37°C, 1:200, Merk Millipore, Bellerica, MA, US) and secondary Alexa-488-conjugated antibody (1h, RT, 1:200, Life Technologies, Monza, Italy) antibody were applied in PBS with 2% gelatin. After washing (3x5min), nuclei were stained with 4′,6-Diamidino-2-phenylindole dihydrochloride (DAPI) for 15 min at RT. Fluorescence images were acquired using a Leica (Leica Microsystems, Wetzlar, Germany) epifluorescent microscope equipped with S Fluor 40x/1.3 objective using MetaMorph (Molecular Devices, Sunnyvale, CA, US) software.

2.8. Statistical analysis

Two-tail Student's t-test or one-sample t-test were used for statistical analysis. Differences were considered significant at $p < 0.05$.

3. Results

3.1. Differential effects of $A\beta_{42}$ and pro-inflammatory agents on expression of astrogliosis-related genes

In the first series of experiments we explored the effects of 24 hour treatment with $A\beta_{42}$, TNFα, IL-1β, and LPS on the mRNA expression of GFAP, vimentin and S100β. As shown in Fig. 1, $A\beta_{42}$ somewhat increased expression of GFAP and vimentin although these changes did not reach significance, whereas expression of S100β was significantly augmented. Conversely, treatment of astrocytes with TNFα, IL-1β and LPS markedly inhibited expression of all three genes under study, this effect being the most prominent after LPS treatment. Immunocytochemical analysis after 72 hours using an anti-GFAP antibody confirmed the mRNA data (Fig. 1D). GFAP staining of $A\beta_{42}$-treated astrocytes was not much different from control cells,

whereas cells treated with TNFα, IL-1β and LPS demonstrated weaker immunoreactivity. A lower density of astrocytes was noted in samples treated with IL-1 and LPS.

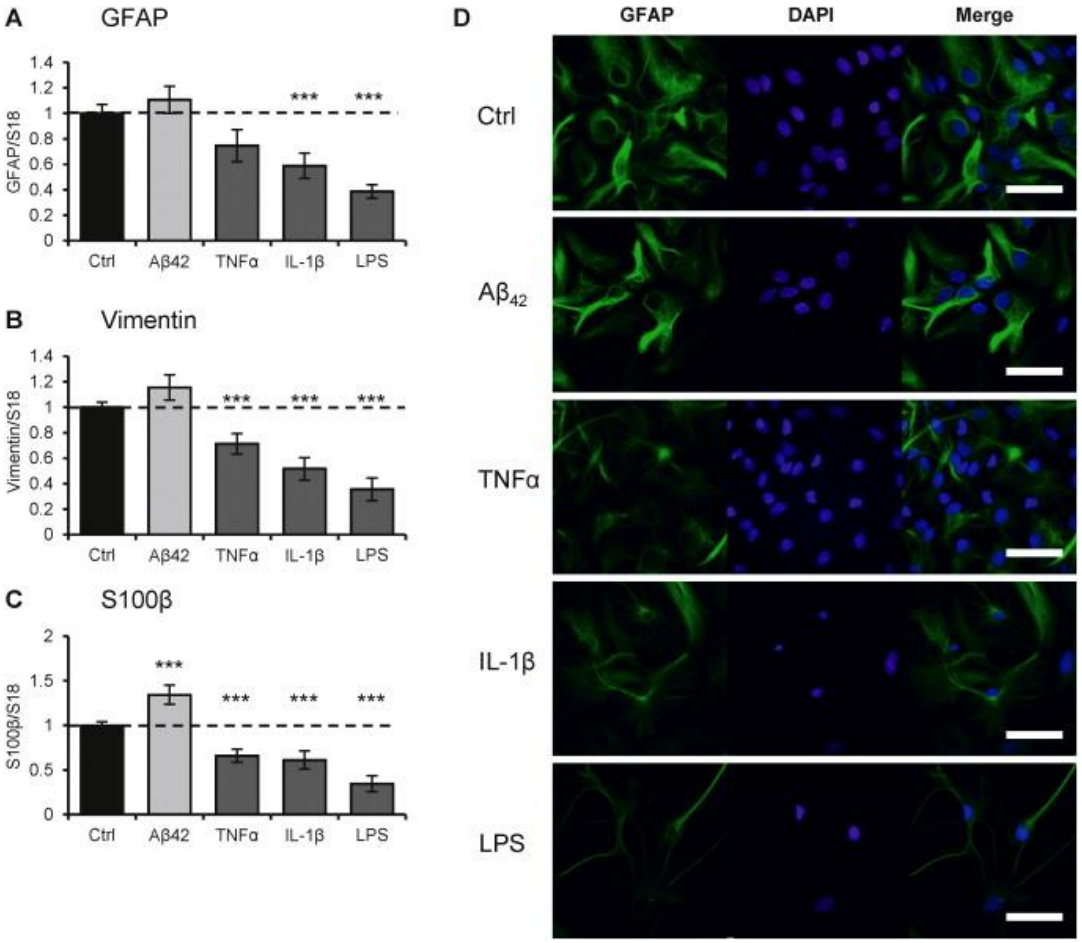

Figure 1. Differential effects of $A\beta_{42}$, TNFα, IL-1β and LPS on expression of markers of astrocytic activation

Rat primary hippocampal astrocytes were treated with 100 nM $A\beta_{42}$, 20 ng/ml TNFα, 10 ng/ml IL-1β or 100 ng/ml LPS for 24 h (for real-time PCR, panels **A**, **B** and **C**) or for 72 h (for immunocytochemistry, panel **D**).

Real-time PCR data were normalized to S18 ribosomal protein mRNA and expressed as mean ± SEM reported to control. The data are from 6-7 independent cultures performed in triplicate. ***$p < 0.001$. For immunocytochemistry (**C**) astrocytes were probed for GFAP (green) and nuclei were counterstained with DAPI (blue). Representative fields are taken from 2 independent cultures prepared in triplicate. Scale bar in (**D**) 45 μm.

3.2. DHPG-induced calcium responses are different in hippocampal astrocytes treated with Aβ$_{42}$, TNFα, IL-1β and LPS

Previously, we have demonstrated that Aβ$_{42}$ potentiated Ca^{2+} responses to the group I metabotropic glutamate receptor agonist DHPG in hippocampal astrocytes [10,11]. Here, we compared DHPG-induced Ca^{2+} signals in astrocytes following treatment with Aβ$_{42}$, TNFα, IL-1β and LPS. In control astrocytes, 50 μM DHPG induced a rapid Ca^{2+} rise in the cytosol (which peaked at 0.59 ± 0.003 norm. ratio, n = 172, Fig. 2A) that was followed by a plateau that lasted for up to 10 minutes. To quantify this long-lasting cytosolic Ca^{2+} elevation alongside with the peak of the transient we measured the area under the curve (AUC) during 200 seconds from the moment of addition of DHPG. The measurements were performed only for cells in which Ca^{2+} transients reached 0.1 of normalized ratio value. These cells were considered as responders and the fraction of these cells over total cell number was also calculated (Fig. 2F). As shown in Fig. 2, and in line with our previous reports, Aβ$_{42}$ significantly increased both the peak (0.68 ± 0.003 norm. ratio vs. control 0.59 ± 0.003 norm.ratio, p = 0.005, n = 169) of the DHPG-induced Ca^{2+} transient and the AUC (44.1 ± 0.027 a.u. vs. 31.15 ± 0.025 a.u. in control cells, p = 5.8e-9) without affecting the percentage of responding cells. None of the pro-inflammatory factors (TNFα, IL-1β, and LPS) altered the amplitude of the peak of DHPG-induced Ca^{2+} response, while dramatically reducing both the AUC of responding cells (24.29 ± 0.052 a.u., p = 0.0083, n = 89 for TNFα; 23.32 ± 0.041 a.u., p = 0.0006, n = 94 for IL-1β; and 24.54 ± 0.056 a.u., p = 0.027, n = 97 for LPS with respect to control cells) and the fraction of responding cells (percentage of responding cells was 60 ± 4.5%, p = 0.0081 for

TNFα; 68 ± 4.84%, p = 0.043 for IL-1β; and 50 ± 4.81%, p = 0.002 for LPS whereas in control conditions 89 ± 3.58% cells generated Ca^{2+} signal).

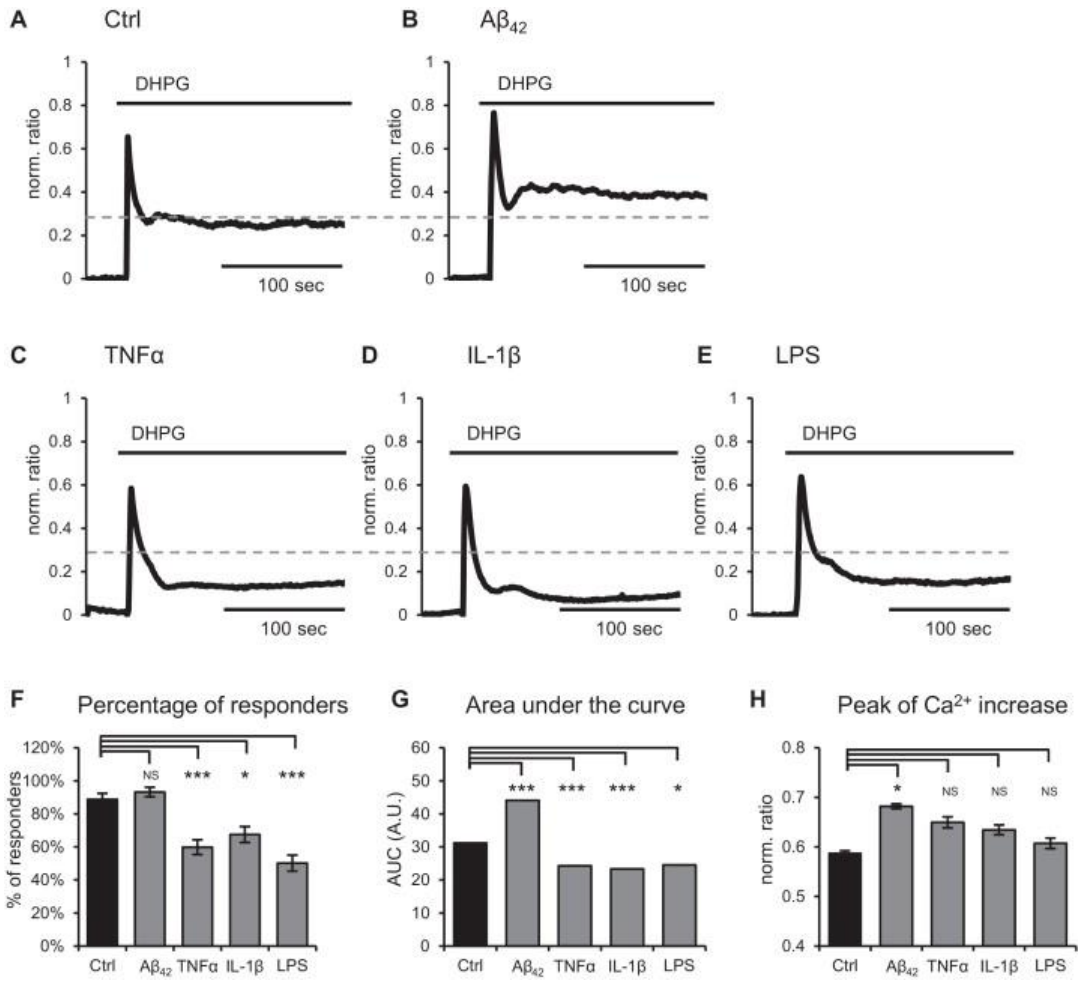

Figure 2. DHPG-induced Ca^{2+} responses are potentiated by $A\beta_{42}$ but inhibited by TNFα, IL-1β and LPS.

Representative traces of hippocampal astrocytes were either not treated (**A**) or treated with $A\beta_{42}$, TNFα, IL-1β and LPS for 72 h (**B**, **C**, **D** and **E**, respectively). On the day of the experiment, cells were loaded with Fura-2-AM and stimulated with 50 μM DHPG. Histograms illustrate the percentage of responding cells (**F**), area under the curve (AUC) (**G**) and peaks of the first Ca^{2+} transients (**H**) for each condition. Data are expressed as mean ± SEM for 94-172 cells acquired from 3-4 independent cultures and 4-6 coverslips per culture. *p < 0.05; ***p < 0.001; NS not significant.

3.3. Differential effect of $A\beta_{42}$ and pro-inflammatory factors on mRNA expression of glutamate metabotropic receptors and $InsP_3$ receptors

Subsequently, we analyzed whether TNFα, IL-1β and LPS induced different transcriptional changes in Ca^{2+} signalling genes. For this purpose, we performed quantitative real-time PCR experiments using specific primers for mGluR5, mGluR3, $InsP_3R1$ and $InsP_3R2$ (Fig. 3). As we had previously shown that the effects of $A\beta_{42}$ are in part mediated by NF-kB, we also investigated the involvement of this transcription factor using a NF-kB nuclear translocation inhibitor, JSH-23 [20]. The expression of the four studied genes in control non-stimulated cells was significantly reduced by pre-treatment with JSH-23 (Fig. 3A), suggesting a role of NF-kB in maintaining basal mRNA levels. To correct for this, all data in stimulated cells in the presence of JSH-23 were normalized to control JSH-treated cells. In line with our previous finding, $A\beta_{42}$ increased mRNA expression of the key components of the astroglial Ca^{2+} signalling, mGluR5, $InsP_3R1$ and $InsP_3R2$. This increase was not apparent when cells were pre-incubated with the NF-kB nuclear translocation inhibitor JSH-23 [20]. The expression of mGluR3 was also increased by 100 nM $A\beta_{42}$ in an NF-kB dependent manner. Similarly, and as previously shown in the literature, the three pro-inflammatory agents, TNFα, IL-1β and LPS, increased significantly the expression of mGluR3 (Fig. 3C). The effects of $A\beta_{42}$, TNFα and LPS were not evident in the presence of JSH-23, suggesting the involvement of NF-kB. On the other hand, TNFα, IL-1β and LPS all exerted a strong inhibitory effect on expression of mGluR5 (Fig. 3B), $InsP_3R1$ (Fig. 3D) and $InsP_3R2$ (Fig. 3E). Inhibition of NF-kB strongly attenuated the effects of TNFα and IL-1β, while it had a more complex effect on stimulation with LPS. These data confirm the results of Ca^{2+} imaging experiments and emphasize the differential effect of $A\beta_{42}$ and pro-inflammatory factors on astrocytic Ca^{2+} signalling.

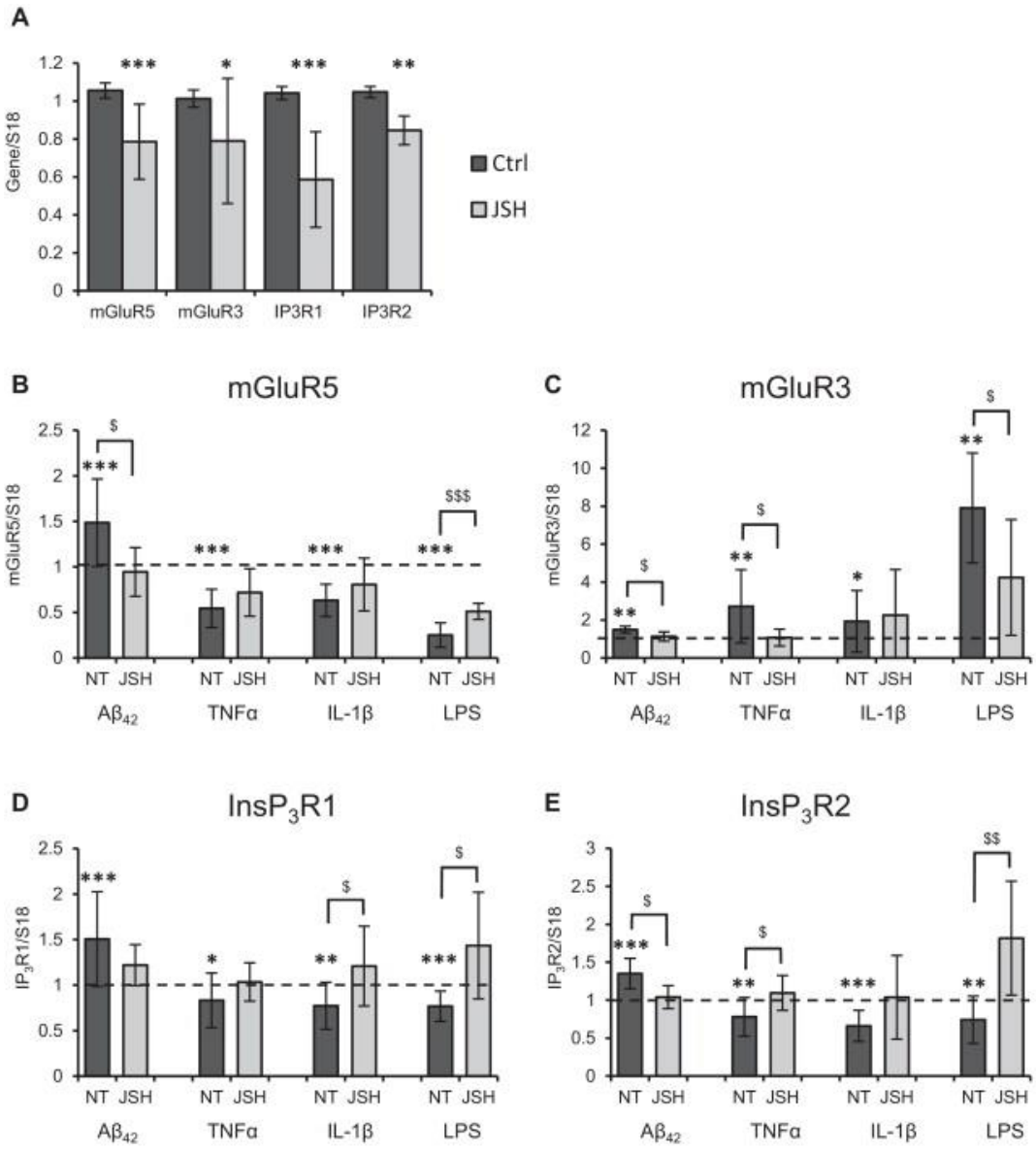

Figure 3. Differential effect of Aβ$_{42}$, TNFα, IL-1β and LPS on mRNA levels of metabotropic glutamate receptors and InsP$_3$ receptors type 1 and 2.

(**A**) Effect of JSH-23 (20 μM, light-grey bars) on basal expression of the indicated genes. Data is normalized to control samples. (**B-E**) Effect of Aβ$_{42}$, TNFα, IL-1β or LPS in control (dark grey bars) or JSH-23 pre-treated (light grey bars) samples on mGluR5 (panel **B**), mGluR3 (panel **C**), InsP$_3$R1 (panel **D**), or InsP$_3$R2 (panel **E**). Given the effect of JSH-23 on basal levels (panel **A**), samples were normalized to respective controls (i.e. non pre-treated or pre-treated with JSH-23).

The data are expressed as mean ± SD from 3-9 independent cultures performed in duplicate or triplicate. *$p < 0.05$; **$p < 0.01$; ***$p < 0.001$ vs non-pre-treated respective control; $^{\$}p < 0.05$; $^{\$\$}p < 0.01$, $^{\$\$\$}p < 0.001$ JSH-23 pre-treated cells and stimulated with the indicated substance vs non JSH-23 pre-treated cells stimulated with the indicated substance.

3.4. Effect of $A\beta_{42}$ on degradation of IkBα is calcineurin-dependent, whereas effects of TNFα, IL-1β and of LPS are not

Since in hippocampal astrocytes the Ca^{2+}-dependent phosphatase calcineurin (CaN) is involved in the $A\beta_{42}$-induced NF-kB activation [11] we analyzed if this may also be the case for TNFα, IL-1β and LPS, because all these three drugs activate NF-kB [13]. We monitored NF-kB activation by measuring the degradation of its endogenous inhibitor IkBα at different time-points after addition of the stimulus (Fig. 4). 100 nM $A\beta_{42}$ induced a significant reduction in IkBα protein quantity 4-7 hours after addition of $A\beta_{42}$. The reduction was fully restored by pre-incubation of astrocytes with 100 nM FK506, a potent calcineurin inhibitor (Fig. 4A). In astrocytes, TNFα is known to produce a biphasic degradation of IkBα, the first phase peaking before 1 hour of treatment and the second phase between 2 and 4 hours [21]. We thus investigated CaN sensitivity of these phases (Fig. 4B). Addition of 20 ng/ml TNFα induced rapid degradation of IkBα, which peaked 20-30 minutes after addition of TNFα. In our experiments, the IkBα protein was fully re-synthesized within 1 hour. The second phase of IkBα degradation was less marked but lasted for all the duration of the experiment (9 hours). For both phases, pre-treatment with FK506 had no effect on degradation of IkBα.

IL-1β is a potent NF-kB activator. As shown in Fig. 4C, IL-1β induced a rapid reduction in IkBα protein level, which peaked at 0.5 hours and was restored by about 80% at 4 hours after addition of IL-1β. IL-1β-induced IkBα degradation in hippocampal astrocytes was insensitive to inhibition of CaN.

Finally, IkBα degradation induced by LPS treatment reached its through peak around 2 hours of treatment with a very slow recovery, which was not sensitive to inhibition of CaN (Fig. 4D).

Figure 4. Degradation of IkBα induced by $A\beta_{42}$ is calcineurin-dependent, while the effects induced by TNFα, IL-1β and LPS are not.

Astrocytes were pre-treated (open bars in histograms) or not (black bars) with 100 nM FK506 for 2-4 h and then stimulated with $A\beta_{42}$ (**A**), TNFα (**B**), IL-1β (**C**) and LPS (**D**). Representative images are shown from three independent cultures performed in duplicate. Data in histograms are expressed as mean ± SEM. *$p < 0.05$; **$p < 0.01$; ***$p < 0.001$.

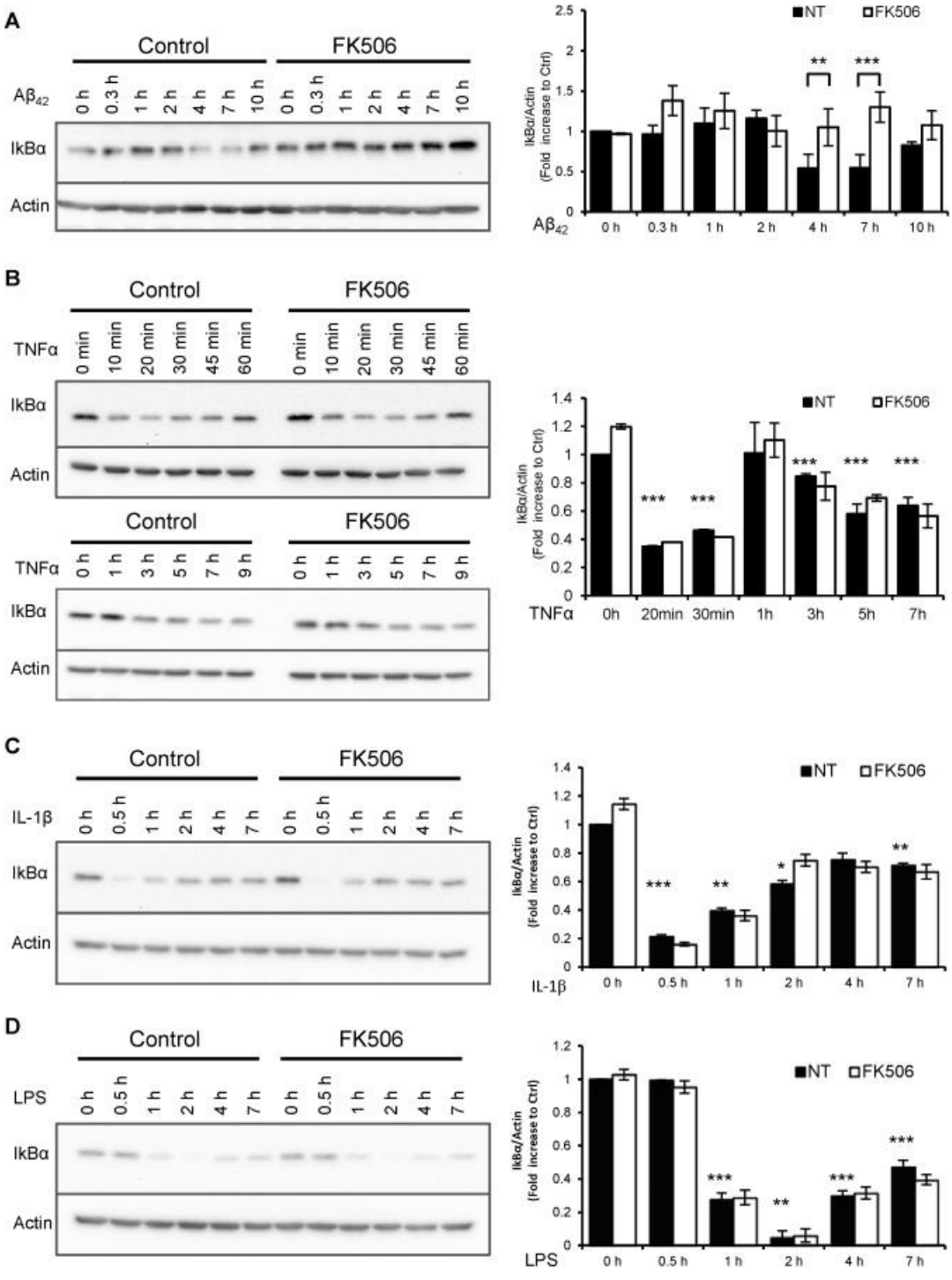
A
Control
FK506
Aβ42
0 h
0.3 h
1 h
2 h
4 h
7 h
10 h
IkBα
Actin
NT
FK506
IkBα/Actin
(Fold increase to Ctrl)
B
TNFα
0 min
10 min
20 min
30 min
45 min
60 min
0 h
1 h
3 h
5 h
7 h
9 h
C
IL-1β
0.5 h
D
LPS

3.5. DHPG-induced calcium entry in hippocampal astrocytes is mediated mainly by SOCE

Although the G-protein-coupled receptor (GPCR)-$InsP_3Rs$ axis represents the major route to initiate the Ca^{2+} increase in the cytosol of an astrocyte, Ca^{2+} entry through the plasma membrane (PM) constitutes the main source for long-lasting Ca^{2+} elevations [22]. Two main mechanisms for Ca^{2+} entry have been proposed, namely, store operated calcium entry (SOCE) activated by the Ca^{2+} depletion of the ER and the receptor operated calcium entry (ROCE) governed by the plasmalemmal receptors [23]. It is generally acknowledged that SOCE is mainly regulated by Orai proteins, whereas channels of TRP family are preferentially responsible for ROCE [24], although this matter remains controversial [23]. To reveal the nature of the plateau phase of DHPG-evoked Ca^{2+} responses we studied its dependence on extracellular Ca^{2+}. As shown in Fig. 5A, stimulation of astrocytes with 50 μM DHPG in Ca^{2+}-free solution containing 100 μM EGTA resulted in a Ca^{2+} transient which rapidly decayed to the baseline level in contrast to the cells stimulated in presence of 2 mM Ca^{2+}. In the subsequent experiment we stimulated the astrocytes in presence of Ca^{2+} and after about 100 sec switched the perfusion to Ca^{2+}-free solution (Fig. 5B). Withdrawal of Ca^{2+} from the perfusion medium rapidly and completely inhibited the plateau of the Ca^{2+} transient (i.e. cytosolic free Ca^{2+} returned to the baseline level), confirming thus the essential role of the transmembrane Ca^{2+} entry for maintaining the long lasting Ca^{2+} plateau. Similar results were obtained when a specific blocker of mGluR5 (MTEP, 500 nM) was applied in the presence of 2 mM Ca^{2+} (Fig. 5C) confirming the mGluR5 specificity of the Ca^{2+} response [10] and indicating that continuous stimulation of the mGluR5 is necessary for opening of the Ca^{2+} channels responsible for the Ca^{2+} entry.

Next we investigated the mechanism by which Ca^{2+} enters the astrocyte. It has been proposed that pyrazole compounds (i.e. Pyr6 and Pyr10) are able to discriminate between SOCE and ROCE [19]. Although it might be claimed that Pyr6 preferentially affects Orai-mediated responses and Pyr10 preferentially affects

TRPC-mediated responses, this has only been directly proven for Orai1 and TRPC3 [19]. First, we analyzed whether Pyr6 and Pyr10 acted on astrocytes similarly to HEK293/RBL-2H3 cells expressing TRPC3 [19]. We found that Pyr6 (5 □M) but not Pyr10 effectively inhibited tBHQ-induced SOCE in cultured hippocampal astrocytes (Suppl. Fig. 1). Next, we used Pyr compounds to investigate the nature of the DHPG-induced Ca^{2+} entry in untreated hippocampal astrocytes. As shown in Fig. 5E, pre-incubation with 5 μM Pyr6 completely abolished the plateau phase of Ca^{2+} elevation (0.055 ± 0.016 norm. ratio, n = 70 for Pyr6 vs 0.21 ± 0.022 norm. ratio, n = 85 for control, p = 6.5e-6, Fig. 5D), whereas Pyr10 had little, if any, effect on this plateau phase (0.22 ± 0.054 norm. ratio, n = 65, p = 0.15, Fig. 5F). Interestingly, Pyr10 reduced the peak of the initial Ca^{2+} transient induced by application of the agonist (0.57 ± 0.012 norm. ratio for Pyr10 vs. 0.63 ± 0.031 norm. ratio for control, p = 0.04), suggesting that a PyR10-sensitive component contributes to the transient. We also investigated whether DHPG-induced Ca^{2+} entry was modified in $A\beta_{42}$-treated astrocytes. As expected, the total Ca^{2+}-peak and the plateau phase of Ca^{2+} elevation was increased (Fig. 5F-G), but Ca^{2+}-entry remained solely sensitive to Pyr6, as in untreated cells (0.03 ± 0.005 norm. ratio, n = 37 for Pyr6 vs 0.31 ± 0.028 norm. ratio, n = 28 for $A\beta_{42}$-treated cells, p = 2e-16, 0.22 ± 0.054 norm. ratio for Pyr10, p = 0.1 vs $A\beta_{42}$-treated cells, Fig. 5E).

Figure 5. DHPG-induced Ca^{2+} entry in hippocampal astrocytes is mediated by SOCE.

(**A**) Primary hippocampal astrocytes were loaded with Fura-2 and stimulated with 50 μM DHPG in Ca^{2+}-free solution. (**B**) Cells were stimulated with DHPG in Ca^{2+}-containing solution which, after 100 sec, was switched to Ca^{2+}-free solution. (**C**) Cells were stimulated with DHPG in presence of Ca^{2+}, and after 100 sec were perfused with 500 nM MTEP. Representative traces from at least 5 independent experiments are shown.

(**D**) Control astrocytes (treated with 0.1% DMSO) and astrocytes pre-treated with Pyr6 or Pyr10 (5 min, 5 μM) were stimulated with 50 μM DHPG in Ca^{2+} containing KRB solution. (**E**) Astrocytes were pre-treated with 100 nM $A\beta_{42}$ for 72 h prior to addition of Pyr compounds. Average traces from representative experiments are shown (control (vehicle), black lines; Pyr6, grey lines; Pyr10, light-gray lines). (**F**) Quantification of the intracellular Ca^{2+} levels at 150 sec after DHPG stimulation as indicated by vertical dashed line in **D** and **E**. (**G**) Quantification of the amplitude of the Ca^{2+} peaks. Data are expressed as mean ± SEM of 28-85 cells from 6-8 coverslips from 3 independent cultures. **p < 0.01; ***p < 0.001; NS non significant.

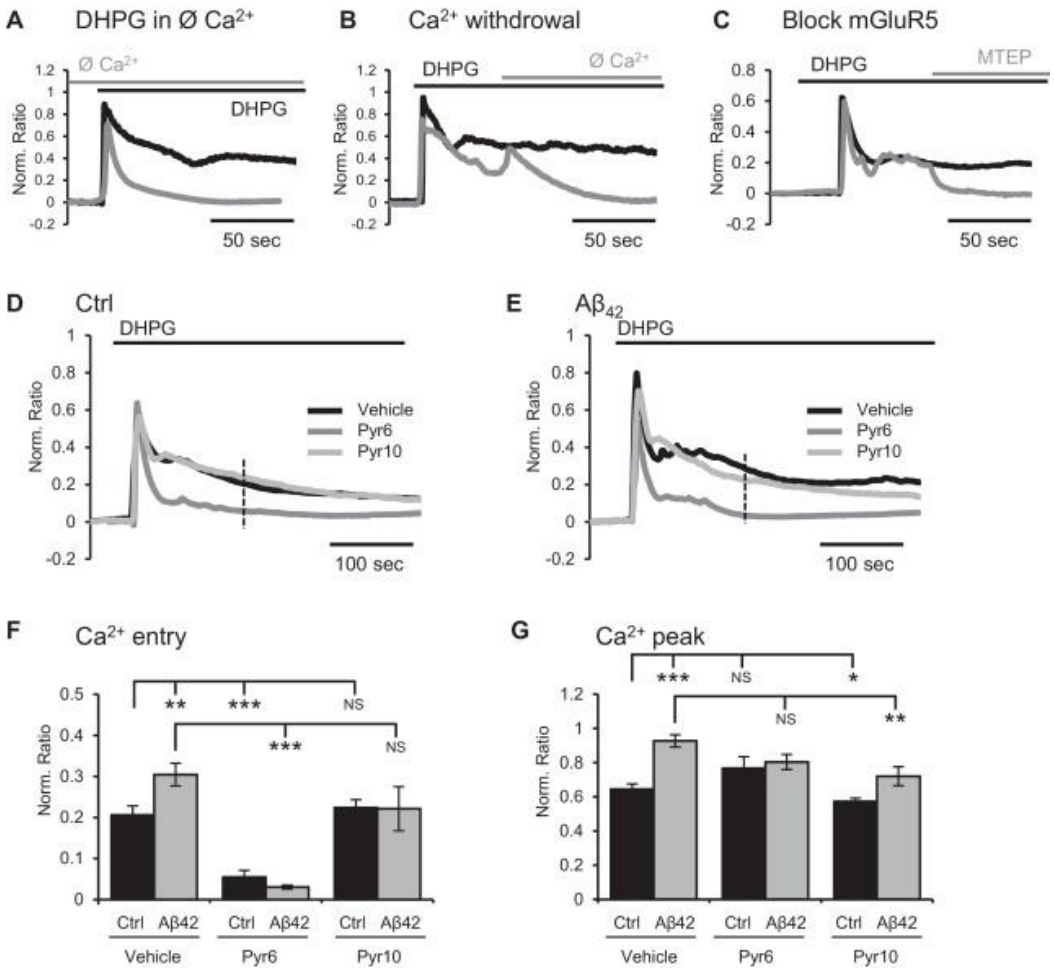

3.6. Differential effect of $A\beta_{42}$ and pro-inflammatory drugs on expression of Orai and TRPC mRNA

Next, we analyzed the mRNA levels of TRPC and Orai channels in cultured astrocytes. First, employing real-time PCR we evaluated relative expression of TRPC channel genes that have been previously shown to be expressed and functional in astrocytes. Fig. 6A shows that TRPC1 and TRPC4 are expressed at the same level and their mRNA quantity is about 8-fold more abundant than mRNA level of TRPC5 with almost undetectable levels of TRPC3, which indicates that TRPC1 and TRPC4 are major contributors. In the next series of experiments we explored the effects of $A\beta_{42}$, TNFα, IL-1β and LPS on expression of TRPC channels. TRPC1 and TRPC5 mRNA were up-regulated by 24 hours pre-treatment with 100 nM $A\beta_{42}$, and conversely, TRPC1, TRPC4 and TRPC5 were down-regulated by TNFα and IL-1β. LPS had a significant stimulatory effect on TRPC5 expression at the same time significantly down-regulating TRPC1 and TRPC4 (Fig. 6B, D). Subsequently, we compared relative expression of Orai genes in cultured hippocampal astrocytes. Surprisingly, two pairs of primers specific to different regions of Orai1 mRNA failed to produce any product, although Orai2 and Orai3 were expressed. Quantitative analysis confirmed this finding and demonstrated that Orai3 was the predominant isoform expressed in hippocampal rat astrocytes being 6 fold more abundant than Orai2 mRNA (Fig. 6F). Orai2 was significantly up-regulated by 100 nM $A\beta_{42}$, TNFα and LPS, but was unchanged after IL-1β treatment (Fig. 6G), although Orai3 was significantly down-regulated by all three pro-inflammatory factors (Fig 6H). The above data show that $A\beta_{42}$ treatment for 24 h affects TRPCs and Orais mRNA levels differently compared to TNFα, Il-1β and LPS. Yet, it is difficult to reconcile the changes seen with the functional data in Fig. 5 and with the data on Pyr6 and Pyr10. Further experiments on protein levels and cellular localization of these channels as well as a more thorough understanding of the specificity of Pyr6 and Pyr10 compounds would be warranted to understand the underlying mechanisms that lead

to an increase of Ca^{2+} entry in $A\beta_{42}$-treated cells and a decrease upon TNFα, Il-1β and LPS treatment.

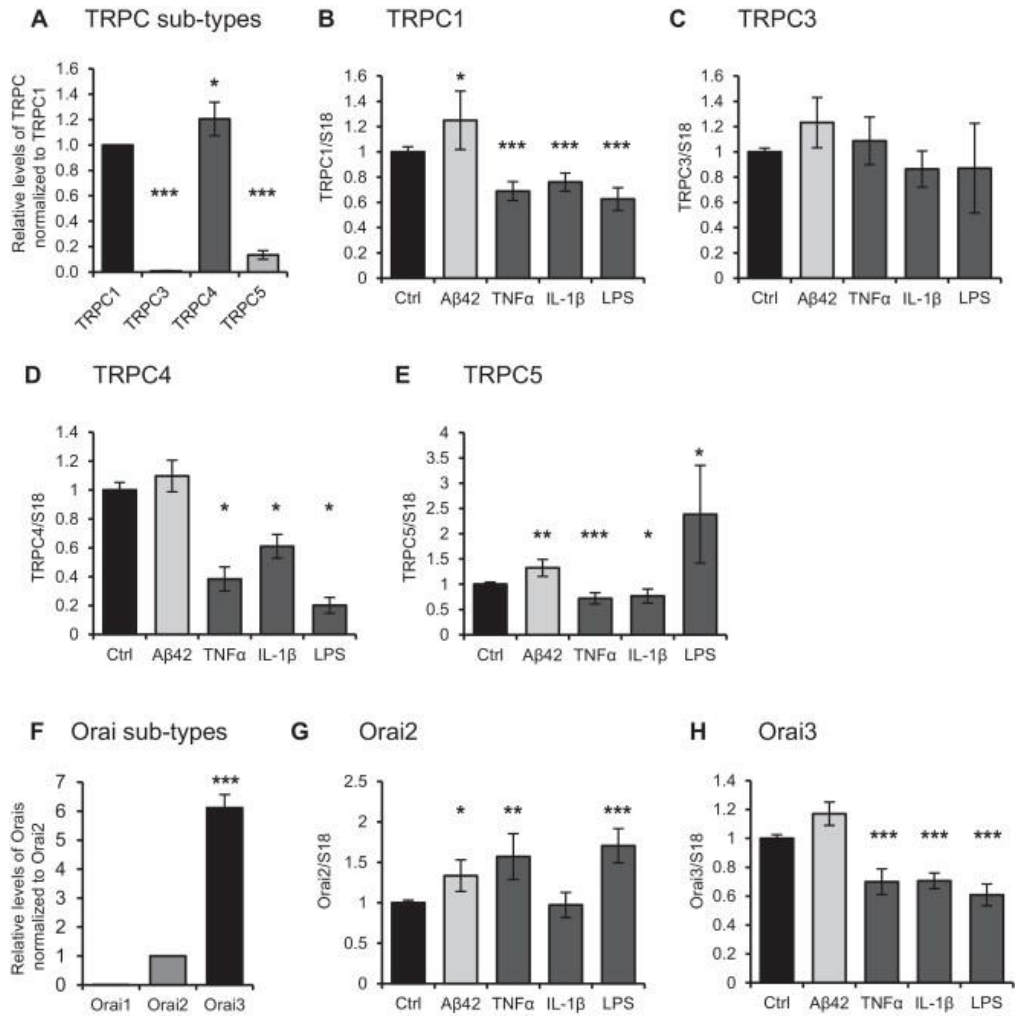

Figure 6. Differential effect of $A\beta_{42}$, TNFα, IL-1β and LPS on mRNA levels of Orai and TRPC.

Relative mRNA levels of TRPC (**A**) and Orai (**F**) gene families members in untreated cultured rat hippocampal astrocytes. Astrocyte were stimulated with $A\beta_{42}$, TNFα, IL-1β and LPS for 24 h and then used for real-time analysis using specific primers for TRPC1, TRPC3, TRPC4 and TRPC5 (**B**, **C**, **D**, and **E**, respectively) or for Orai2 and Orai3 (**G** and **H**, respectively). Data are expressed as mean ± SEM of three independent cultures performed in triplicate. *$p < 0.05$; **$p < 0.01$; ***$p < 0.001$.

3.7. Store-operated calcium entry is potentiated in Aβ$_{42}$-treated hippocampal astrocytes and in astrocytes from 3xTg-AD mice

Next, we directly measured SOCE in control and Aβ$_{42}$-treated astrocytes by a classical protocol of re-addition of Ca^{2+} in the perfusate after depletion of Ca^{2+} stores with tBHQ (50 μM for 5 min). As shown in Fig. 7A, 72 h pre-treatment with 100 nM Aβ$_{42}$ resulted in a 10% increase of Ca^{2+} entry compared to control cells as was measured in terms of AUC. This increase, however, was highly significant (121.49 ± 2.7 a.u., n = 572 for control vs. Aβ$_{42}$ 134.78 ± 2.87 a.u., n = 542 for Aβ$_{42}$-treated cells, p = 0.00078; Fig. 7A, B). This result is in line with mRNA expression data and supports the hypothesis that Aβ$_{42}$-potentiated long-lasting Ca^{2+} signals induced by DHPG are mediated by SOCE. Given the absence of the plateau phase in TNFα, IL-1β and LPS, these experiments were not performed.

To investigate whether the changes in astrocytic SOCE produced by exogenous Aβ$_{42}$ treatment might be relevant to the AD pathology, we dissociated hippocampal astrocytes from wild-type (WT) and 3xTg-AD mice pups and measured SOCE after the depletion of internal Ca^{2+} stores with 1 μM thapsigargin. Fig. 7C demonstrates that in 3xTg-AD astrocytes SOCE was more than twice higher in terms of AUC (12.6 ± 1.07 a.u., n = 36) as compared with WT astrocytes (5.86 ± 0.76 a.u., p = 4.01e-6, n = 22). To confirm that exogenous Aβ$_{42}$ treatment affected mouse hippocampal astrocytes in a similar manner compared to rat astrocytes, the astrocytes from WT mice were treated for 72 h with 100 nM oligomeric Aβ$_{42}$. As shown in Fig. 7C (open diamonds), SOCE was significantly increased (14.9 ± 1.48 a.u., n = 24) and was not different from that of the 3xTg-AD astrocytes (p = 0.204). At the same time exogenous Aβ$_{42}$ failed to affect SOCE in 3xTg-AD astrocytes (13.5 ± 1.48 a.u., n = 30, p = 0.29) which is in line with our previous report in which Aβ$_{42}$ failed to further increase ATP-induced Ca^{2+} transients in hippocampal astrocytes from 3xTg-AD mice [7]. These results confirm our experiments with exogenously added Aβ$_{42}$ and indicate that the increased SOCE may have a role in derangement of Ca^{2+} homeostasis in AD.

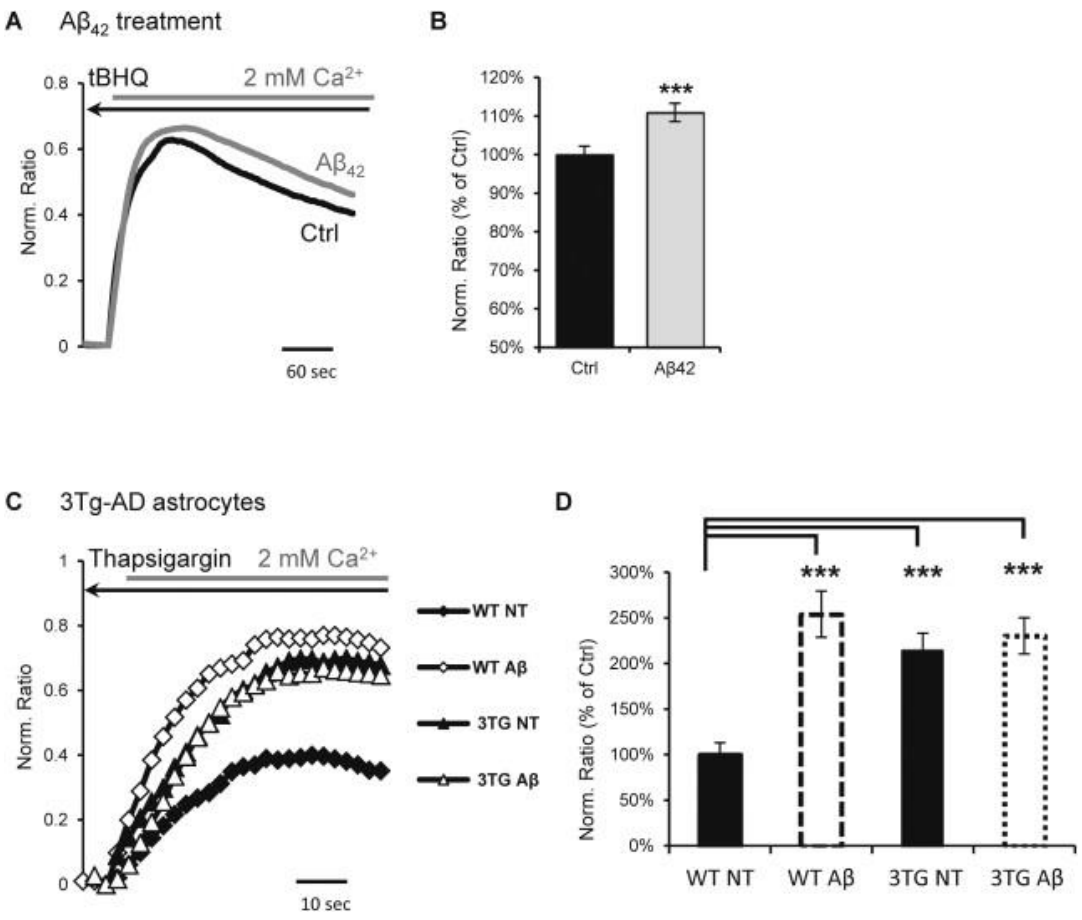

Figures 7. Store operated Ca^{2+} entry is potentiated in $A\beta_{42}$-treated rat hippocampal astrocytes and in hippocampal astrocytes from 3xTg-AD mice.

(**A**) Cultured rat primary hippocampal astrocytes were treated with 100 nM $A\beta_{42}$ for 72 h. On the day of experiment, cells were loaded with Fura-2 and internal Ca^{2+} stores were depleted with 50 μM tBHQ for 5 min. After that, 2 mM Ca^{2+} was added and SOCE was measured as the area under the curve (AUC) of the Ca^{2+} transients in control (black line in **A** and black bar in **B**) and $A\beta_{42}$-treated astrocytes (grey line in **A** and grey bar in **B**). (**C**) Astrocytes form WT and 3xTg-AD (3TG) mice were treated (open diamonds and triangles on **C** and open bars on **D**) or not treated (filled diamonds and triangles on **C** and filled bars on **D**) with $A\beta_{42}$ for 72h. At the day of the experiments, cells were loaded with Fura-2 and the internal Ca^{2+} stores were depleted by perfusing with 1 μM thapsigargin. After that, perfusion was switched to the solution containing 2 mM Ca^{2+} and the SOCE was measured as above. Data in histograms in **B** and **D** are expressed as mean ± SEM for 6-9 coverslips from 3 independent cultures.

4. Discussion

In the present study we analyzed whether $A\beta_{42}$, TNFα, IL-1β and LPS had differential effects on calcium signalling and on the transcriptional regulation of genes related to the calcium toolkit in rat primary hippocampal astrocytes.

Our main observation is that the effects of $A\beta_{42}$ and pro-inflammatory factors on the Ca^{2+} signalling toolkit and on cytosolic Ca^{2+} dynamics are different. To the best of our knowledge, this is the first attempt to compare effects of these substances on astroglial signalling pathways. The most striking of these differences is probably represented by the potentiation of SOCE by $A\beta_{42}$ and the inhibition of SOCE by the other three agents. We may therefore conclude that $A\beta_{42}$ cannot be regarded as a traditional pro-inflammatory agent; to the contrary $A\beta_{42}$ employs idiosyncratic pathways to affect the astroglial state and function.

It is important to note that the qPCR data in this manuscript reflects mRNA changes after 24 hour treatments, while Ca^{2+}-signalling experiments were performed at 72 hours. We have previously shown for mGluR5 and $InsP_3R1$ that an increase in mRNA levels at 24 hours is followed by an increase in protein levels at 72 hours and similar data on GFAP is presented here (Fig.1). Yet, we do not have data on inflammatory cytokines and other genes and therefore a direct relationship between qPCR experiments (Fig. 3 and 6) and Ca^{2+}-signalling (Fig. 2 and 5) cannot be established, as other post-trascriptional events (mRNA and protein stability, translation, localization, etc) could also play a part. The only exception to this caution is given by results obtained with Pyr6. So far, Pyr6 had been shown to inhibit SOCE via Orai1. Given that our cells do not have detectable levels of Orai1 but that Pyr6 is able to inhibit SOCE, it must be reasoned that other channels are affected by Pyr6, and this requires further investigation.

It is important to note that the changes observed in this manuscript confirm reports by others. For example, mGluR5 was found to be down-regulated specifically in astrocytes by TNFα, IL-1β and LPS [25–27] and astrocytic mGluR3 mRNA was up-regulated by TNFα and IL-1β [27]. Aβ has been shown to up-regulate mGluR5 [8].

On the contrary the effect on $InsP_3R$ was unexpected, because TNFα has been shown to up-regulate $InsP_3Rs$ expression in neurons [28,29], in osteoclasts [30] and in human mesangial cells [31], although in cultured neurons from 3xTg-AD mice TNFα-induced up-regulation of $InsP_3R2$ was significantly suppressed with respect to WT neurons [32].

Regarding function, we are not aware of manuscripts which have tackled the effects of pro-inflammatory agents on SOCE, with a single exception. In this former work, shorter exposures with IL-1β on cortical astrocytes increased 1-Oleoyl-2-acetyl-*sn*-glycerol (OAG)-induced Ca^{2+} entry, but it is unclear how the experiments protocol employed in this study [24] relates to the one described here. Nonetheless, it is unclear why chronic exposure with pro-inflammatory agents should decrease Ca^{2+} entry, a phenomenon which could be directly related to further cytokine release.

Yet, $A\beta_{42}$ and the three pro-inflammatory agents do not induce opposite direction changes in all circumstances. For example, it has been shown previously that TNFα and IL-1β induce strong up-regulations of mGluR3 [27] and we were able to reproduce this finding. $A\beta_{42}$ also induced an up-regulation of mGluR3, albeit to a smaller extent.

A somewhat surprising element in our study was that the three pro-inflammatory factors reduced expression of markers of astrogliosis GFAP, vimentin and S100. Nonetheless some time ago it was noticed that LPS down-regulates GFAP in astrocytic primary cultures [33]. The down-regulation of GFAP has been observed also for TNFα and IL-1β-treated astrocytes [26,27,34]. Vimentin, another protein associated with astrogliosis has previously also been shown to be down-regulated by LPS [26].

We also show that the four agents compared all activate the NF-kB pathway, but to different extents, different time-frames and via different mechanisms (e.g. CaN-sensitive vs. insensitive).

A crucial question is whether the effects observed in this study pertain to AD pathology. Indeed, we have previously shown that levels of mGluR5 and calcineurin

are higher in astroglial cells around plaques in AD post-mortem brains [11], and the data on mGluR5 has also been confirmed in a mouse AD model [35]. We now show that astrocytes from 3xTg-AD animals possess increased SOCE similar to that which we are able to obtain by treating cultured healthy astrocytes with $A\beta_{42}$. Yet, we must acknowledge that in a complex disease such as AD, pro-inflammatory cytokines and $A\beta_{42}$ would be present simultaneously, also given the participation of microglia [36], and therefore it is likely that astrocytic changes in AD would reflect this.

Acknowledgements

We thank Dr. Christian Zurlo and Dr. Marco Vacchiano for the help in the conduction of our experiments. This work was supported by Fondazione Cariplo (grant n° 2008-2319 to AAG, DL); and by MIUR (PRIN 2010-2011, SynAD, to AAG, DL).

The authors declare no conflict of interests.

References

[1] A. Verkhratsky, M.V. Sofroniew, A. Messing, et al., Neurological diseases as primary gliopathies: a reassessment of neurocentrism, ASN Neuro. 4 (2012).

[2] M.V. Sofroniew, Molecular dissection of reactive astrogliosis and glial scar formation, Trends Neurosci. 32 (2009) 638–647.

[3] A. Verkhratsky, M. Olabarria, H.N. Noristani, C.-Y. Yeh, J.J. Rodriguez, Astrocytes in Alzheimer's disease, Neurother. J. Am. Soc. Exp. Neurother. 7 (2010) 399–412.

[4] K.V. Kuchibhotla, C.R. Lattarulo, B.T. Hyman, B.J. Bacskai, Synchronous hyperactivity and intercellular calcium waves in astrocytes in Alzheimer mice, Science. 323 (2009) 1211–1215.

[5] C.-Y. Yeh, B. Vadhwana, A. Verkhratsky, J.J. Rodríguez, Early astrocytic atrophy in the entorhinal cortex of a triple transgenic animal model of Alzheimer's disease, ASN Neuro. 3 (2011) 271–279.

[6] M. Kulijewicz-Nawrot, A. Verkhratsky, A. Chvátal, E. Syková, J.J. Rodríguez, Astrocytic cytoskeletal atrophy in the medial prefrontal cortex of a triple transgenic mouse model of Alzheimer's disease, J. Anat. 221 (2012) 252–262.

[7] A.A. Grolla, J.A. Sim, D. Lim, J.J. Rodriguez, A.A. Genazzani, A. Verkhratsky, Amyloid-β and Alzheimer's disease type pathology differentially affects the calcium signalling toolkit in astrocytes from different brain regions, Cell Death Dis. 4 (2013) e623.

[8] C.S. Casley, V. Lakics, H.-G. Lee, et al., Up-regulation of astrocyte metabotropic glutamate receptor 5 by amyloid-beta peptide, Brain Res. (2009).

[9] H.M. Abdul, J.L. Furman, M.A. Sama, D.M. Mathis, C.M. Norris, NFATs and Alzheimer's Disease, Mol. Cell. Pharmacol. 2 (2010) 7–14.

[10] A.A. Grolla, G. Fakhfouri, G. Balzaretti, et al., Aβ leads to Ca^{2+} signaling alterations and transcriptional changes in glial cells, Neurobiol. Aging. 34 (2013) 511–522.

[11] D. Lim, A. Iyer, V. Ronco, et al., Amyloid beta deregulates astroglial mGluR5-mediated calcium signaling via calcineurin and Nf-kB, Glia. 61 (2013) 1134–1145.

[12] W. Liu, Y. Tang, J. Feng, Cross talk between activation of microglia and astrocytes in pathological conditions in the central nervous system, Life Sci. 89 (2011) 141–146.

[13] I.M. Adcock, Transcription factors as activators of gene transcription: AP-1 and NF-kappa B, Monaldi Arch. Chest Dis. Arch. Monaldi Mal. Torace Fondazione Clin. Lav. IRCCS Ist. Clin. Tisiol. E Mal. Appar. Respir. Univ. Napoli Secondo Ateneo. 52 (1997) 178–186.

[14] C. Li, R. Zhao, K. Gao, et al., Astrocytes: implications for neuroinflammatory pathogenesis of Alzheimer's disease, Curr. Alzheimer Res. 8 (2011) 67–80.

[15] S. Oddo, A. Caccamo, J.D. Shepherd, et al., Triple-transgenic model of Alzheimer's disease with plaques and tangles: intracellular Abeta and synaptic dysfunction, Neuron. 39 (2003) 409–421.

[16] L. Fresu, A. Dehpour, A.A. Genazzani, E. Carafoli, D. Guerini, Plasma membrane calcium ATPase isoforms in astrocytes, Glia. 28 (1999) 150–155.

[17] T.N. Glasnov, K. Groschner, C.O. Kappe, High-speed microwave-assisted synthesis of the trifluoromethylpyrazol-derived canonical transient receptor potential (TRPC) channel inhibitor Pyr3, ChemMedChem. 4 (2009) 1816–1818.

[18] D. Obermayer, T.N. Glasnov, C.O. Kappe, Microwave-assisted and continuous flow multistep synthesis of 4-(pyrazol-1-yl)carboxanilides, J. Org. Chem. 76 (2011) 6657–6669.

[19] H. Schleifer, B. Doleschal, M. Lichtenegger, et al., Novel pyrazole compounds for pharmacological discrimination between receptor-operated and store-operated Ca(2+) entry pathways, Br. J. Pharmacol. 167 (2012) 1712–1722.

[20] H.-M. Shin, M.-H. Kim, B.H. Kim, et al., Inhibitory action of novel aromatic diamine compound on lipopolysaccharide-induced nuclear translocation of NF-kappaB without affecting IkappaB degradation, FEBS Lett. 571 (2004) 50–54.

[21] I. Kemler, A. Fontana, Role of IkappaBalpha and IkappaBbeta in the biphasic nuclear translocation of NF-kappaB in TNFalpha-stimulated astrocytes and in neuroblastoma cells, Glia. 26 (1999) 212–220.

[22] A. Verkhratsky, J.J. Rodríguez, V. Parpura, Calcium signalling in astroglia, Mol. Cell. Endocrinol. 353 (2012) 45–56.

[23] M.D. Salmon, J. Ahluwalia, Pharmacology of receptor operated calcium entry in human neutrophils, Int. Immunopharmacol. 11 (2011) 145–148.

[24] O. Beskina, A. Miller, A. Mazzocco-Spezzia, M.V. Pulina, V.A. Golovina, Mechanisms of interleukin-1beta-induced Ca2+ signals in mouse cortical astrocytes: roles of store- and receptor-operated Ca2+ entry, Am. J. Physiol. Cell Physiol. 293 (2007) C1103–1111.

[25] E. Aronica, J.A. Gorter, A.J. Rozemuller, B. Yankaya, D. Troost, Interleukin-1 beta down-regulates the expression of metabotropic glutamate receptor 5 in cultured human astrocytes, J. Neuroimmunol. 160 (2005) 188–194.

[26] S. Tilleux, J. Berger, E. Hermans, Induction of astrogliosis by activated microglia is associated with a down-regulation of metabotropic glutamate receptor 5, J. Neuroimmunol. 189 (2007) 23–30.

[27] J.V. Berger, A.O. Dumont, M.C. Focant, et al., Opposite regulation of metabotropic glutamate receptor 3 and metabotropic glutamate receptor 5 by inflammatory stimuli in cultured microglia and astrocytes, Neuroscience. 205 (2012) 29–38.

[28] K.M. Park, D.I. Yule, W.J. Bowers, Tumor necrosis factor-alpha potentiates intraneuronal Ca2+ signaling via regulation of the inositol 1,4,5-trisphosphate receptor, J. Biol. Chem. 283 (2008) 33069–33079.

[29] K.M. Park, D.I. Yule, W.J. Bowers, Tumor necrosis factor-alpha-mediated regulation of the inositol 1,4,5-trisphosphate receptor promoter, J. Biol. Chem. 284 (2009) 27557–27566.

[30] L. Xia, D. Zhang, C. Wang, F. Wei, Y. Hu, PC-PLC is involved in osteoclastogenesis induced by TNF-α through upregulating IP3R1 expression, FEBS Lett. 586 (2012) 3341–3348.

[31] Y. Wang, Z. Li, J. Fu, Z. Wang, Y. Wen, P. Liu, TNFα-induced IP3R1 expression through TNFR1/PC-PLC/PKCα and TNFR2 signalling pathways in human mesangial cell, Nephrol. Dial. Transplant. Off. Publ. Eur. Dial. Transpl. Assoc. - Eur. Ren. Assoc. 26 (2011) 75–83.

[32] K.M. Park, D.I. Yule, W.J. Bowers, Impaired TNF-alpha control of IP3R-mediated Ca2+ release in Alzheimer's disease mouse neurons, Cell. Signal. 22 (2010) 519–526.

[33] M.L. Letournel-Boulland, C. Fages, B. Rolland, M. Tardy, Lipopolysaccharides (LPS), up-regulate the IL-1-mRNA and down-regulate the glial fibrillary acidic protein (GFAP) and glutamine synthetase (GS)-mRNAs in astroglial primary cultures, Eur. Cytokine Netw. 5 (1994) 51–56.

[34] C. Song, Y. Zhang, Y. Dong, Acute and subacute IL-1β administrations differentially modulate neuroimmune and neurotrophic systems: possible implications for neuroprotection and neurodegeneration, J. Neuroinflammation. 10 (2013) 59.

[35] A.N. Shrivastava, J.M. Kowalewski, M. Renner, et al., β-amyloid and ATP-induced diffusional trapping of astrocyte and neuronal metabotropic glutamate type-5 receptors, Glia. 61 (2013) 1673–1686.

[36] J.M. Rubio-Perez, J.M. Morillas-Ruiz, A review: inflammatory process in Alzheimer's disease, role of cytokines, ScientificWorldJournal. 2012 (2012) 756357.

SUPPLEMENTARY MATERIALS

Index

Supplementary Table 1. Oligonucleotide primers used for quantitative real-time PCR.

Gene	Accession number	Forward Reverce	Sequence 5' to 3'
GFAP	NM_017009	Forward Reverce	GGTGGAGAGGGACAATCTCA GAGTTCTCGAACTTCCTCCTCA
S100β	NM_013191	Forward Reverce	ATTCAGGGAGAGAGGGTGACA TCTTCGTCCAGCGTCTCCAT
Vimentin	NM_031140	Forward Reverce	CCCGTGTCGAGGTGGAGA ACGTGCCAGAGAAGCATTGT
mGluR5	NM_017012	Forward Reverce	GCCATGGTAGACATAGTGAAGAGA TAAGAGTGGGCGATGCAAAT
mGluR3	NM_001105712		CATTGCAGGAGTCATTGGTG TGGTGGAGGCGTAGCTTATC
$InsP_3R1$	NM_001007235	Forward Reverce	GGCTACAGAGTGCCTGACCT CCATTCGTAGATCCCTCTGC
$InsP_3R2$	NM_031046	Forward Reverce	TCCAAAAGACGTTGGACACA TTCATCCCCTTCCTCTGGAT
Orai1 (6-134)	NM_001013982	Forward Reverce	GCCGGCGGAGGTG GAAGCTCCGGATTGCTGTT
Orai1 (429-567)	NM_001013982	Forward Reverce	ACTACCCGCCAGGGTTACTC ACGGAGTTGAGGTTGTGGAC
Orai2	NM_001170403	Forward Reverce	ACACAGACGCTAGCCACGAG ACATTGAGCTCGGCACTCAT
Orai3	NM_001014024	Forward Reverce	GCTAAGCTCAAAGCCTCCAG GATCGCTCTCCAGCTGTACC
TRPC1	NM_053558	Forward Reverce	GAGGTGAAGGAGGAGAACACC ACAGCATTTCTCCCAAGCAC
TRPC3	NM_021771	Forward Reverce	GAGATCTGGAATCGGTGGAA AAAAGCTGCTGTTGGCAGTT
TRPC4	NM_080396	Forward Reverce	CAGGAAAGAGGTGGTTGGAG GCCAAGATGATAGGCGTGAT
TRPC5	NM_080898	Forward Reverce	GAGGTGGTAGGAGCTGTGGA GATGGGTGTGATGTCTGGTG
S18	NM_213557	Forward Reverce	TGCGAGTACTCAACACCAACA CTGCTTTCCTCAACACCACA
GAPDH	NM_017008	Forward Reverce	CAAGGTCATCCATGACAACTTTG GGGCCATCCACAGTCTTCTG
RP2a	XM_002727723	Forward Reverce	GCACCATCAAGAGAGTGCAG GGATCCATTAGTCCCCCAAG

Supplementary Figure 1. Effect of Pyr6 and Pyr10 compounds on store-operated Ca^{2+} entry in rat hippocampal astrocytes.

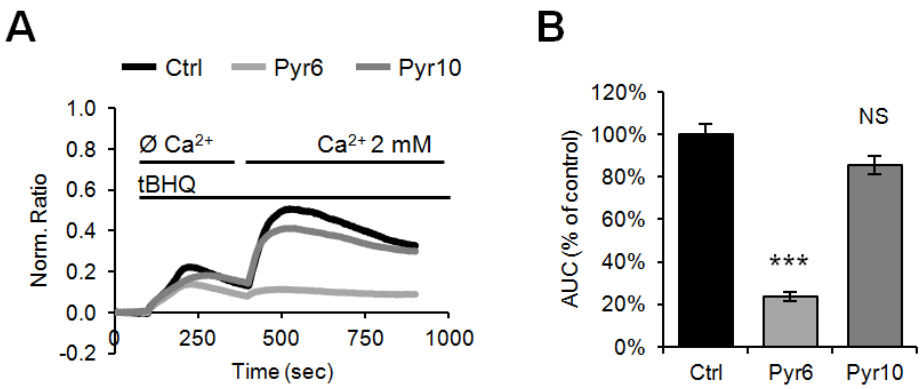

Rat rimary hippocampal astrocytes were loaded with Fura-2 and treated with DMSO (0.1%, Ctrl, black line and column), 5 μM Pyr6 (grey line and column) or 5 μM Pyr10 (light-grey line and column) for 5 min. SOCE was assessed using classical protocol of re-addition of Ca^{2+} (2 mM) after emptying internal Ca^{2+} stores with tert-Butylhydroquinone (tBHQ, 50 μM) in Ca^{2+}-free solution supplemented with 100 μM EGTA. Representative traces (**A**) and summarizing histogram (**B**) are shown for 22 (Ctrl), 54 (Pyr6) and 58 (Pyr10) cells recorded from at least 3 independent experiments. The data are expressed as mean ± SEM. *** $p < 0.001$.

Supplementary Figure 5. Western blot analysis of mGluR5 and IP_3R1 proteins in Aβ-treated hippocampal mixed and pure glial cultures.

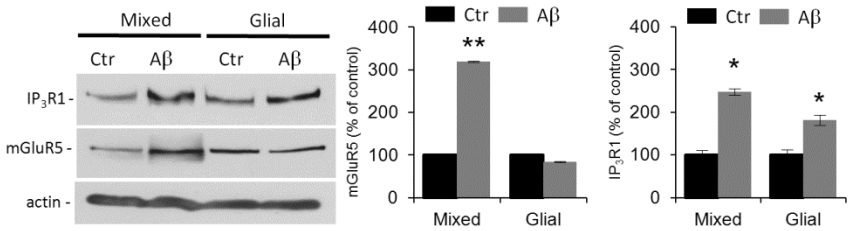

Control and Aβ-treated (1 µM, 48h) Mixed and Glial cultures were lysed and assayed by Western blotting using anti-IP3R1 and anti-mGluR5 primary antibody. Anti -actin antibodies were used for normalization. The band intensities are expressed as mean percent of control ± S.E.M. of 3 independent cultures. Differences are significative at: $p < 0.01$, **; $p < 0.05$, *.

Chapter 5

Discussion

The scenario that emerges from these findings suggests that the neurocentric view of Alzheimer's Disease might not be enough to explain the complex effects and aspects of the pathology. Indeed, astrocytes have been shown to be involved in AD not as inert bystanders, but as one of the main actors. Imagine the brain as a chess game (Figure 1). The only role, which neurons can play best is of course the king. Neurons are the essence of any brain activities as the king is the beginning and the end of the chess game. Anyway, even if the king is the most important piece of the game and from which depends the final result of the entire game, he cannot fight alone. Other pieces as the queen or the bishop are the real player and the real strategists of this fight.

Figure 1. The brain as a chess game.

They fight to support and save their king as astrocytes do in the brain. Indeed, astrocytes support neurons thanks to their structural and trophic functions and they can "advise the king" taking part to the tripartite synapses. Nevertheless, even the best king's advisers can sometimes rebel and fight against their sovereign. That's what happens in neurodegenerative disorders as Alzheimer's disease (AD).

Reactive and hypotrophic astrocytes, which are typical of neuroinflammation, surrounding the amyloid plaques are a hallmark of the pathology [1]. What is particularly interesting is that atrophic astrocytes have been seen also in 3xTg-AD mice at 3 months of age [2], very earlier before the plaques development, thus to confirm the involvement of astrocytes also in this stage of the disease and not only when the pathology is full-blown. For this reason, astrocytes can be an interesting point of view to learn something more about AD. In our hands astrocytes involvement in AD is demonstrated by a strong deregulation of calcium signalling inside these cells. Specifically, we have seen an increase in the DHPG, a specific agonist for glutamate metabotropic receptors type I, Ca^{2+} response in rat hippocampal astrocytes treated with $A\beta_{42}$. This effect is mediated by mGluR5 as the Ca^{2+} transient can be abolished by MTEP, a selective mGluR5 antagonist, but is insensitive to AIDA, the antagonist of mGluR1. Furthermore, the increased glutamatergic response is dependent on the up-regulation of the mGluR5 expression, as well as its downstream targets, the InsP3 receptors [3]. At this point, our question is how Aβ is able to induce these transcriptional changes. The calcium/calmodulin-dependent phosphatase calcineurin (CaN) is the best candidate as it has been previously demonstrated its ability in regulating the InsP3Rs expression [4]. Moreover CaN has been found up-regulated in reactive astrocyte surrounding the amyloid plaques in transgenic mice [5], as well as in post-mortem studies [6]. Furthermore, *in vivo* studies on transgenic APP/PS1 and Tg2576 have demonstrated the neuroprotective role of FK506, the inhibitor of CaN, on synaptic plasticity and neuronal arborization, as well as in the improvement of the mice performances in the

cognitive tests [7-10]. In line with these findings, we demonstrated the involvement of CaN in the altered glutamatergic signalling through mGluR5, in $A\beta_{42}$ oligomers treated astrocytes. Indeed, the pre-treatment of the cells with two CaN inhibitors, FK506 and cyclosporine A (CsA), can block not only the augmented Ca^{2+} response, but also the up-regulation of mGluR5, as well as insP3R1 and InsP3R2. According to the classical pathway of CaN, an increase in $[Ca^{2+}]i$ activates CaN, which in turn dephosphorylates the cytoplasmic subunit of the NFAT transcription complex. The dephosphorylated NFAT translocates into the nucleus, to regulate genes transcription. Because of NFAT is rapidly exported from the nucleus, a continuous elevation of $[Ca^{2+}]i$, as well as the continuous activity of CaN are necessary to maintain NFAT nuclear localization and activities on genes expression [11]. In our experiments, a 4-6 h treatment of $A\beta_{42}$ oligomers is sufficient to significantly increase the basal Ca^{2+} in a subpopulation of hippocampal astrocytes. Moreover, the pre-treatment of Aβ treated astrocytes with the calcium chelator BAPTA, as well as the TRP channels inhibitor, 2-APB, can keep the mRNA levels of mGluR5 and InsP3Rs at control levels. While the importance of the extracellular Ca^{2+} for this pathway is evident, it's difficult to draw conclusions about the role of TRP channels, as 2-APB is a non-specific inhibitor. How Aβ could induce this $[Ca^{2+}]i$ increment and activate CaN, is still a matter of debate. One explanation might be the postulated role of Aβ as a ionophore. Indeed, the organization of Aβ oligomers into β-sheets to form pores permeable to Ca^{2+} has been observed [12-15] also in post-mortem AD brains [16]. The CaN/NFAT pathway could not be the only way to mediate the Aβ effects. Indeed, an increased immunoreactivity of NFκB has been observed in correspondence of the amyloid plaques in post-mortem brain of AD patients [17]. It should be acknowledged that the promoter region of the gene coding for mGluR5 (GRM5) doesn't have the NFAT binding site, but the binding site for NFκB is present [18]. Finally, in T cells, CaN is reported to interact and de-phosphorylate B cell lymphoma 10 (Bcl10) [19]. This is a step for the recruitment of Carma1 and Malt1 to form the CBM complex, which finally leads to the degradation of IkB and the

nuclear translocation of NFκB [19]. We have observed by immunocytochemistry that $A\beta_{42}$ oligomers treatment could induce p65 NFκB subunit translocation into nucleus and this effect is blocked by the inhibition of CaN by CsA as well as FK506. Furthermore, we have confirmed the interaction between the active subunit of CaN (CaNA) and Bcl10 in rat hippocampal astrocytes. CaNA/Bcl10 interaction is augmented after $A\beta_{42}$ treatment, effect which can be blocked by CaN inhibition. In line with these findings, the inhibition of the NFκB nuclear translocation, by CAPE and JSH-23, affectes also the Ca^{2+} signalling, decreasing the percentage of DHPG responding astrocytes after $A\beta_{42}$ treatment. Moreover, CAPE and JSH-23 treatment can revert the $A\beta_{42}$ induced up-regulation of mGluR5 and InsP3R2, as observed after CaN inhibition. Interestingly, NFκB inhibition have no effects on the mRNA levels of InsP3R1 of the $A\beta_{42}$ treated cells, thus to suggest the co-existence of different pathways regulated by Aβ. Taken together, our data suggest that, with a still unknown mechanism, Aβ can increase the resting $[Ca^{2+}]i$, which in turn leads to an abnormal activation of CaN. CaN can then follow its classical pathway to up-regulates InsP3R1 and a non-canonical one to overexpress mGluR5 and Insp3R2, resulting in an increased Ca^{2+} response to glutamate in $A\beta_{42}$ oligomers treated astrocytes. This model is also supported by immunohistochemistry analysis on the hippocampus of human AD brains. Indeed, mGluR5 is overexpressed in astrocytes surrounding the amyloid plaques and this effect is correlated by an increased expression of CaN, as well as p65, which both co-localize with mGluR5.

This profound Ca^{2+} signalling remodelling, consequent of Aβ, might be reflected in astrocytes Ca^{2+}-dependent processes as gliotransmission and reactive inflammation. Indeed, atrophic and reactive astrocytes, which are a hallmark of neuroinflammation, have been observed around the amyloid plaques in the full-blown pathology, as well as in the early stages of the disease [1, 2]. For this reason, we investigated if the observed alterations in Ca^{2+} signalling were something specific for Aβ or could be compared with those induced by a pro-inflammatory environment. We have

compared the response to DHPG in rat hippocampal astrocytes treated with Aβ42 oligomers, with the DHPG response of astrocytes treated with three classical pro-inflammatory stimuli, TNFα, IL-1β and LPS. The fast Ca^{2+} transient, which reflects the Ca^{2+} release from the ER, is augmented in Aβ treated cells, as described before, while the treatment with TNFα, IL-1β and LPS have no effects on this transient, but significantly reduce the percentage of responding astrocytes. Because of the increased Ca^{2+} response after Aβ treatment is mediated by alteration at transcriptional level, we analysed if was the case also for the effects of the three pro-inflammatory stimuli. The comparison between the mRNA levels of mGluR5, as well as the InsP3Rs reveals that data of Aβ treatment are confirmed, with the up-regulation of all of the three genes, on the contrary the TNFα, IL-1β and LPS treatments reduce the expression of all of the three receptors. The reduction of mGluR5 after TNFα, IL-1β and LPS exposure has been reported yet [20, 21], whereas the effects on InsP3Rs are unexpected. Indeed, TNFα is reported to up-regulate Insp3Rs in neurones [22] as well as in mesanglial cells [23]. Somewhat interesting is that, even if the effects of $Aβ_{42}$ compared to those of the three pro-inflammatory agents are just the opposite, they are basically mediated by NFκB since the expression of mGluR5 and Insp3Rs is normal after pre-treatment with JSH-23. Because of the ability of Aβ to activate NFκB through CaN, we have analysed the time-course of IkB degradation (so NFκB activation) to verify if this is also the case of TNFα, IL-1β and LPS or not. IkB degradation is affected by CaN inhibition only in Aβ treated astrocytes, while FK506 treatment have no effect in TNFα, IL-1β and LPS treated cells. Moreover, after stimulation with the three pro-inflammatory stimuli, IkB is rapidly degraded, and such degradation is immediately followed by a recovery. This is s not the case of Aβ treatment, where the IkB degradation is in a time delay way, thus to support the existence of an NFκB activation pathway specific for Aβ and different from the way triggered by the pro-inflammatory stimuli. Another aspect of the Ca^{2+} response to DHPG is the slow $[Ca^{2+}]i$, which follows the Ca^{2+} release from the ER. Such $[Ca^{2+}]i$ was a Store Operated Ca^{2+} Entry (SOCE), a

mechanism leading to the Ca^{2+} entry from the extracellular space to restore the ER Ca^{2+} content after ER Ca^{2+} release (see the introduction), as far as it's abolished by the absence of extracellular Ca^{2+} and by Pyr6 a specific SOCE inhibitor [24]. Also in this case the effect of Aβ is the opposite as these of TNFα, IL-1β and LPS, indeed, Aβ potentiates the SOCE, whereas TNFα, IL-1β and LPS treatment significantly decreases this mechanism. Our hypothesis is that in the case of SOCE, as well as in the first part of the DHPG Ca^{2+} response, the effects of the four agents can be mediated by transcriptional changes. The screening of the receptor involved in SOCE in rat hippocampal astrocytes, the cells used in these experiments, revealed that the channels involved in this mechanism are TRPC1 and TRPC4, as well as Orai3. Aβ can up-regulate TRPC1, while TNFα, IL-1β and LPS decrease the expression of all of the three involved genes, thus to explain, at least, the differential effects of the four stimuli on the SOCE. A reduction of SOCE in APP knock out mice has been reported [25], while we are not aware of manuscripts which have explored the effects of pro-inflammatory stimuli on SOCE. Finally, in order to confirm that the altered SOCE in Aβ treated astrocytes is not an artefact, but it can be found also in a model nearer to reality, we have analysed SOCE in primary hippocampal astrocytes of 3xTg-AD mice. We have compared four different situations: wild type astrocytes treated with Aβ, wild type astrocytes not treated with Aβ, 3xTg-AD astrocytes treated with Aβ and 3xTg-AD astrocytes not treated with Aβ. $Aβ_{42}$ treatment of wild type astrocytes induces the expected increase in the SOCE, while the treatment have no effects on the SOCE of transgenic cells. What is particularly interesting is that the SOCE level of transgenic untreated astrocytes is higher than wild type untreated cells, especially the SOCE of transgenic untreated astrocytes is almost the same as the wild type astrocytes treated with $Aβ_{42}$, thus to confirm the effect of Aβ on this mechanism.

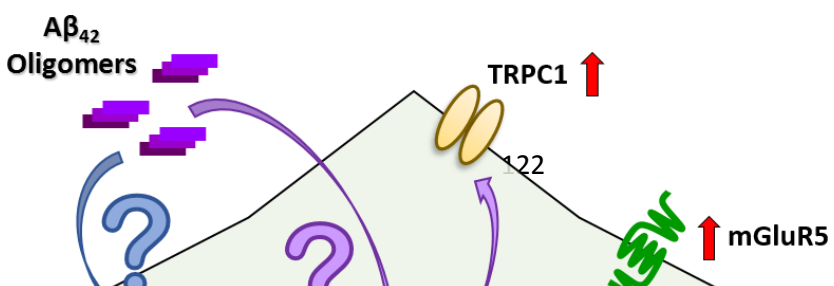

All of our findings demonstrate that Aβ can modify astrocytic Ca^{2+} signalling, increasing the resting Ca^{2+}, as well as the glutamate response through the mGluR5 pathway and the SOCE. These effects are mediated at transcriptional level and are something specific for Aβ, indeed, a pro-inflammatory environment induces the opposite effects both on mGluR5 response and on the SOCE. This model is a good model for an *in vitro* situation, but of course reality is more complicated as astrocytes, neurons and microglia co-exist as well as Aβ and pro-inflammatory stimuli are present at the same time. Many critical questions remain unsolved. First, how can Aβ trigger the Ca^{2+} alterations in primary cultures, as well as in *in vivo* experiments on transgenic mice models? Is the ability of Aβ to behave as a ionophore sufficient to explain these effects or other mechanism/receptors are involved? Second, are the glial Ca^{2+} abnormalities a consequence of neuronal dysfunction or neuronal dysfunctions are a consequence of glial alterations? Are these two events correlated or are something independent? Our findings on Ca^{2+} signalling in primary cultures from neonatal transgenic mice support the involvement of astrocytes in the early phases of the disease, suggesting that astrocytes are among the first to be affected. Third, how astrocytic Ca^{2+} signalling is relevant in the disease initiation and progression? Is it the responsible for a failure in astrocytic protection of neuronal network, leading to neurodegeneration? Fourth, how important is inflammation in AD? An improvement in memory tests of 3xTg-AD mice has been observed after the COX-1 inhibitor SC-560 administration [26]. Could the cure of inflammation be a strategy in the fight against AD? Is inflammation a consequence of AD or vice versa? Despite the great strides science has made in AD understanding, these questions are still far from an answer.

References

[1]. Parpura V, Heneka MT, Montana V, Oliet SH, Schousboe A, Haydon PG, Stout RF Jr, Spray DC, Reichenbach A, Pannicke T, Pekny M, Pekna M, Zorec R, Verkhratsky A. Glial cells in (patho)physiology. J Neurochem. 2012 Apr;121(1):4-27. doi: 10.1111/j.1471-4159.2012.07664.x. Epub 2012 Feb 2

[2]. Kulijewicz-Nawrot M, Verkhratsky A, Chvatal A, Sykova E, Rodriguez JJ (2012) Astrocytic cytoskeletal atrophy in the medial prefrontal cortex of a triple transgenic mouse model of Alzheimer's disease. J Anat 221:252-62

[3]. Grolla AA, Fakhfouri G, Balzaretti G, Marcello E, Gardoni F, Canonico PL, DiLuca M, Genazzani AA, Lim D (2013) Ab leads to Ca^{2+} signaling alterations and transcriptional changes in glial cells. Neurobiol Aging 34:511-22

[4]. Genazzani AA, Carafoli E, Guerini D. Calcineurin controls inositol 1,4,5-trisphosphate type 1 receptor expression in neurons. Proc Natl Acad Sci U S A. 1999; 96:5797-801.

[5]. Norris CM, Kadish I, Blalock EM, Chen KC, Thibault V, Porter NM, Landfield PW, Kraner SD (2005) Calcineurin triggers reactive/inflammatory processes in astrocytes and is upregulated in aging and Alzheimer's models. J Neurosci 25:4649-58

[6]. Abdul HM, Sama MA, Furman JL, Mathis DM, Beckett TL, Weidner AM, Patel ES, Baig I, Murphy MP, LeVine H, 3rd, Kraner SD, Norris CM (2009) Cognitive decline in Alzheimer's disease is associated with selective changes in calcineurin/NFAT signaling. J Neurosci 29:12957-69

[7]. Taglialatela G, Hogan D, Zhang WR, Dineley KT. Intermediate- and long-term recognition memory deficits in Tg2576 mice are reversed with acute calcineurin inhibition. Behav Brain Res. 2009 Jun 8;200(1):95-9.

[8]. Hong HS, Hwang JY, Son SM, Kim YH, Moon M, Inhee MJ. FK506 reduces amyloid plaque burden and induces MMP-9 in AβPP/PS1 double transgenic mice. J Alzheimers Dis. 2010;22(1):97-105.

[9]. Rozkalne A, Hyman BT, Spires-Jones TL. Calcineurin inhibition with FK506 ameliorates dendritic spine density deficits in plaque-bearing Alzheimer model mice. Neurobiol Dis. 2011 Mar;41(3):650-4.

[10]. Cavallucci V, Berretta N, Nobili A, Nisticò R, Mercuri NB, D'Amelio M.Calcineurin inhibition rescues early synaptic plasticity deficits in a mouse model of Alzheimer's disease. Neuromolecular Med. 2013 Sep;15(3):541-8.

[11]. Crabtree GR. Calcium, calcineurin, and the control of transcription. J Biol Chem. 2001 Jan 26;276(4):2313-6. Epub 2000 Nov 28.

[12]. Arispe N, Rojas E, Pollard HB (1993) Alzheimer disease amyloid beta protein forms calcium channels in bilayer membranes: blockade by tromethamine and aluminum. Proc Natl Acad Sci U S A 90:567-71

[13]. Lashuel HA, Hartley D, Petre BM, Walz T, Lansbury PT, Jr. (2002) Neurodegenerative disease: amyloid pores from pathogenic mutations. Nature 418:291

[14]. Demuro A, Smith M, Parker I. Single-channel $Ca(^{2+})$ imaging implicates Aβ1-42 amyloid pores in Alzheimer's disease pathology. J Cell Biol. 2011 Oct 31;195(3):515-24.

[15]. Johnson RD, Schauerte JA, Wisser KC, Gafni A, Steel DG. Direct observation of single amyloid-β(1-40) oligomers on live cells: binding and growth at physiological concentrations. PLoS One. 2011;6(8):e23970.

[16]. Inoue S. In situ Abeta pores in AD brain are cylindrical assembly of Abeta protofilaments. Amyloid. 2008 Dec;15(4):223-33.

[17]. Ferrer I, Martí E, López E, Tortosa A. NF-kB immunoreactivity is observed in association with beta A4 diffuse plaques in patients with Alzheimer's disease. Neuropathol Appl Neurobiol. 1998 Aug;24(4):271-7.

[18]. Corti C, Clarkson RW, Crepaldi L, Sala CF, Xuereb JH, Ferraguti F. Gene structure of the human metabotropic glutamate receptor 5 and functional analysis of its multiple promoters in neuroblastoma and astroglioma cells. J Biol Chem. 2003 Aug 29;278(35):33105-19. Epub 2003 Jun 3.

[19]. Palkowitsch L, Marienfeld U, Brunner C, Eitelhuber A, Krappmann D, Marienfeld RB. The Ca2+-dependent phosphatase calcineurin controls the formation of the Carma1-Bcl10-Malt1 complex during T cell receptor-induced NF-kappaB activation. J Biol Chem. 2011 Mar 4;286(9):7522-34.

[20]. Berger JV, Dumont AO, Focant MC, Vergouts M, Sternotte A, Calas AG, Goursaud S, Hermans E. Opposite regulation of metabotropic glutamate receptor 3 and metabotropic glutamate receptor 5 by inflammatory stimuli in cultured microglia and astrocytes. Neuroscience. 2012 Mar 15;205:29-38.

[21]. Aronica E, Gorter JA, Rozemuller AJ, Yankaya B, Troost D. Interleukin-1 beta down-regulates the expression of metabotropic glutamate receptor 5 in cultured human astrocytes. J Neuroimmunol. 2005 Mar;160(1-2):188-94. Epub 2005 Jan 21.

[22]. Park KM, Yule DI, Bowers WJ. Tumor necrosis factor-alpha potentiates intraneuronal Ca2+ signaling via regulation of the inositol 1,4,5-trisphosphate receptor. J Biol Chem. 2008 Nov 28;283(48):33069-79.

[23]. Wang YR, Li ZG, Fu JL, Wang ZH, Wen Y, Liu P. TNFα-induced IP3R1 expression through TNFR1/PC-PLC/PKCα and TNFR2 signalling pathways in human mesangial cell. Nephrol Dial Transplant. 2011 Jan;26(1):75-83.

[24]. Glasnov TN, Groschner K, Kappe CO. High-speed microwave-assisted synthesis of the trifluoromethylpyrazol-derived canonical transient receptor potential (TRPC) channel inhibitor Pyr3. ChemMedChem. 2009 Nov;4(11):1816-8.

[25]. Linde CI, Baryshnikov SG, Mazzocco-Spezzia A, Golovina VA (2011) Dysregulation of Ca^{2+} signaling in astrocytes from mice lacking amyloid precursor protein. Am J Physiol Cell Physiol 300:C1502-12

[26]. Choi SH, Aid S, Caracciolo L, Minami SS, Niikura T, Matsuoka Y, Turner RS, Mattson MP, Bosetti F. Cyclooxygenase-1 inhibition reduces amyloid pathology and improves memory deficits in a mouse model of Alzheimer's disease. J Neurochem. 2013 Jan;124(1):59-68.

Chapter 6

List of publications

1. Lim D, Iyer A, **Ronco V**, Grolla AA, Canonico PL, Aronica E, Genazzani AA. Amyloid beta deregulates astroglial mGluR5-mediated calcium signaling via calcineurin and Nf-kB. Glia. 2013 Jul;61(7):1134-45. doi: 10.1002/glia.22502.

2. **Ronco V**, Grolla AA, Glasnov TN, Canonico PL, Verkhratsky A, Genazzani AA, Lim D. Differential deregulation of astrocytic calcium signalling by amyloid-β, TNFα, IL-1β and LPS. Cell Calcium. 2014 Apr;55(4):219-29.

3. Lim D, **Ronco V**, Grolla AA, Verkhratsky A, Genazzani AA. Glial Calcium Signalling in Alzheimer's Disease. Rev Physiol Biochem Pharmacol. 2014 Jun 17.

Acknowledgments

First, I would like to thank Prof. Armando Genazzani for this extraordinary journey in neuroscience. Thanks for all the advice in science and life.

I would like to thank Ambra Grolla, Cristina Travelli and last but not least Sarah Cargnin. We have been a great team!!!

I would like to thank Prof. Alex Verkhratsky for his collaboration and Dr. Toma Glasnov for his precious PyR compounds.

I cannot forget to thank all of the lab members for their support: Beatrice Riva, Simone Torretta, Dmitry Lim, Salvatore Terrazzino and Roberta Zaninetti. Thanks for all!